REPORT DOCUMENTATION FORM
WATER RESOURCES RESEARCH CENTER
University of Hawaii at Manoa

[1]Report Number Tech. Rep. No. 119	[2]FCST Category II-B
[3]Title *Mesoscale Structure of Hawaiian Rainstorms*	[4]Report Date September 1978
	[5]No. of Pages x + 69
	[6]No. of Tables 14 / [7]No. of Figures 49
[8]Author(s) Thomas A. Schroeder	[9]Grant or Contract Agency Office of Water Research and Technology, U.S. Dept. of the Interior
	[10]Grant or Contract No. 14-34-0001-8013 (A-072-HI)

[11]Keywords *Descriptors:* Rainfall, Meteorological satellites, Flash floods, Storms, Meteorology, Rainfall disposition, Hawaii.
Identifiers: Synchronous Meteorological Satellite, Contingency indices.

[12]Abstract (Purpose, method, results, conclusions)

I. Three significant Hawaiian rainstorms were analyzed using conventional meteorological data and photographs from Synchronous Meteorological Satellite (SMS-2). The impact of the satellite on analysis and forecasting was evaluated. Gridding inaccuracies and the distinctive nature of Hawaiian rains limit the impact of the satellite to the scale of synoptic analysis. The storms studied illustrate the range of Hawaiian flood-producing systems and the limitations of the detection network. The most important meteorological determinant of flood location is the low-level wind direction. Forecast and detection capabilities are evaluated in terms of developments in the coterminus United States, and it is concluded that the absence of meteorological radar in Hawai'i inhibits significant progress.

II. Contingency indices (CI) were computed for 103 rain gages in the Hawaiian Islands. Results are presented in matrices of CI and in individual island maps on which CIs are plotted and analyzed relative to representative stations. The secondary CI maximum with increasing station separation, which has been attributed to spacing of convective updrafts, does not appear in Hawaiian examples. Orography dominates the CI patterns which resemble isohyets. The analysis was extended to interisland comparisons using representative windward and leeward stations. CIs decrease with distance in both samples but more so for windward (trade wind) stations.

2540 Dole Street, Holmes Hall 283 • Honolulu, Hawaii • U.S.A.

MESOSCALE STRUCTURE OF HAWAIIAN RAINSTORMS

by

Thomas A. Schroeder

Technical Report No. 119
UHMET 78-03

September 1978

Project Completion Report
for
Studies of Hawaiian Mesoscale Rainfall Regimes
Utilizing Satellite Imagery, Phase II

OWRT Project No.: A-072-HI
Project Period: 1 October 1977 to 30 September 1978
Principal Investigator: Thomas A. Schroeder

The work upon which this publication is based was supported in part by funds provided by the Office of Water Research and Technology, U.S. Department of the Interior, Washington, D.C., as authorized by the Water Research and Development Act of 1978.

ABSTRACT

Three significant Hawaiian rainstorms were analyzed using conventional meteorological data and photographs from the Synchronous Meteorological Satellite (SMS-2). The impact of the satellite on analysis and forecasting was evaluated. Gridding inaccuracies and the distinctive nature of Hawaiian rains limit the impact of the satellite to the scale of synoptic analysis. The storms studied illustrate the range of Hawaiian flood-producing systems and the limitations of the detection network. The most important meteorological determinant of flood location is the low-level wind direction. Forecast and detection capabilities are evaluated in terms of developments in the coterminus United States, and it is concluded that the absence of meteorological radar in Hawai'i inhibits significant progress.

Contingency indices (CI) were computed for 103 rain gages in the Hawaiian Islands. Results are presented in matrices of CI and in individual island maps on which CIs are plotted and analyzed relative to representative stations. The secondary CI maximum with increasing station separation, which has been attributed to spacing of convective updrafts, does not appear in Hawaiian examples. Orography dominates the CI patterns which resemble isohyets. The analysis was extended to interisland comparisons using representative windward and leeward stations. CIs decrease with distance in both samples but more so for windward (trade wind) stations.

CONTENTS

ILLUSTRATIONS

FIGURES

PLATES

TABLES

I. ANALYSIS OF HAWAIIAN FLASH FLOODS USING DATA FROM GEOSTATIONARY SATELLITES

INTRODUCTION

Floods in Hawai'i

Flash floods of varied severity and extent occur in the Hawaiian Islands. Between 1961 and 1976, 71 events were reported as "RAIN" or "FLOODS" in *Storm Data*, the official National Weather Service (NWS) tabulation of storm reports (Schroeder 1978). This probably underestimates flood frequency. Streamflow data in the U.S. Geological Survey (USGS) annual report series, *An Investigation of Floods in Hawaii* (1959-1971),[1] indicate a much higher incidence of flooding.

Factors that contribute to the high flood incidence are:

1. Topography. The islands are mountainous and watersheds lie close to populated coasts. Fifty percent of the land area is within 8 000 m of the coasts.
2. Watersheds. On the older islands the watersheds are steep (highly eroded) with narrow basins and low capacities.
3. Stream response. Because of the topography and nature of the watersheds, stream response can be rapid. Usually less than 1 hr elapses between peak rainfall and flood peak (Wang, Wu, and Lau 1970).
4. Flood-producing weather types. Floods are primarily winter phenomena (Schroeder 1977). However, the associated synoptic-scale weather patterns are sufficiently varied to produce floods in any month. Blumenstock and Price (1967) specified four flood-producing systems:
   a. Cold fronts—winter features
   b. Kona lows (Simpson 1952)—winter features
   c. Rains induced by upper tropospheric troughs—any season
   d. Tropical storms—late summer and autumn.

For purposes of this discussion, winter comprises the months, October through April; and summer, the months, June through August.

---
[1]Series succeeded in 1976 by *Water Resources Data for Hawaii and Other Pacific Areas*.

Recent Significant Floods in the Continental U.S.

A series of devastating flash floods has awakened the American public to the hazard posed by flash floods. The most significant have been:

1. Big Thompson, Colorado, 31 July 1976. One hundred thirty-nine persons killed as a result of flash flooding produced by 305 mm of rain in 6 hr (Maddox et al. 1977).
2. Johnstown, Pennsylvania, 19-20 July 1977. Seventy-six persons killed and $200 million property damage caused by a 280 mm rainfall in 9 hr over seven counties (NOAA 1977*a*; Hoxit et al. 1978).
3. Kansas City, Missouri, 12 September 1977. Twenty-five persons killed and $90 million property damage due to floods caused by two "100-yr" rainfalls within 24 hr (NOAA 1977*b*; Hales 1978; Larson and Vochatzer 1978).
4. Toccoa, Georgia, 6 November 1977. Forty persons killed by flood waters produced when heavy rains caused failure of an earthen dam (Land 1978).

In response to heightened awareness of the flood problem, the American Meteorological Society (AMS) in 1978 prepared a statement of concern which declared:

> Flash floods now rank as the major killers and destroyers among weather-related disasters in the United States.

In the same policy statement it was noted:

> Unfortunately, there are substantial gaps in our knowledge and understanding of how such extremely heavy rains of short duration are produced.

PURPOSES OF THE PRESENT RESEARCH PROGRAM

The AMS statement mentioned above included nine recommended steps as "positive action" to reduce the death toll and property damages arising from flash floods. Three of the steps summarize the purposes for which this present research program was originally undertaken (Schroeder 1976):

1. Improve the ability to monitor and detect flash flood conditions, partly by increased use of automated ground measurements, radar, and weather satellites
2. Increase the capability to forecast the location and magnitude of rainfall

3. Improve the capability to forecast intense small-scale phenomena.

The impetus for flood research effort came with the launching of the Synchronous Meteorological Satellite (SMS-2) in the spring of 1975. Since December 1975, SMS-2 has been in orbit above 0° north latitude, 135° east longitude, providing continuous surveillance over the Hawaiian Islands. This allows unprecedented observations of weather systems in a "data sparse" region. Furthermore, since it is obvious that cataclysm must occur before the National Weather Service will provide weather radar for Hawai'i, the satellite must perform two roles: description of large-scale systems (its normal role) and detection of individual clouds with high resolution (the traditional role of radar but becoming routine for satellites). A preliminary study (Schroeder 1976, 1977) describes the pre-SMS detection and forecast capability. In the following discussion three recent flood episodes are described with the use of satellite data being emphasized in each instance. In conclusion, prospects for further developments in flood detection and forecasting are assessed.

RECENT SIGNIFICANT HAWAIIAN FLOODS

The period 1975 through 1977 has been characterized by drought in Hawai'i. Absence of major winter storms has resulted in low flood frequencies. Nevertheless, three significant rainstorms occurred that demonstrated the variable scale of Hawaiian rains and their interdependence with topography and synoptic scale weather patterns. Two "rainstorms" occurred as consequences of one synoptic event, an intense low pressure system, Kona storm, between 4 and 8 February 1976; the third resulted from development of an isolated cumulus tower.

4-5 February 1976

Southeasterly winds in advance of an intense frontal system deposited heavy rain on the southeast slopes of Mauna Loa and the southern flank of Kīlauea. Heaviest rains fell during the evening of 4 February and the early morning of 5 February. Flooding occurred along the flood-prone strip of Highway 11 between Nā'ālehu and Pāhala (Fig. 1).

RAINFALL DATA. Data were assembled for all NWS rain gages (standard and recording). Analysis of 24-hr totals during the flood period showed the

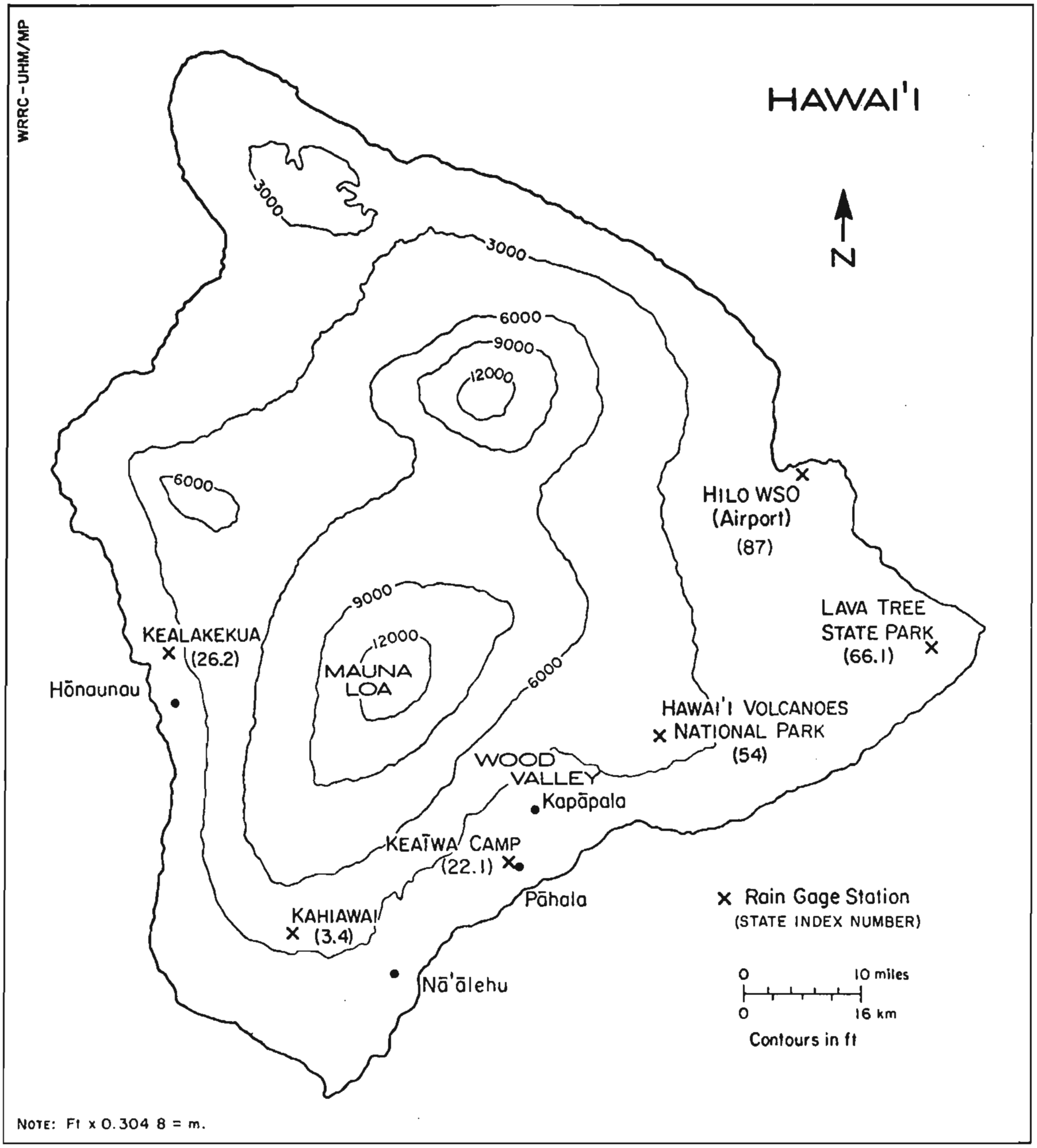

FIGURE 1. MAP OF SELECTED RAIN GAGE STATIONS AND GEOGRAPHIC FEATURES, HAWAI'I ISLAND

rainfall to be centered over the Pāhala-Kapāpala area (Fig. 2). Recording rain gage data show that the "flood rain" fell between 2000 hr 4 February and 0100 hr 5 February when 189 mm were recorded at Keaīwa Camp and 98 mm at Hawaii Volcanoes National Park Headquarters (Fig. 3).

Analysis of areal and temporal distributions of storm rains showed several distinctive features:

1. Rainfall for the flood period was limited to less than half of the

island. The 0-mm isopleth was oriented almost exactly southwest-northeast (Fig. 2). (It should be noted that analysis of upper elevations is hindered by a lack of rainfall gages.)

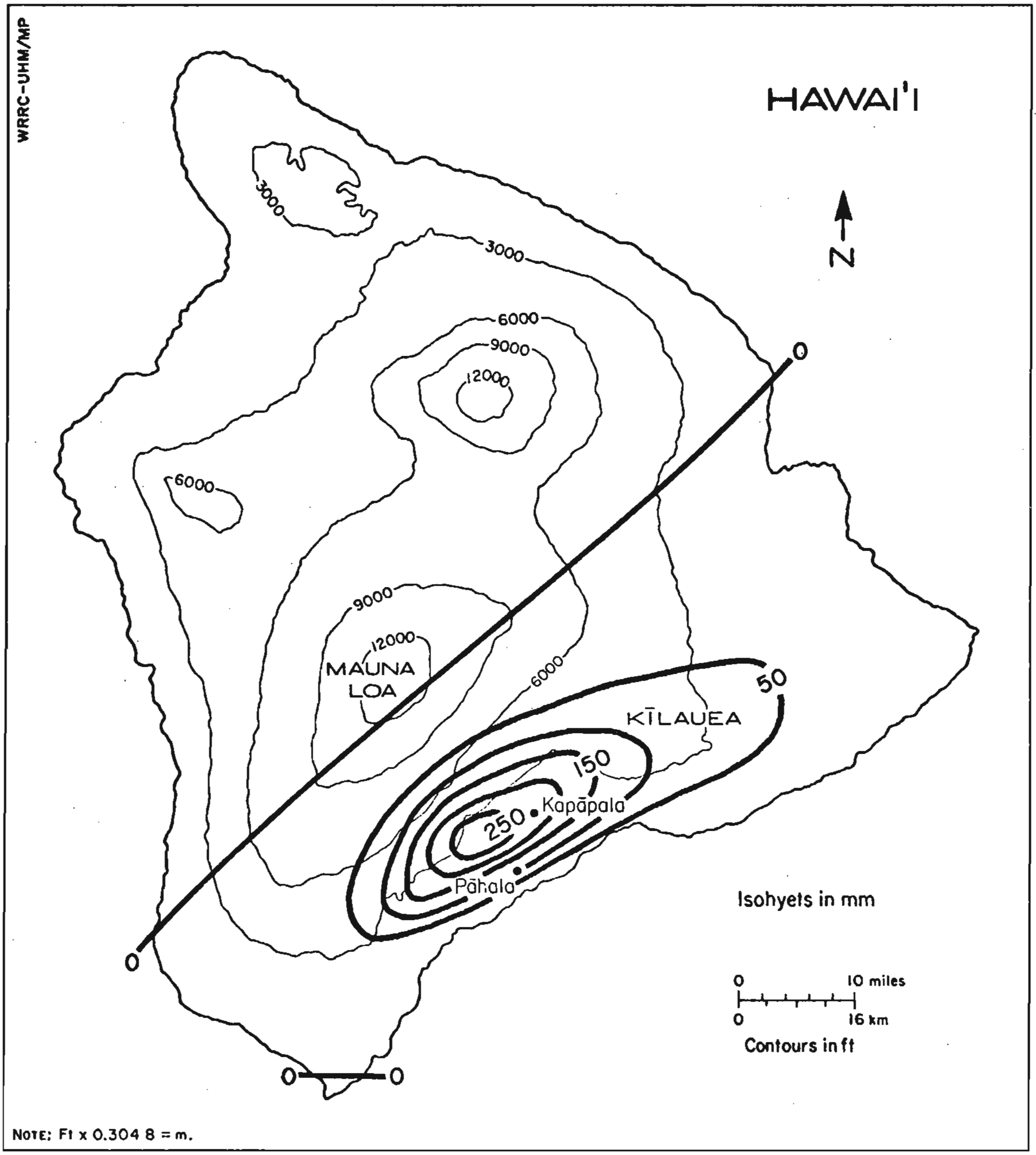

FIGURE 2. 24-HR RAINFALL FOR THE PERIOD 0800 HR, 4 FEBRUARY TO 0800 HR, 5 FEBRUARY 1976, PĀHALA-KAPĀHALA, HAWAI'I ISLAND

2. Though orographic influences are obvious, there was temporal variability between adjacent rain gages. The convective character of the clouds

could be inferred from considerable differences between adjacent gages (Fig. 3).

3. There were several periods of lighter rain in succeeding days (Fig. 3).

SATELLITE IMAGERY. The following discussion makes extensive use of enhanced infrared (IR) satellite imagery. Visible satellite images sample reflected sunlight and, although variations in cloud-top reflectivity help locate cumulonimbus clouds, little detail of cloud structure or depth can be determined. Since the infrared (IR) sensor on SMS-2 measures infrared radiation, it is possible to translate radiation measured into equivalent black body temperature of the radiating body, e.g., cloud top. By assigning grey scales based on temperature intervals, shade-contoured images are possible. Cloud-top height may be estimated by assigning to the satellite-observed, cloud-top temperature the height corresponding to that temperature in an adjacent sounding.

The visible image at 1619 hr (Pl. 1) shows a mass of cumulonimbus cloud south of Hawai'i. Some detail at anvil level could be seen due to shadow effects. At 1815 hr (Pl. 2) enhanced IR indicated cloud-top temperatures of less than -70°C (approximate elevation 14 000 m) south and southeast of the island. Much more vigorous convection was occurring northwest of the state in the cold front zone. By 0016 hr (Pl. 3) cloud tops had lowered near Hawai'i with a small patch reaching 10 000 m (-42.2°C). At 0615 hr (Pl. 4) no tall clouds appeared over the island.

Radar reports, not weather radar, from Mt. Ka'ala, O'ahu, indicated no significant echoes to the south or southeast. Perhaps attention was focused on the frontal zone to the northwest. Hilo Weather Service Office (WSO) reported no thunder during the period.

LOW-LEVEL WINDS. Low-level southeasterly winds blew at Hilo throughout the period. Between 1400 hr 4 February and 1400 hr 5 February the southeast winds below 1 500 m increased significantly (Table 1). Orography acts on southeasterlies to create a rainfall maximum along the southeast flank of Mauna Loa. Convergence is enhanced by the south rift of Mauna Loa and the east rift of Kīlauea. Southeasterlies occasionally produce similar local rains in the Ka'ū district. An annual rainfall maximum occurs in a similar region but is due to local, mountain-induced circulations.

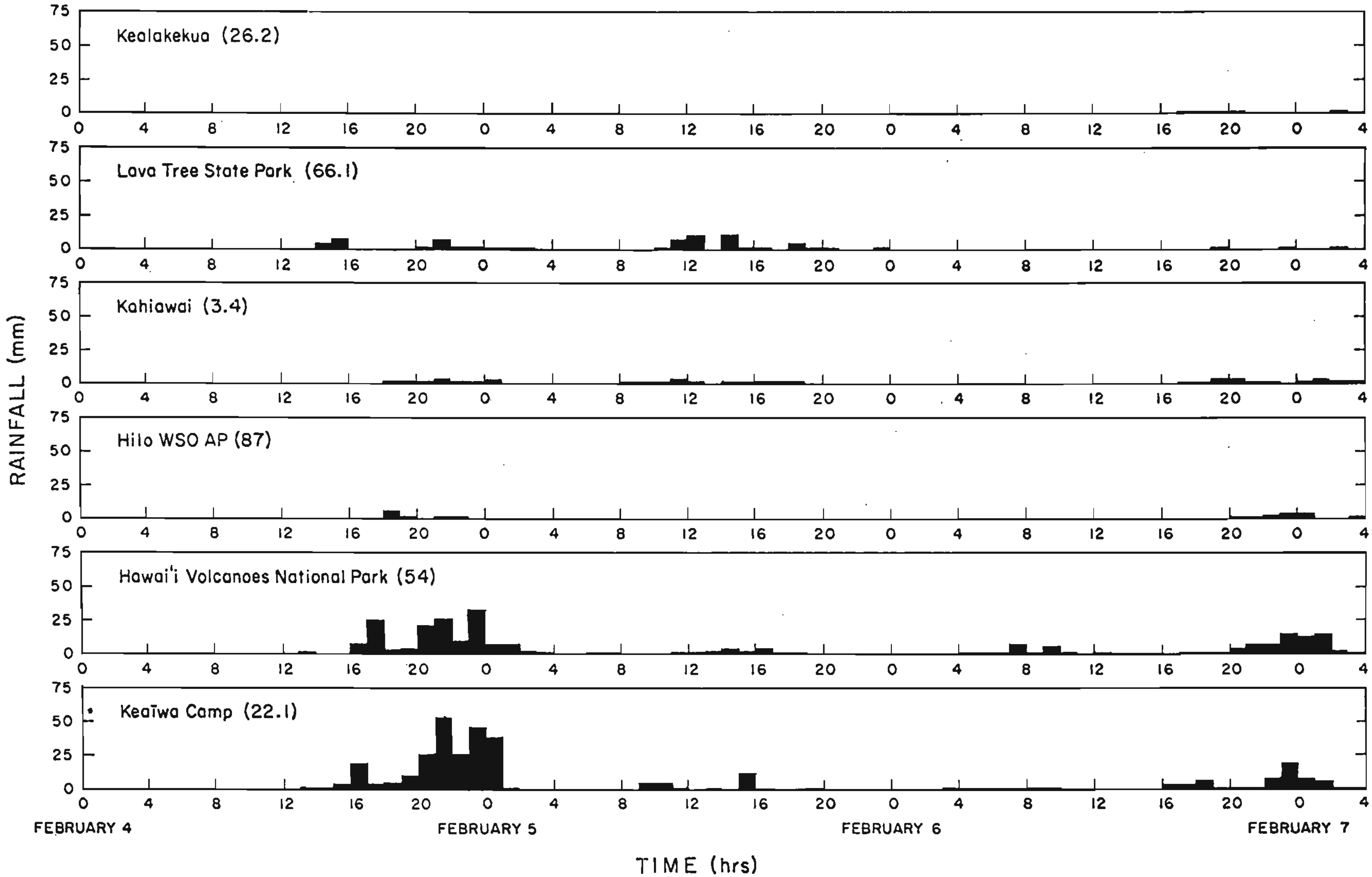

FIGURE 3. HOURLY RAINFALL FOR SIX STATIONS, HAWAI'I ISLAND, 4-7 FEBRUARY 1976

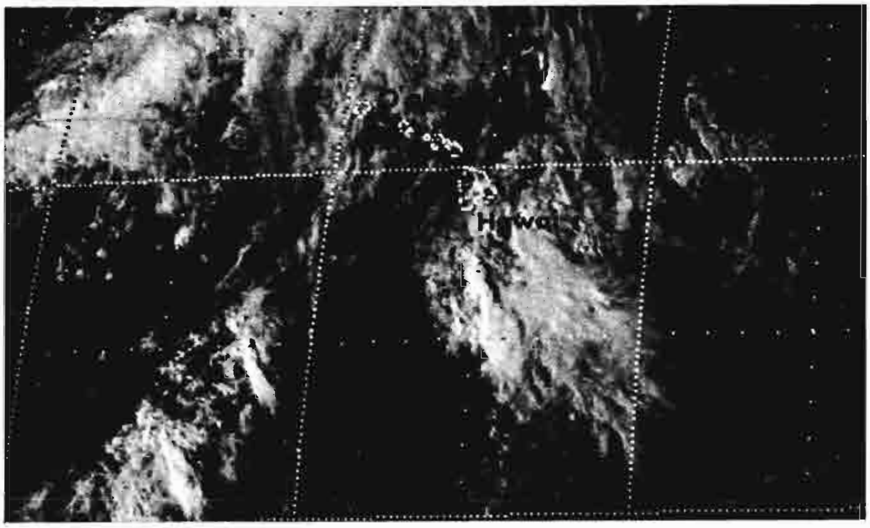

NOTE: An area of cumulonimbus cloud is south and southeast of Hawai'i Island.

PLATE 1. SMS-2 VISIBLE IMAGE FOR 1619 HR, 4 FEBRUARY 1976

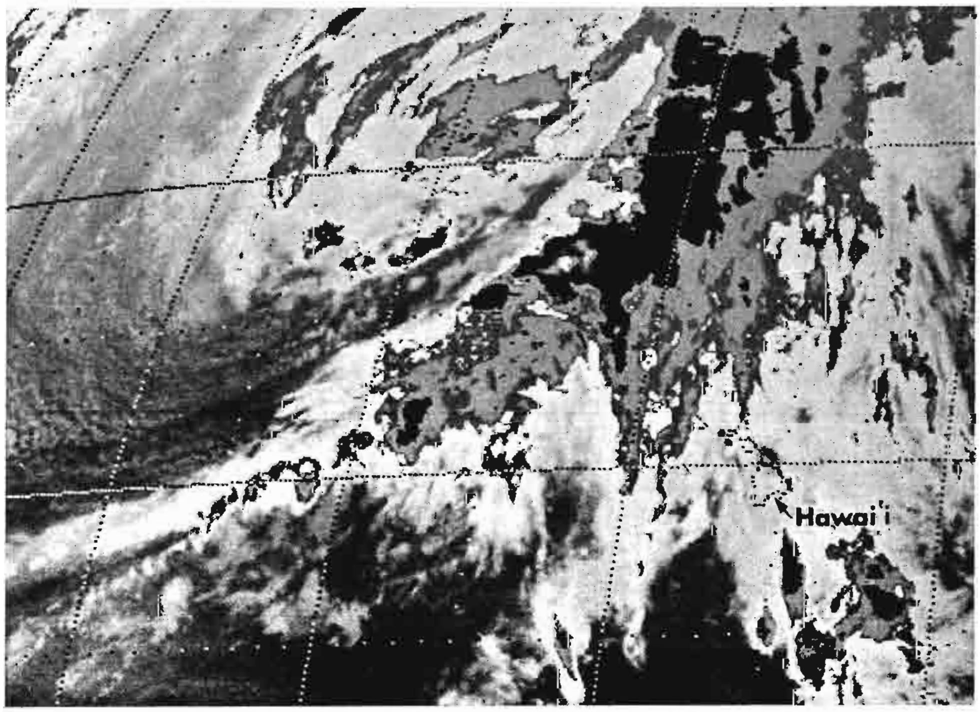

NOTE: A number of active cumulonimbi appear south and southeast of Hawai'i Island.

PLATE 2. ENHANCED INFRARED IMAGE (IR) FOR 1815 HR, 4 FEBRUARY 1976

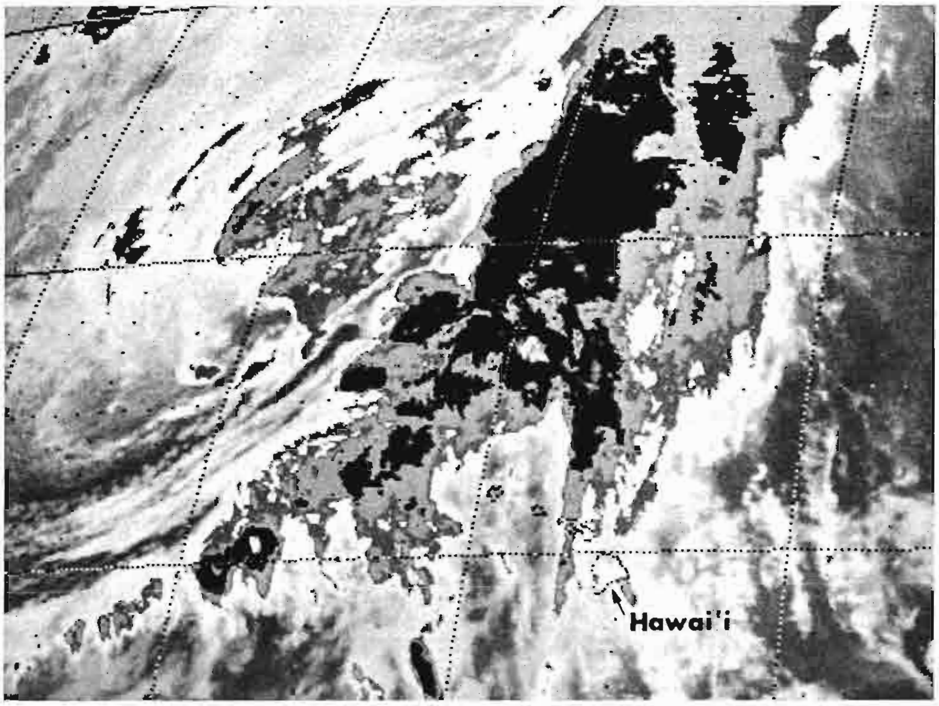

NOTE: One high cloud area is immediately southeast of Hawai'i Island.

PLATE 3. ENHANCED IR IMAGE FOR 0016 HR, 5 FEBRUARY 1976 SHOWING PERIOD OF HEAVIEST RAIN

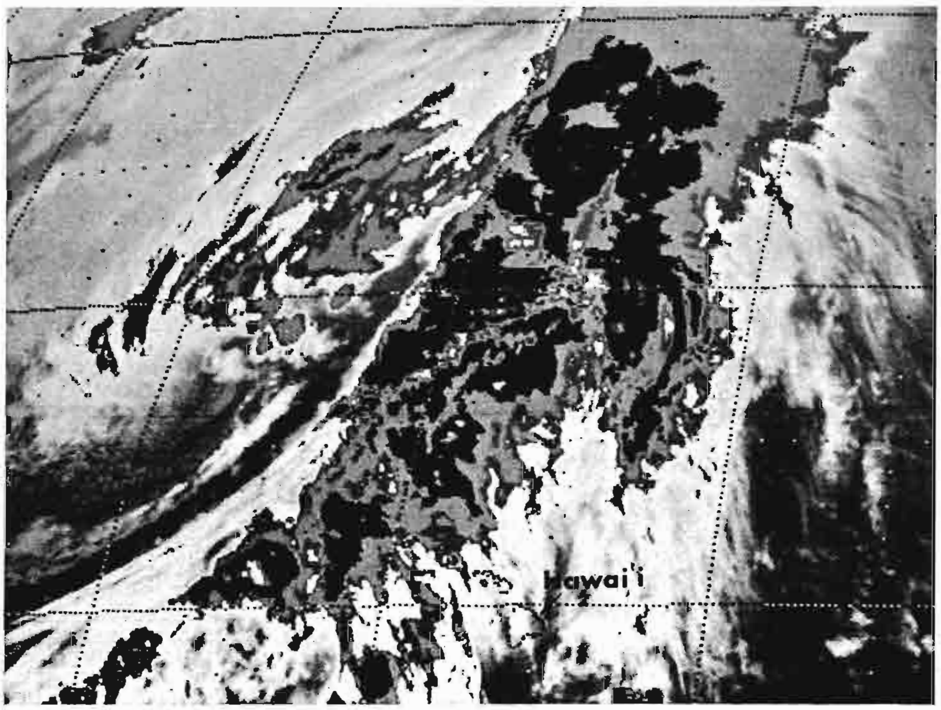

NOTE: No active tops are apparent near Hawai'i Island. Vigorous convection is occurring west and north of the state.

PLATE 4. ENHANCED IR IMAGE FOR 0615 HR, 5 FEBRUARY 1976

TABLE 1. WINDS ALOFT OVER HILO DURING PERIOD OF HEAVY RAINS IN KA'Ū AND PUNA, HAWAI'I ISLAND, 4-6 FEBRUARY 1976

Pressure (mb)		4 Feb. Speed (m/s)	4 Feb. Dir. (°)	1400 hr, 1976 5 Feb. Speed (m/s)	5 Feb. Dir. (°)	6 Feb. Speed (m/s)	6 Feb. Dir. (°)
-----	Surface	4	140	10	130	9	140
1 000	100	4	130	11	140	11	150
850	1 500	8	185	16	200	13	190
700	3 000	10	230	7	230	11	205

SUMMARY. Flooding in the Pāhala area of Hawai'i occurs frequently with southeasterly low-level flow. Orography produces rainfall maxima in the area between the rifts of Mauna Loa (south) and Kīlauea (east). The events of 4-5 February 1976 are interesting in that intense nonthundery rains occurred in an area far removed from the synoptic scale storm (which produced heavy rains in the northern islands). Radar (such as it was) reported no significant tops. Isolated thunderstorms, indicated by satellite imagery to the south of the island, may have moved over land. It seems likely that the principal cause of heavy rains was orography enhanced by increased instability in the prefrontal air mass.

6-8 February 1976

Significant rain occurred on O'ahu from 6-8 February due to the storm system mentioned above. Low-level southwesterly winds produced heaviest rains over the Wai'anae Range. Damage due to rain and wind totaled $250,000 to property and $500,000 to crops and livestock.

RAINFALL DATA. Rainfall data were taken from all rain gages published in *Hourly Precipitation Data* or *Climatological Data* as well as telemetered gages and U.S. Geological Survey gages in the leeward Wai'anae mountains.

Three bursts of rain occurred over O'ahu (Fig. 4). During the morning of 6 February thunderstorm activity covered all of O'ahu, diminishing in the afternoon. Heavy rain began early on 7 February over leeward O'ahu (see, e.g., Lualualei in Fig. 4), reaching highest intensity between 0600 and 0800 hr when 99 mm fell in Mākaha Valley (Fig. 5). A third widespread burst occurred during the evening of 7 February. The duration of the bursts is seen both from plots of hourly rainfall amounts (Fig. 4) and tabulation of consecutive hours of rain (Table 2, p. 15).

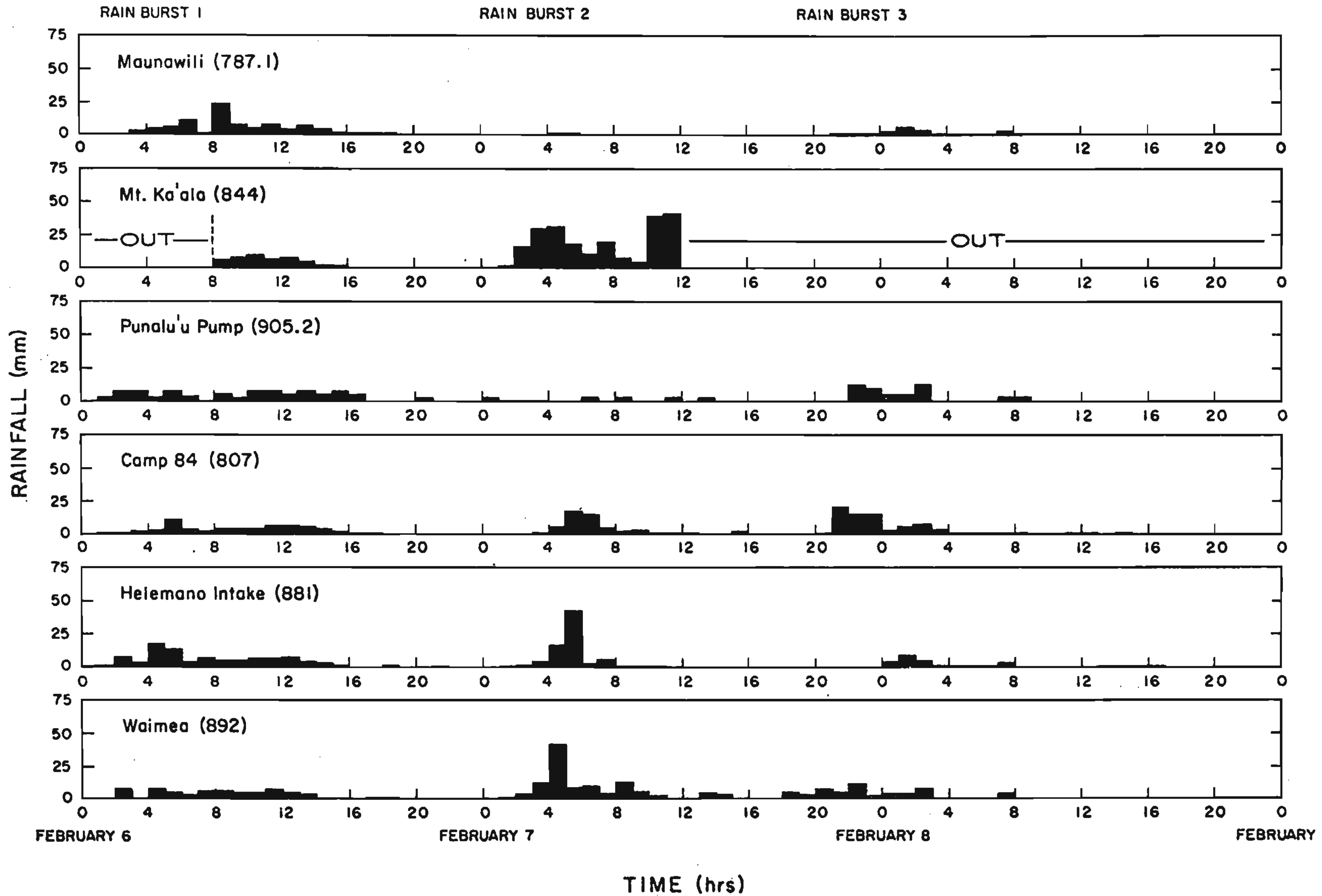

FIGURE 4. HOURLY RAINFALL FOR 18 GAGES ON O'AHU, 4-7 FEBRUARY 1976

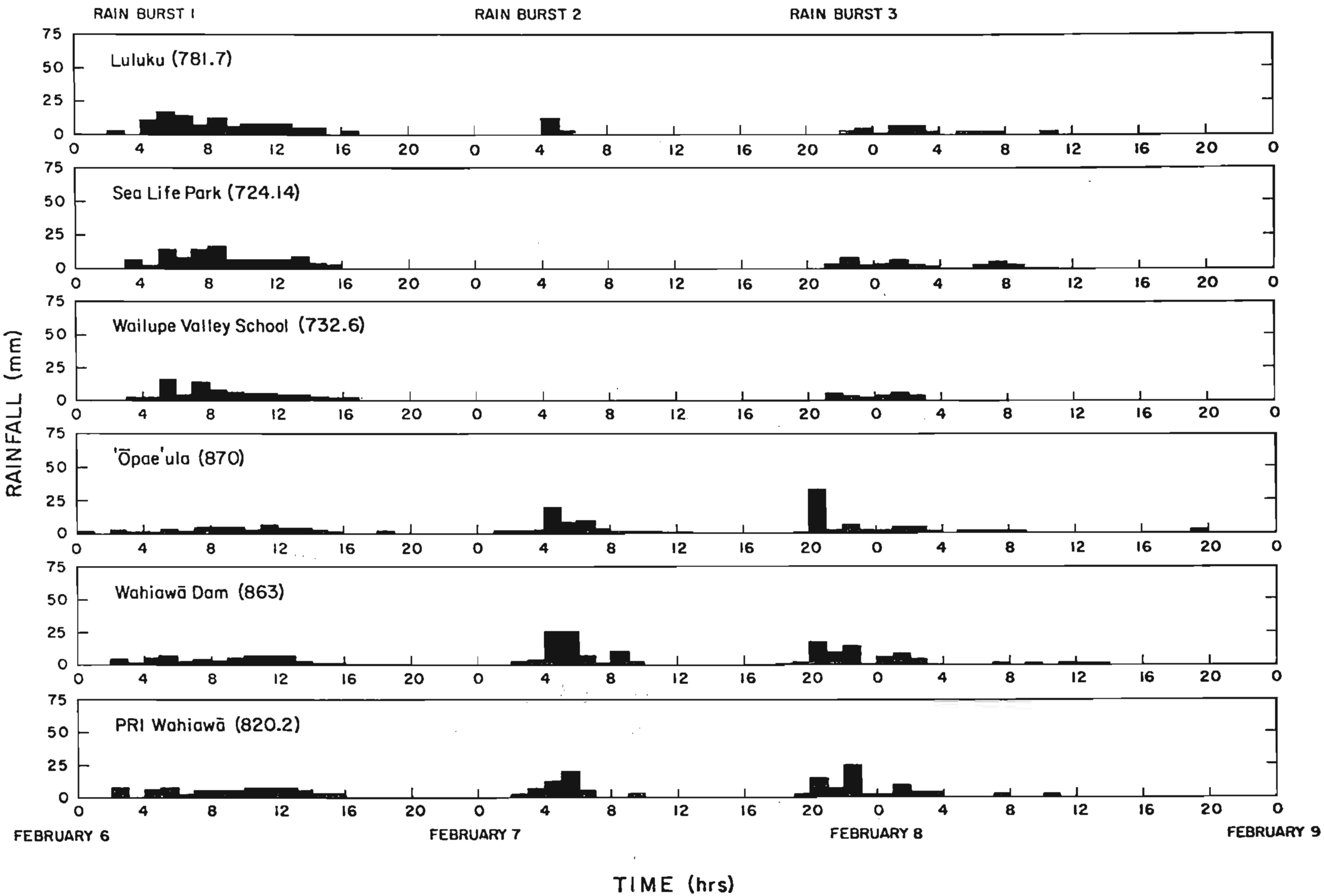

FIGURE 4.—*Continued*

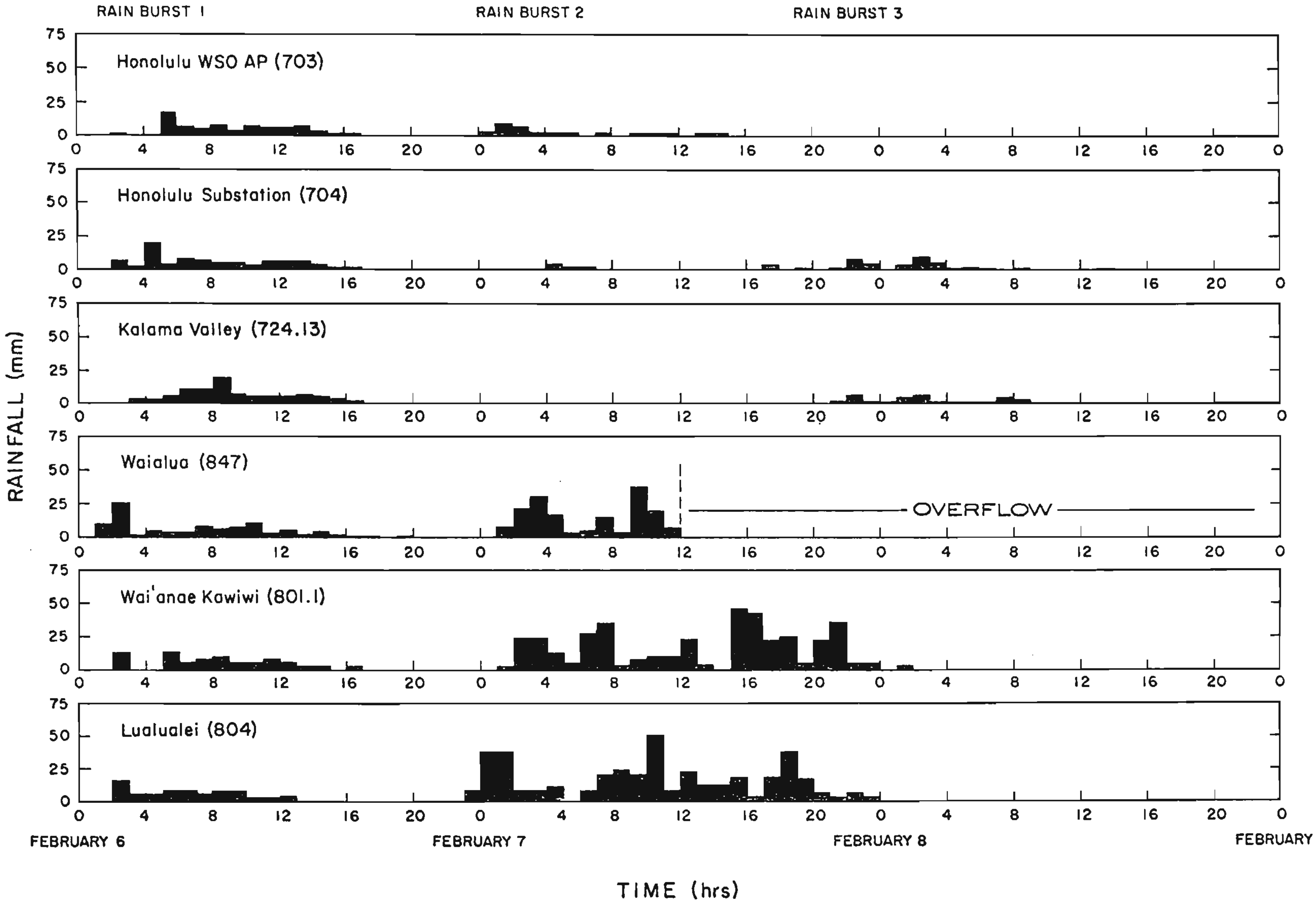

FIGURE 4.—*Continued*

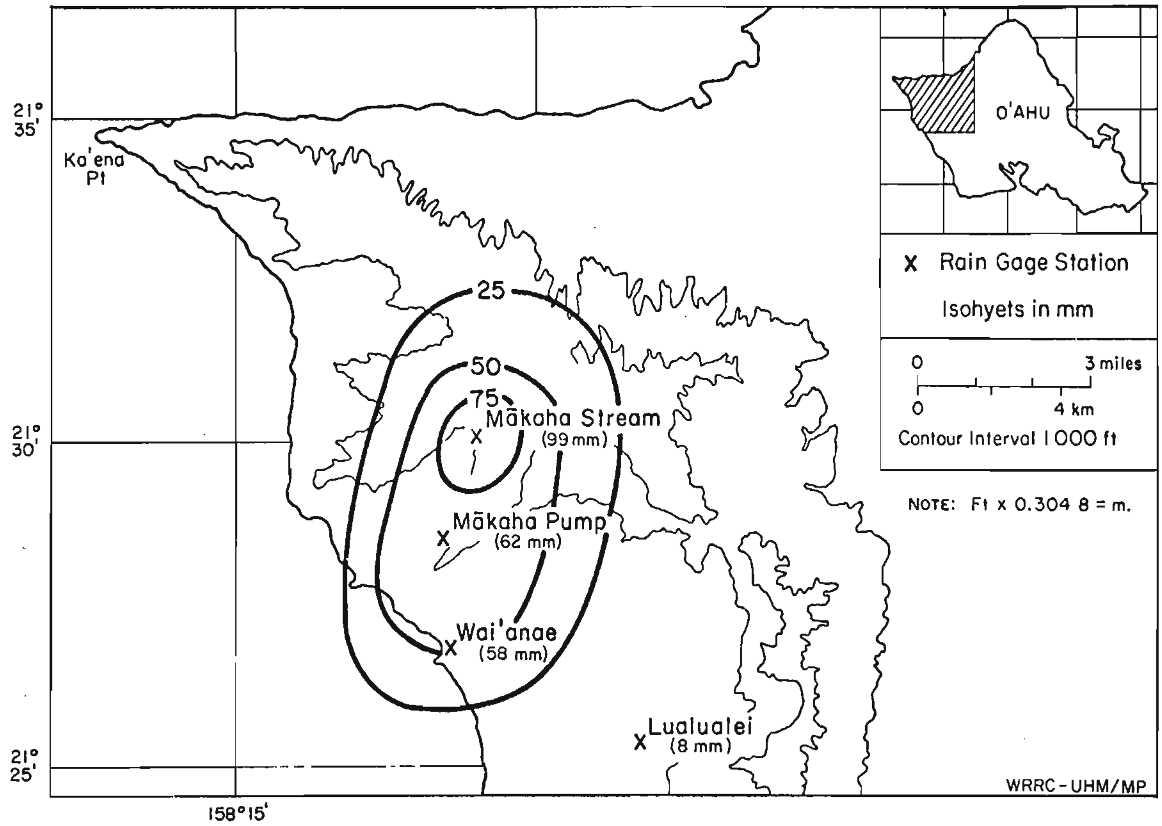

FIGURE 5. GREATEST 1-HR RAIN BETWEEN 0600 AND 0800 HR, 7 FEBRUARY 1976, LEEWARD AREA, O'AHU, HAWAI'I

With the exception of the extreme rainfall episode between 0600 and 0800 hr, 7 February rainfall intensities were considerably less than those of the 19 April 1974 record O'ahu flood (Schroeder 1976). Twenty-four-hr analyses show that areal distributions also differed from the record flood of 1974. For the 24 hr ending at 0800 hr 7 February, all available O'ahu gages recorded at least 50 mm of rain with 200 mm maximum over the Wai'anae Range (Fig. 6). The next day (Fig. 7) the maximum remained in the same location, but accumulations were greater over much of the leeward area while southern and eastern portions of O'ahu were relatively dry. The large gradient across central O'ahu is supported by ground-based (author's) and satellite observations of the location of precipating clouds on 7 February.

SATELLITE IMAGERY. One SMS-2 picture has been selected to typify conditions during each of the bursts. Vigorous convection on the morning of 6 February was evidenced by numerous cloud tops above 14 000 m over O'ahu and surrounding waters (Pl. 5). In the early morning of 7 February, tops were

TABLE 2. CONSECUTIVE HOURS OF MEASURED RAINFALL AT SELECTED O'AHU STATIONS FOR THE THREE RAIN BURSTS OF 6 TO 8 FEBRUARY 1976

STATION		RAIN BURSTS		
		1	2	3
Name	No.	02/6	02/7	02/7-8
Camp 84	807	16	10	13
Helemano Intake	881	18	10	14
Hokuloa	725.2	13	10*	--
Honolulu Airport	703	12	0	13
Kailua Fire Station	791.3	15	0	16
Kalama Valley	724.13	14	0	14
Mākaha Pump	800.2	12	17†	--
Maunawili	787.1	16	0	15
Momilani	835.1	13	8	14
'Ōpae'ula	870	15	12	13‡
Sea Life Park	724.14	13	0	14
Wahiawā Dam	863	18	9	14
Wailupe Valley Sch.	723.6	14	0	15

NOTE: Fischer-Porter gages not included, although one of these (Lualualei [804]) recorded 23 hr of rain on 7 February 1976.
*Out; overflow.
†Out.
‡13 of 14.

below 12 000 m over O'ahu (Pl. 6) though rainfall rates on leeward O'ahu attained their storm maxima (Fig. 5). The third burst was characterized by development of a broad area of 12 000-m high clouds which moved over O'ahu (Pl. 7). There was little, if any, thunder associated with the second and third bursts of activity.

Radar estimates of cloud tops were 10 000 m for the morning of 6 February (burst 1), 9 000 m for burst 2 (early 7 February), and 8 000 m for the evening of 7 February (burst 3). Considering the nonmeteorological nature of the radars (wavelengths ∿20 cm), it is no surprise to find such a discrepancy between radar and satellite estimates of cloud tops.

Gridding accuracy of the enhanced infrared pictures is a problem. During intense winter storms copious cirrus clouds cover the islands so that landmarks normally used in gridding are unavailable. Acceptable gridding

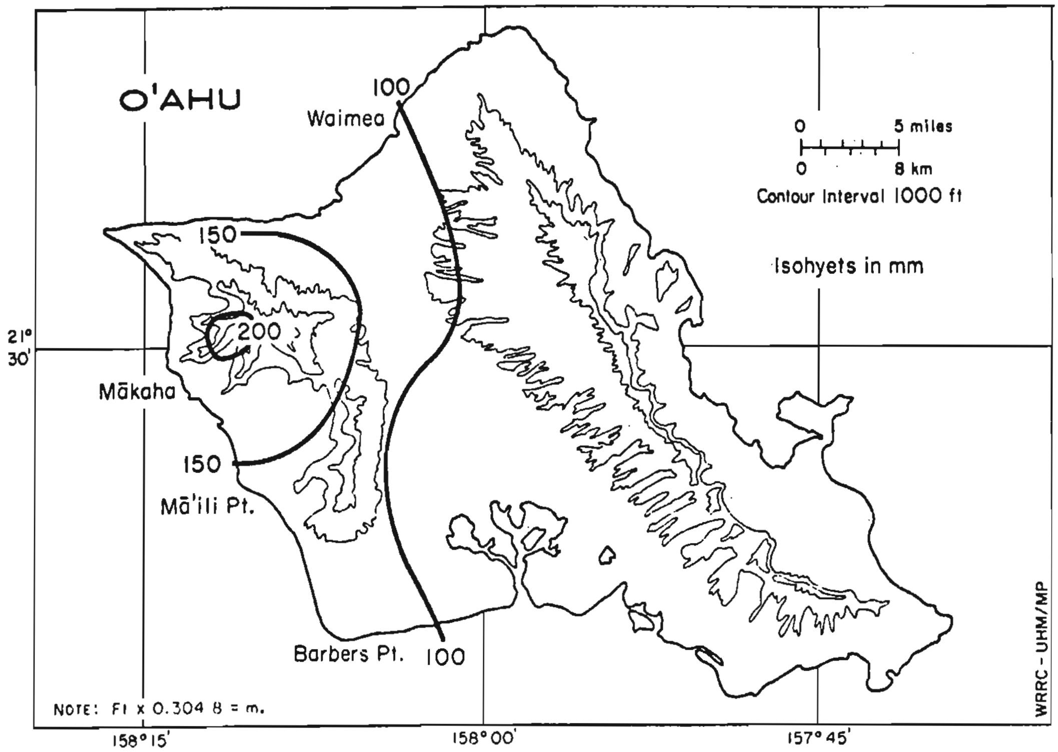

FIGURE 6. 24-HR RAINFALL OVER O'AHU FOR PERIOD ENDING 0800 HR, 7 FEBRUARY 1976

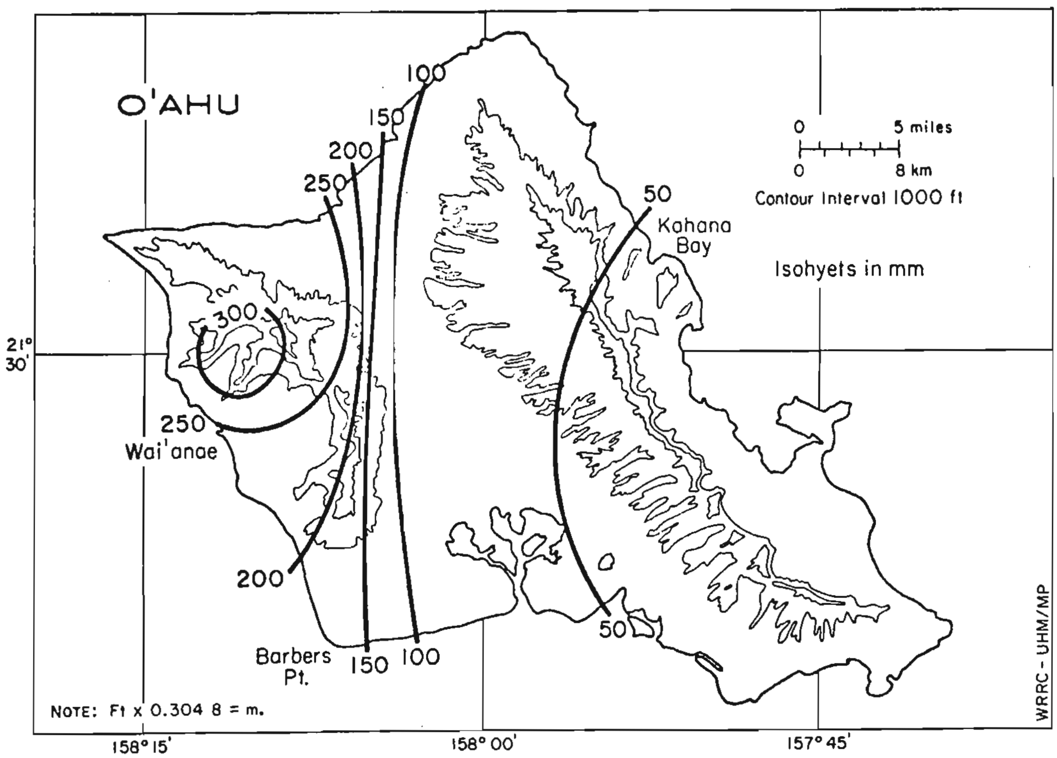

FIGURE 7. 24-HR RAINFALL OVER O'AHU FOR 0800 HR, 7 FEBRUARY TO 0800 HR, 8 FEBRUARY 1976

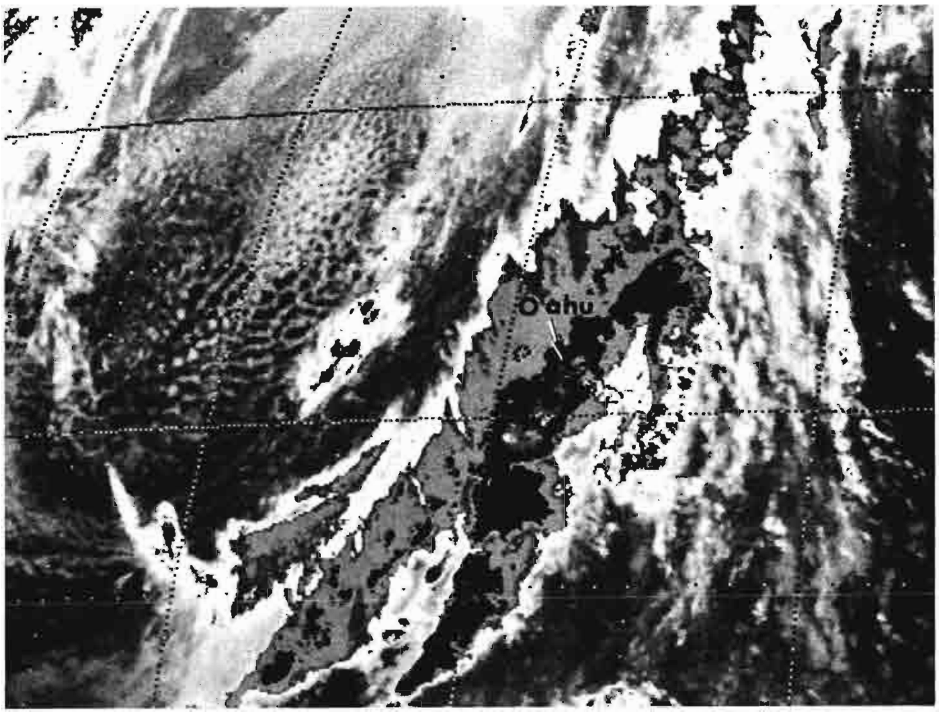

PLATE 5. SMS-2 ENHANCED IR IMAGE FOR 1015 HR, 6 FEBRUARY 1976 (O'AHU "BURST" 1)

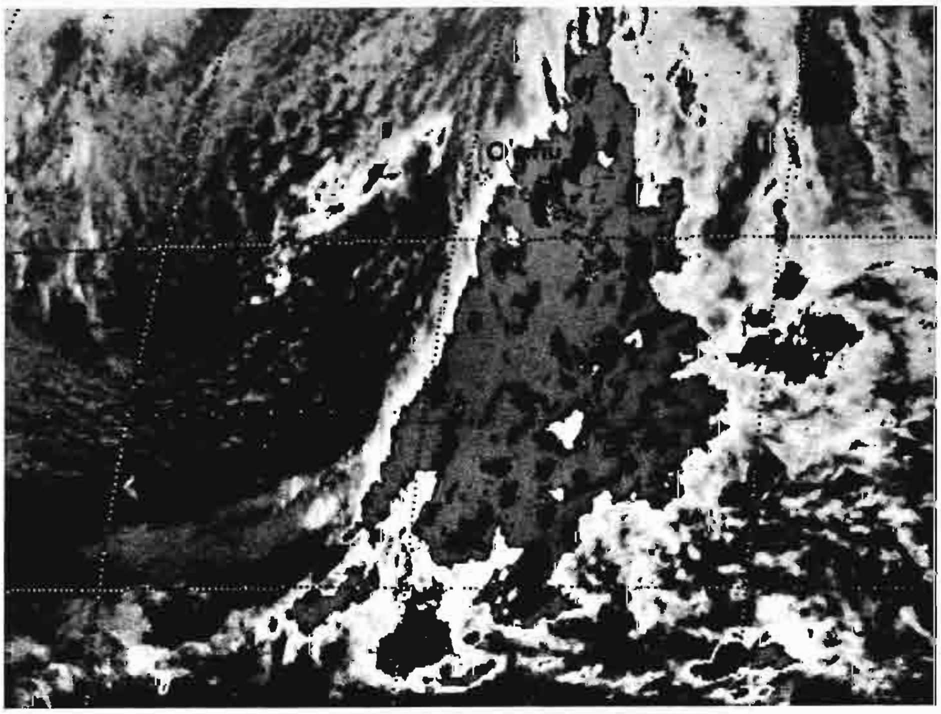

PLATE 6. SMS-2 ENHANCED IR IMAGE FOR 0615 HR, 7 FEBRUARY 1976 (O'AHU "BURST" 2)

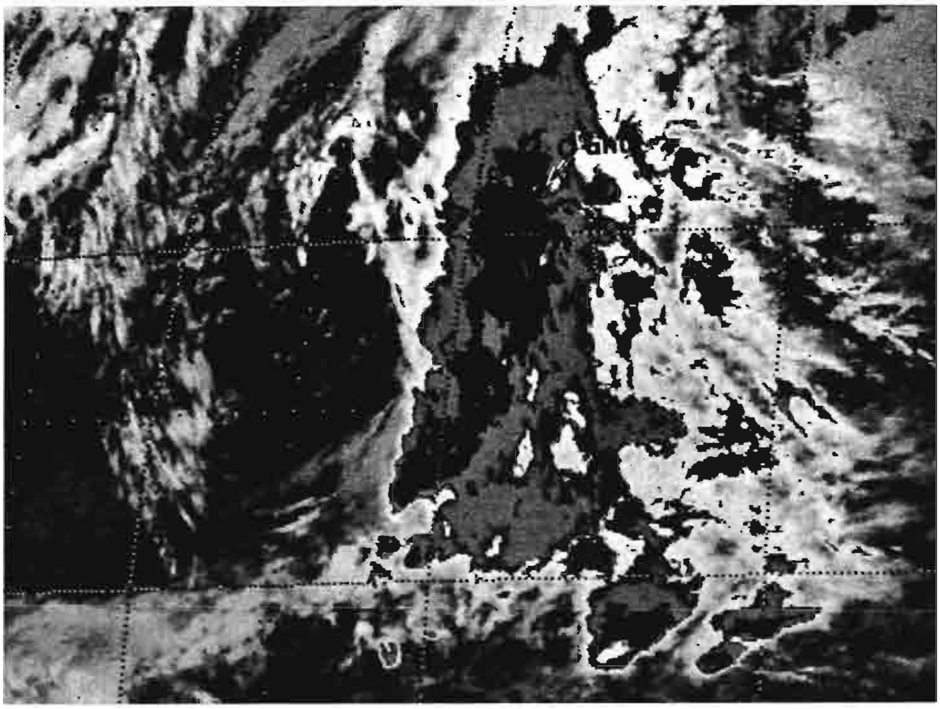

PLATE 7. SMS-2 ENHANCED IR IMAGE FOR 2115 HR, 7 FEBRUARY 1976 (O'AHU "BURST" 3)

accuracy is 35 000 m (NOAA 1976). In the case of an island the size of O'ahu this can be the difference between placing a line of precipitating clouds over the island or not. For the morning of 7 February the shower line extended inland only 30 000 m. This fact is confirmed by visual observations, radar reports, and rain gage data (Fig. 7).

LOW-LEVEL WINDS. Winds were south-southwesterly over O'ahu during the storm period. Līhu'e winds (Table 3) support this except for the afternoon of 6 February when the surface front had moved past Līhu'e, resulting in north-northeasterly winds. Strong winds caused damage on Kaua'i and O'ahu on 5 February. Līhu'e 3 000-m winds were 34 m/s. At Ka'ena Point, O'ahu, hourly mean winds reached 34 m/s on the afternoon of 5 February.

South-southwesterly winds result in orographic augmentation of rain on what normally are leeward areas of O'ahu. On the mesoscale the valleys of Wai'anae coast can serve as convergence centers similar to the southeast Mauna Loa features described previously. For each day of heavy rains the maximum rain fell over Mākaha Valley. On the day of heaviest rain, 7 February, a line of convective cells lay over Mākaha, and the torrential rains resulted from the interaction of the line of convective cells with the local topography.

TABLE 3. WINDS ALOFT OVER LĪHU'E, KAUA'I, DURING HEAVY RAIN PERIOD ON O'AHU, FEBRUARY 1976

Pressure (mb)	Elevation (m)	1400 hr 4 Feb. Speed (m/s)	Dir. (°)	1400 hr 5 Feb. Speed (m/s)	Dir. (°)	1400 hr 6 Feb. Speed (m/s)	Dir. (°)	1400 hr 7 Feb. Speed (m/s)	Dir. (°)
-----	surface	8	190	12	210	1	20	3	240
1 000	100	9	190	14	210	2	45	5	230
850	1 500	13	230	21	190	4	215	20	170
700	3 000	20	230	34	205	16	220	13	175

STABILITY ANALYSIS. A number of conventional stability indices were prepared for the Līhu'e soundings of 4 February through 7 February (Table 4).

TABLE 4. STABILITY PARAMETERS FOR LĪHU'E, KAUA'I, SOUNDINGS DURING HEAVY RAIN PERIOD ON O'AHU, FEBRUARY 1976

INDEX	STABILITY PARAMETERS 1400 hr, 1976 4 Feb.	5 Feb.	6 Feb.	7 Feb.
Showalter	+5.0	-2.1	+1.2	+2.5
K	5.5	37.6	33.6	32.0
Total Totals	40.4	51.4	43.7	44.7
SWEAT	297	507	212	230

Each index attained the most unstable value on the afternoon of 5 February. The SWEAT index (Miller 1972) reflects thermodynamic and shearing instabilities. The value of SWEAT for 5 February exceeded that of all documented tornado outbreaks for Hawai'i (Schroeder 1977). The "Total Totals" index (Miller 1972) of 51.4°C translates as possible isolated tornadoes or waterspouts. K (George 1960) infers an 80% chance of thunderstorms. It is interesting that, as the rains set in, the Līhu'e air mass became more stable.

SUMMARY. Heavy rains resulted from the interaction of topographic features with a prefrontal zone. Conventional stability analysis showed that stability increased as the rains set in. This was confirmed by radar data (nonmeteorological), satellite cloud-top estimates, and ground-based observations. Heaviest rains fell on 7 February, one day after significant thunderstorm activity and tallest cloud development over O'ahu. The clouds of 7 February were at the threshold of thunderstorm size, yet produced much greater rains probably due to orographic enhancement of low-level convergence over the Wai'anae Range.

26 April 1976

This was a localized event. Damage occurred in the vicinity of Hōnaunau on Hawai'i's Kona coast where a blocked drainage culvert produced washouts of the main highway, caused water damage to several buildings, and disinterred numerous corpses in a graveyard. Because this event went completely undetected by existing meteorological networks and represents the extreme of small-scale floods, which are particularly frequent over the Kona slopes, it was chosen for analysis.

RAINFALL DATA. Rainfall data were collected for available stations in the Hōnaunau area as well as stations representative of other sea breeze regimes on Hawai'i (Fig. 8). The official Hōnaunau gage was not read the morning of the flood so the two-day total (151 mm) was prorated according to totals of a nearby private gage (G. Steffen, Hōnaunau). The Steffen gage recorded 78 mm in 90 min. Apparently at least 100 mm fell further upslope.

SATELLITE IMAGERY AND SOUNDINGS. Satellite imagery (Pl. 8-10), as well as movie loops, indicated light easterly drift at low levels, becoming calm near the islands. A weak frontal remnant lay north of the islands and an upper level jet stream axis south of the islands. A weak disturbance had cleared Hawai'i early on 26 April 1976 as shown by drying of the Hilo sounding between 0200 (Fig. 9) and 1400 hr (Fig. 10).

Sea breeze developed on all coasts in the early morning (Pl. 8). By 1645 hr the island was completely obscured by cloud (Pl. 9). Jet stream cirrus had overrun the southern cape, and a peculiar northwest-southeast cloud band had developed along the Kona coast. Individual cumulus elements could be seen along the coast. By 1745 hr (Pl. 10) as the sun was sinking, a tall cloud element cast a long shadow on surrounding altostratus which covered the summits of the major peaks (4 200 m). A computation based on solar elevation and measured cloud shadow indicated that, since this cloud towered 4 200 m above the surrounding cloud field, its top must have reached 8 400 m. It was located over the flood area.

SUMMARY. Damage reports in local newspapers gave the first inkling of a flash flood. National Weather Service had no concrete evidence other than

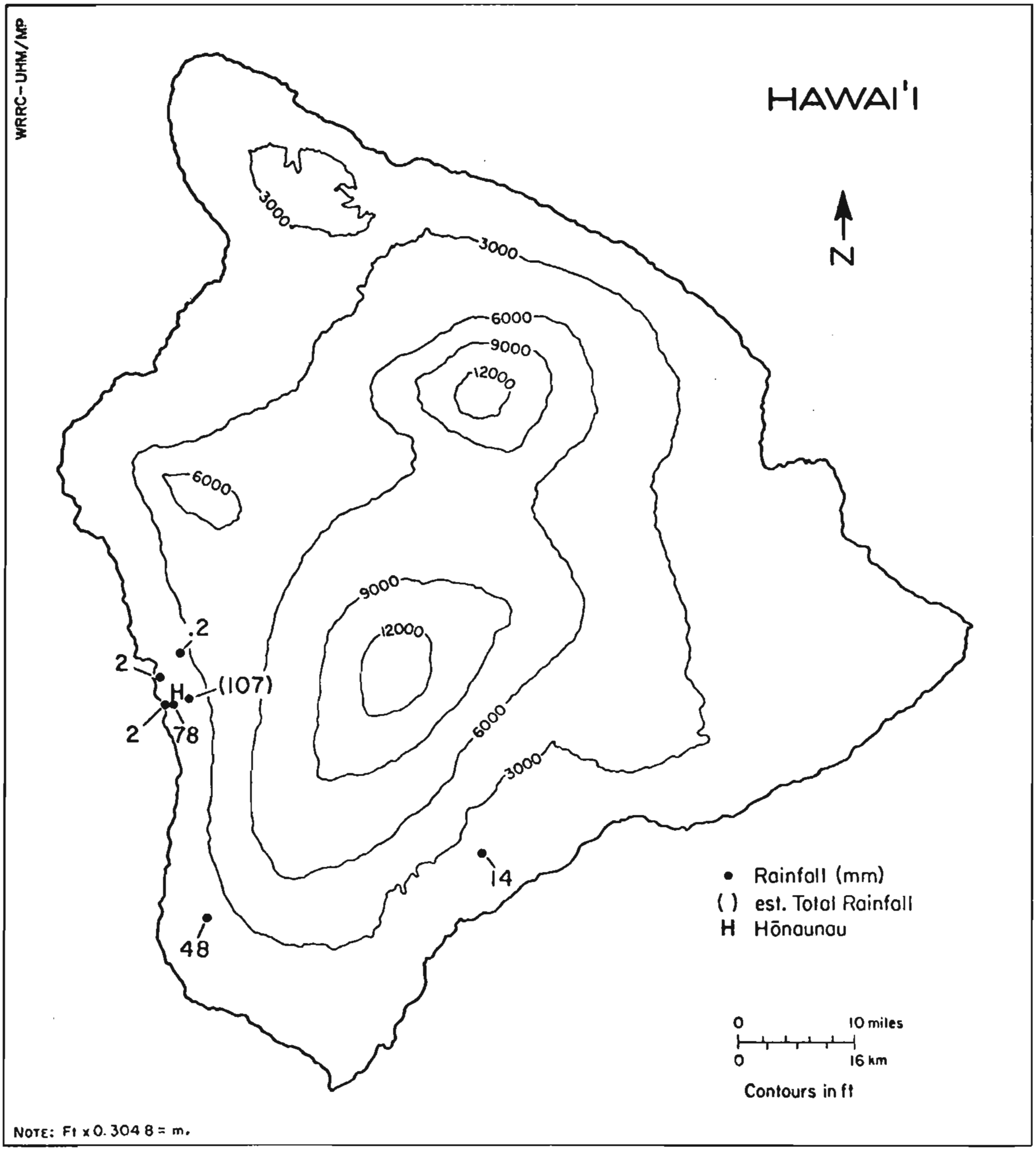

FIGURE 8. 24-HR RAINFALL OVER SELECTED HAWAI'I ISLAND STATIONS FOR 0800 HR, 26 APRIL TO 0800 HR, 27 APRIL 1976

the 2-day rainfall accumulation at the official Hōnaunau rain gage. The isolated turret over Hōnaunau was discovered in the satellite record *one week* after the event. The utility of the satellite pictures on 26 April would have been questionable; the first clue appeared at 1745 hr, well into the event. I believe that *no conceivable detection system in the state of Hawai'i could have given adequate warning.*

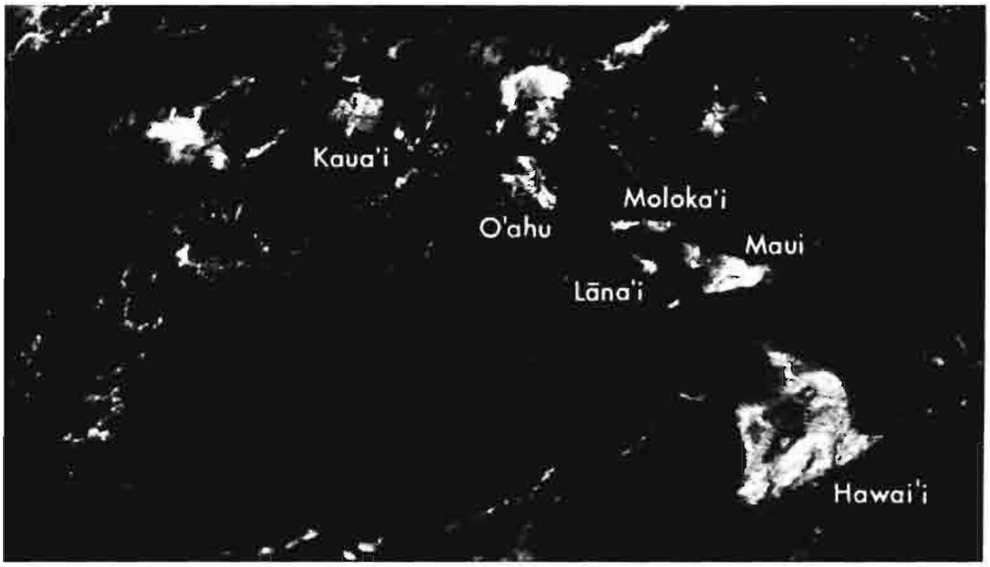

PLATE 8. SMS-2 VISIBLE IMAGE (1-KM RESOLUTION) OF HAWAIIAN ISLANDS AT 1045 HR, 26 APRIL 1976

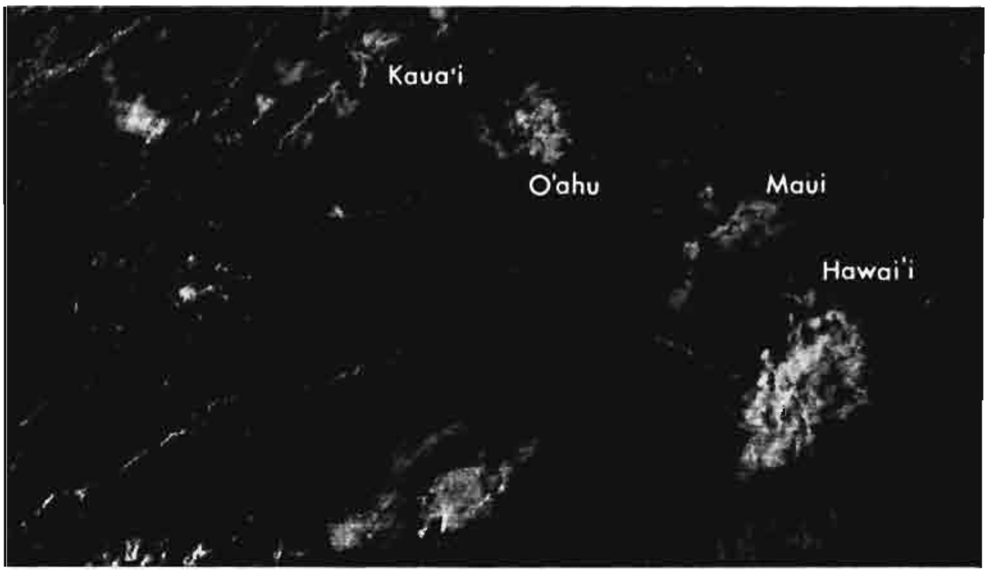

NOTE: A narrow cloud band appears off Hawai'i Island's west coast. The major volcanoes are clouded in.

PLATE 9. SMS-2 VISIBLE IMAGE (1-KM RESOLUTION) AT 1645 HR, 26 APRIL 1976

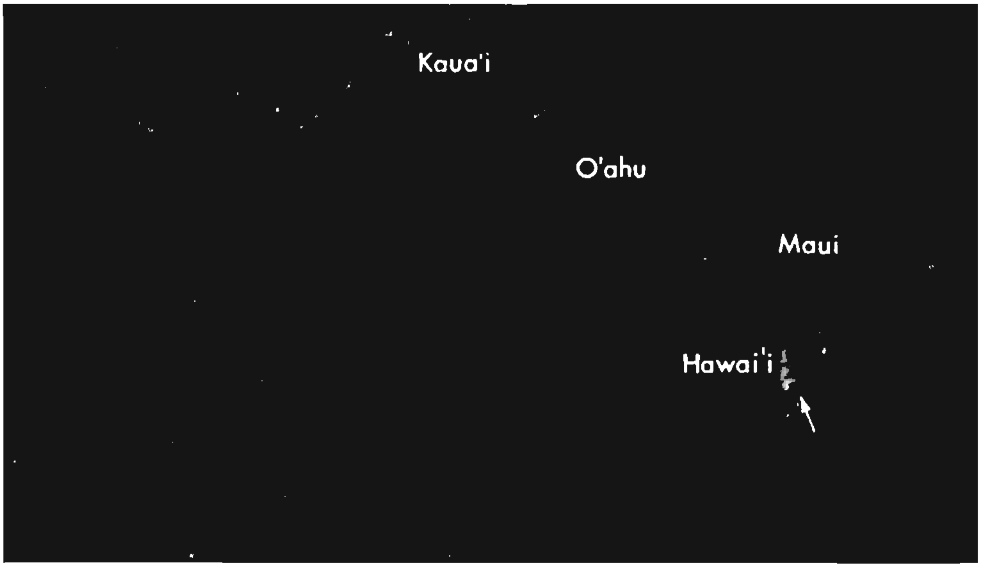

NOTE: An isolated bright top is casting a shadow. Heavy cloud to the south of Hawai'i Island is jet stream cirrus.

PLATE 10. SMS-2 VISIBLE IMAGE (1-KM RESOLUTION) AT 1745 HR, 26 APRIL 1976

The trigger for development of an isolated 8 000-m tall cloud over Hōnaunau is not readily apparent. Hilo soundings indicate that stability was increasing over the island on the afternoon of 26 April. Considerable drying had occurred through all layers. It may be that residual moisture from the passing disturbance of early morning had remained in Kona. Development of cloud covering Mauna Loa and Mauna Kea summits implies more instability than detected by the Hilo soundings. Absence of strong trade winds precluded an interaction between trade winds and sea breeze on the Kona slopes as postulated by Leopold (1949). Leopold attributed heavy rains on the Kona slopes to enhanced convergence between the sea breeze and strong trades funneled through the saddle between Mauna Loa and Mauna Kea and deflected south of Hualālai. The peculiar cloud band which appeared off the coast may represent a traveling disturbance. The origin of the band is unclear, but it may be related to numerous "arc clouds" which formed at the frontal remnant north of the islands. These arcs have been observed to move ahead of frontal zones and convective regions. It appears that the best explanation, in the absence of in situ observations, is that instability in the air mass over Kona was released in concert with a very small-scale convergence line (arc).

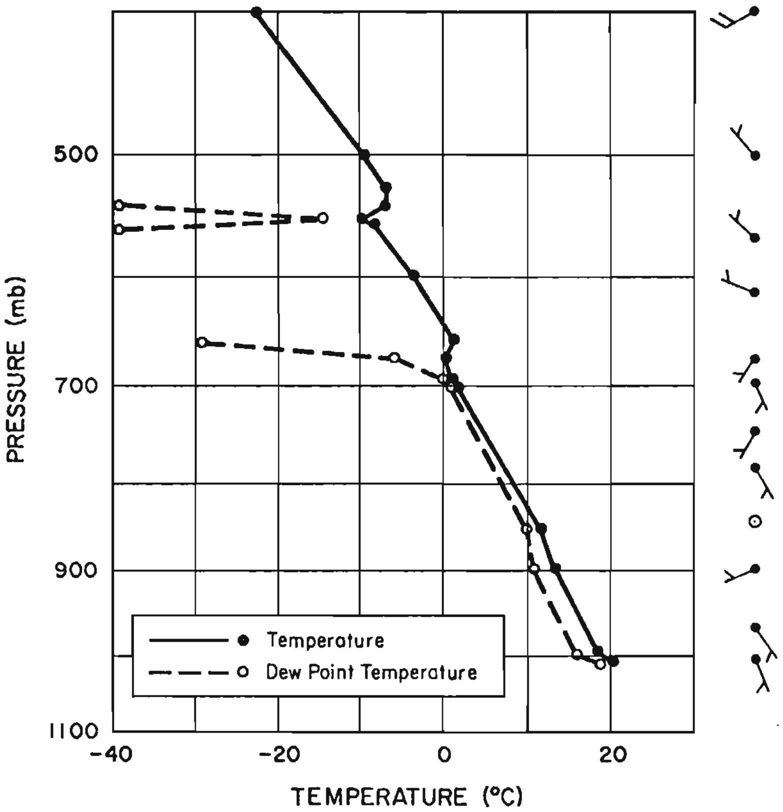

FIGURE 9. HILO SOUNDING FOR 0200 HR, 26 APRIL 1976

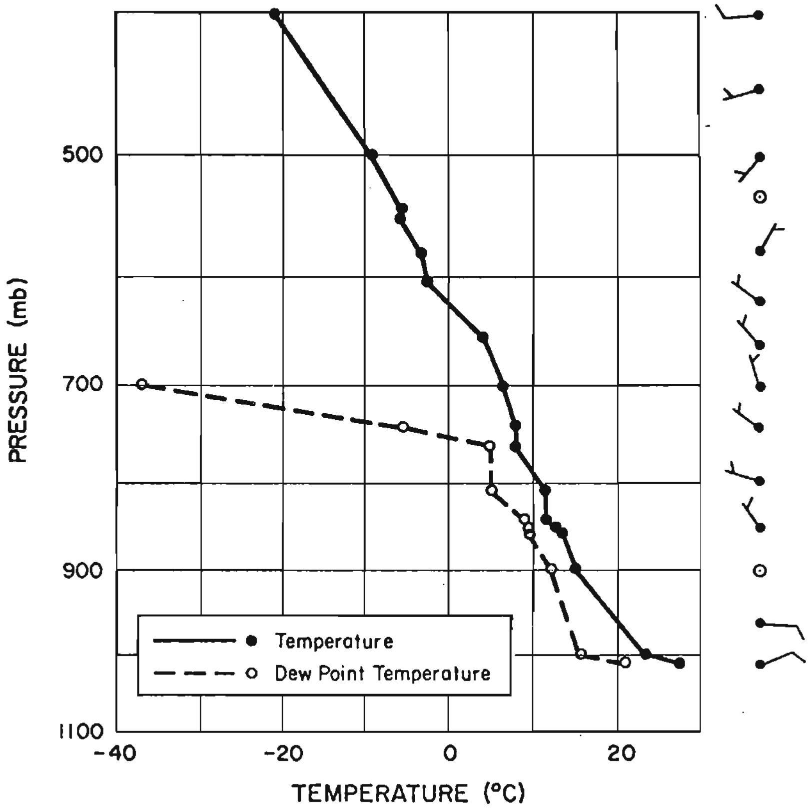

FIGURE 10. HILO SOUNDING FOR 1400 HR, 26 APRIL 1976

SYNOPTIC FEATURES ASSOCIATED WITH FLASH FLOODS

Maddox and Chappell (1978) identified meteorological conditions associated with major flash floods in the continental U.S. Similar studies 30 yr ago led to the development of operational severe storm (tornado) forecasting (Fawbush et al, 1951; Showalter and Fulks 1943). In their preliminary study Maddox and Chappell grouped synoptic situations into five categories, which in turn shared nine characteristics:

1. Convective storms produced the flood rains
2. Storms occurred in regions of high surface dew point temperature
3. Relatively high moisture contents were present through a deep tropospheric layer
4. Weak vertical shear of the horizontal wind was present through the cloud depth
5. Convective storms and/or cells formed repeatedly over the same area
6. The storm area was very near the large-scale ridge position
7. A weak short-wave trough helped to destabilize, trigger, and focus the storms
8. Storms often occurred during the night
9. Severe thunderstorm phenomena (hail, tornadoes, damaging winds) were usually absent in the heavy rain area.

Seven years earlier Ramage (1971) summarized conditions associated with torrential rains in monsoon regions. Specifically, the storms

1. Are associated with synoptic scale disturbances
2. Draw on a plentiful supply of moisture either along a coast or from a flooded river plain
3. Are usually anchored by a discontinuity in surface roughness, such as a coastline or mountain range.

Hawaiian studies (Schroeder 1977, 1978) have in general supported the Ramage conclusions.

The conclusions of Maddox and Chappell (1978) and Ramage (1971) do not differ in any significant fashion. A favorable synoptic environment must be present; then local influences, such as orography or differential heating, determine the location and duration of heavy rains. Maddox and Chappell did find that anchoring of rain cells could result from such diverse causes as stationary frontal systems and mesoscale high pressure areas, e.g., Kansas

City flood of 12 September 1977.

The consistent feature of major Hawaiian floods is the interaction of low-level winds with topography. Under unstable conditions, areas of orographic uplift and local convergence, such as a wide valley, become preferred regions for updrafts. The migration of individual rain cells depends on the nature of horizontal winds through the cloud-bearing layer. Satellite data indicate that a sequence of convective elements moved over the Wai'anae coast of O'ahu on 7 February 1976 when cloud-layer winds were nearly uniformly south-southwesterly. In contrast, the record rains of 19 April 1974 resulted from weak winds and little cell movement.

The discussion above presents a rather simple picture of the synoptic environment of flood-producing systems. Unfortunately, conditions frequently occur which favor major rainstorms with no such result. Furthermore, events such as that of 26 April 1976 defy the forecast rules. The logical approach to genuine alleviation of the flash flood problem lies in improved detection and warning capabilities. The authors of the Johnstown disaster report (NOAA 1977*a*) acknowledge the existing inability to forecast large convective rainstorms. Ramage (1976, 1978*a*), in his provocative articles on the outlook for forecasting, advocates emphasis on development of detection abilities. Recent developments in airport weather service (Beran et al. 1977) are directed at detection. In the following section evaluation of the future of monitoring of flash flood rainfalls is presented.

TECHNIQUES FOR DETECTION OF HEAVY RAINS

Radar

Rainfall intensity can be estimated from radar through use of an expression of the form

$$Z = AR^b \tag{1}$$

where A and b are empirical constants, Z is the radar reflectivity factor, and R is rainfall rate. Since $Z = \Sigma D^6$ where D is drop size diameter, it follows that Z can be related to volume of water (liquid water content) and to rainfall rate. An equation of the form (1) given above defines a Z-R relation. Empirical Z-R relations are derived by using radar with a network of recording rain gages.

Z-R relations have been found to exhibit considerable variability with locale and type of rainfall. Battan (1973) lists 69 different *Z-R* equations of which three apply to Hawai'i Island (Blanchard 1953). Nevertheless, most equations produce similar rainfall rate estimates in the important range between 20 and 200 mm/hr (Battan 1973).

Eccles (1978) compared integrated rainfall estimates based on *Z-R* with weighing gage totals for a dense network in the National Hail Research Experiment (NHRE) network. Examining 12 serious storms, he found that rainfall estimates differed by a factor of at least 2.5 in 42% of the cases. Greene and Saffle (1978) showed that radar-derived rainfalls varied from gage totals by 50% in the Johnstown, Pennsylvania, flood of 19 July 1977.

Interpretation of radar data is very important to analysis of flood-producing systems. In the case of the Big Thompson flood, confusion arose in that high thunderstorm tops did not correspond to high radar reflectivities (NOAA 1976). Maddox et al. (1977) found that this was due to dominance by coalescence processes (*warm rain*) in the lower portion of the cloud and that, in fact, the echo structure of the Big Thompson storm resembled that of a monsoon thunderstorm. A warm rain mechanism may explain the production of prodigious rain totals from nonsevere (in conventional usage, severe = hail, tornado, winds) thunderstorms.

In spite of the uncertainties of rainfall estimation, radar provides high resolution coverage over large areas. Furthermore, in instances of radar-rain gage disagreements, radar estimates were still adequate to indicate flood potential. Unfortunately, the above discussion will prove of little use *in the Hawaiian situation since weather radar is unavailable and not likely to become available.*

Telemetered Rain Gages

The National Weather Service maintains 23 telemetered rain gages on the island of O'ahu (Haraguchi 1977) as well as a few on the neighbor islands. Newer telemetered gages are being developed (Burnash and Twedt 1978) and, based on comments by participants at the Conference on Flash Floods: Hydrometeorological Aspects (Los Angeles, California, 2-3 May 1978), are enthusiastically hailed as *solutions* to the flash flood warning problem. This is unfortunate.

Time and space scales of convective precipitation limit the usefulness of telemetered rain gage data. Let us examine the O'ahu network as it would have performed during the record flash flood of 19 April 1974. There were two centers of flooding: one on the north shore at Hale'iwa and one along Moanalua Stream near Honolulu. There would have been no telemetered gage in the rainfall area of Moanalua Stream. Furthermore, an independent network of seven recording gages in Moanalua Valley showed nearly 100% variation of 3-hr totals within a distance of 2 000 m (Schroeder 1977). On 7 February 1976 the heaviest rains on leeward O'ahu fell well away from any telemetered gage (Fig. 5).

I believe the utility of telemetered gages could best be summed as (1) they are extremely useful as a source of point rainfall data and (2) in flood conditions they are useful as long as the storm happens to be directly over the gage. In a more general sense they aid in determining general geographical distribution of movement of rain areas.

Satellite

Satellites have made a substantial impact on certain phases of meteorology. The impact of satellite imagery on the daily weather forecast has not been well documented (Ramage 1978*b*), but weather depiction in the Hawaiian region has definitely improved. A geostationary satellite such as SMS-2 provides 24-hr coverage, allowing monitoring of development of convective systems responsible for flood rainfalls. The utility of SMS-2 imagery in analyses of flood situations has already been shown. I shall now discuss efforts at using the satellite as pseudo-radar to estimate rainfall intensity.

A variety of techniques has been developed for rainfall estimation using satellites. For monthly and annual time scales, Kilonsky and Ramage (1976) found useful a relationship between monthly rainfall and areal coverage by highly reflective (cumulonimbus) clouds over tropical oceans. Rao and Theon (1977) used the microwave scanning capability of NIMBUS-5 satellite to prepare global rainfall maps. The above techniques require one image per day over any area; thus, polar-orbiting satellites are ideal.

Two similar techniques have been developed for estimation of convective rainfall using data from geostationary satellites (Scofield and Oliver 1977; Woodley et al. 1978; Griffith et al. 1976). Both techniques depend on properties of convective clouds discovered during studies of tropical systems over South Florida (Woodley, Sancho, and Miller 1972). Properties of cumulonimbus anvils are determined from enhanced IR images; and rainfall production is estimated based, among other items, upon:

1. Life cycles of overshooting tops
2. Growth rates of anvils
3. Cloud-top geometry related to wind shear.

The Woodley technique is especially promising in that it was developed in the tropics; radar and rain gage data were used to calibrate the technique, and flash flood clouds even over continental areas appear tropical in nature.

At least two problems inhibit rapid application of these techniques to Hawaiian storms, although the Scofield-Oliver technique is being used in postanalysis by the Honolulu Satellite Field Services Station (SFSS).

1. The gridding resolution for IR is insufficient to locate adequately a cloud relative to an island the size of O'ahu.
2. Torrential rains *do not require* the highest clouds. For example, the heaviest rains of the February 1976 O'ahu storm fell on the day of lowest cloud tops. Neither technique has been tried with torrential orographic rains.

CONCLUSIONS

The primary conclusion to be drawn from this study is that, although SMS-2 imagery has proven of considerable help in the analysis of flood-producing meteorological systems, it has had little effect on detection and warning, areas of most beneficial public impact. The localized nature of Hawaiian rains, orographic influences, watershed sizes, gridding accuracy of IR images, and absence of adequate radar surveillance prevent ready application of existing satellite-based techniques of areal rainfall estimation in the state of Hawai'i.

Three essential components for a flood-detection network are satellite, radar, and rain gages. The Woodley-Griffith and Scofield-Oliver techniques each depend heavily on radar for initial calibration. Radar provides a link between point rain gage data and areal (approximate) satellite imagery. It is my opinion that efforts at applying SMS-2 imagery to quantitative rainfall estimation over the Hawaiian Islands in the absence of radar surveillance will prove to be interesting academic exercises but of little practical value.

The above statement is pessimistic but appropriate. Improved gridding and an independent program to develop techniques of satellite rainfall estimation in orographic regimes may produce significant improvements. The alternative is increased public apathy because of inaccurate island-wide flood warnings. The greatest danger in any area of extreme weather forecasting is overforecasting. This will result in very few misses of significant events, thus saving considerable embarrassment, but it also causes declining credibility. The final product of such a practice is, of course, additional disasters.

II. MESOSCALE ORGANIZATION OF HAWAIIAN RAINS DEDUCED FROM CONTINGENCY INDEX ANALYSIS

INTRODUCTION

Radar studies have shown that even widespread precipitation systems (termed continuous rains) possess substructures of mesoscale dimension (10 000-100 000 m) (Battan 1973). A series of studies have documented mesoscale structure in tropical systems, e.g., Henry and Griffiths (1963); Rainbird (1968). Studies of intense rains in the Hawaiian Islands (Schroeder 1977) have found that orographic influences interact with synoptic (1 000 000 m) scale wind patterns to produce persistent local rains. Ramage (1971) termed such situations "continuous thunderstorms." This study has examined mesoscale structure in Hawaiian rains by use of a statistic termed the contingency index (CI).

The CI was first used by Henry and Griffiths (1963) in the study of daily rainfall patterns in Central America and has subsequently been used by others such as Rainbird (1968) in his examination of Southeast Asia rainfall.

The CI is computed by a 3 x 3 contingency table testing the relationship of simultaneous occurrence at two stations of daily rainfall within three categories: 0, <25 mm, and >25 mm (Rainbird 1968).

	Rainfall (mm)	0	<25 mm	>25 mm	
Station A	0	a_1	a_2	a_3	y_1
	<25	a_4	a_5	a_6	y_2
Station B	>25	a_7	a_8	a_9	y_3
		x_1	x_2	x_3	T

where

$a_1, a_2, \ldots a_9$	are actual frequencies
x_1, x_2, x_3	are column totals
y_1, y_2, y_3	are row totals
T	is grand total

The index is computed by the expression:

$$CI = \frac{(a_1 + a_5 + a_9) - (b_1 + b_5 + b_9)}{T - (b_1 + b_5 + b_9)}$$

where

$b_1 = \frac{x_1 y_1}{T}$, $b_2 = \frac{x_2 y_1}{T}$, ..., are the frequencies expected by chance corresponding to each observed frequency.

A perfect value of CI is 1.0; zero represents random chance, and a negative value represents increasing departure from simultaneous occurrence. The index behaves effectively as a simple correlation.

Figure 11 depicts a typical plot of CI value vs. station separation (Rainbird 1968). The secondary peak is considered as evidence of mesoscale structure, namely, representative of the distance separating thunderstorm cells.

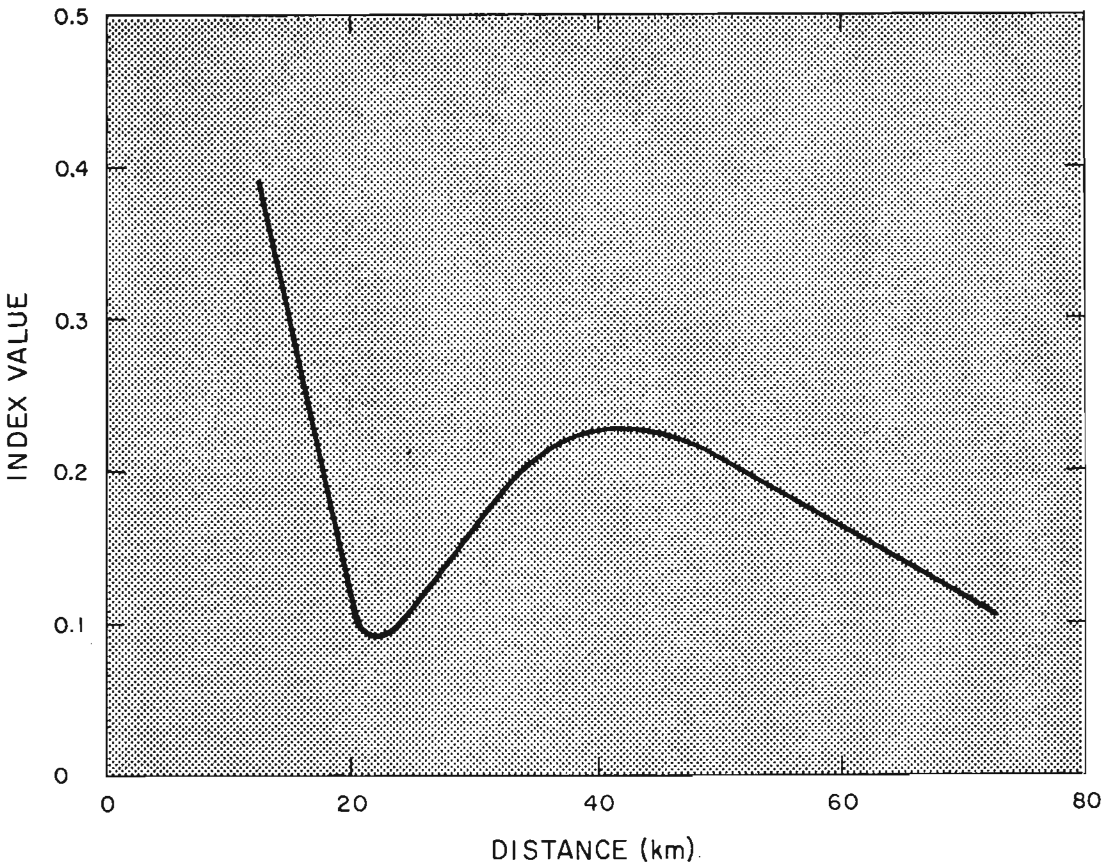

FIGURE 11. TYPICAL PLOT OF CI VALUE VS. STATION SEPARATION SHOWING SECONDARY MESOSCALE MAXIMUM OF CI

DATA USED

Daily rainfall totals were extracted from a magnetic tape containing hourly precipitation data from 103 National Weather Service recording rain gages in the Hawaiian Islands (App. A). The organization of this data set is discussed in a separate report (Schroeder, Kilonsky, and Meisner 1977). Contingency tables were then prepared for each station pair on an island-by-island basis, and CI matrices prepared (App. B). Next, the computations were extended interisland by selecting one representative windward and one leeward station for each island. Contingency tables were prepared for each pair of windward and leeward stations.

ANALYSES BY ISLAND

Hawai'i[1]

Topographic influences are obvious. Windward coastal stations, such as Haina (840) and Hilo (1492), benefit from copious tradewind shower activity. Rainfall rates of 25 mm can occur in the absence of significant synoptic disturbances, and the patterns of Figures 12 and 13 need bear little resemblance to thunderstorm rain distributions. In each case rainfall seems well distributed along the windward coasts; however, Haina will receive significant rains from more northerly winds when Hilo may be relatively dry. There is no evidence of a secondary maximum CI on the leeward side for either case. Keaīwa Camp (Fig. 14) receives heavy rains in southeasterly winds generated by a shift of the Pacific anticyclone or an advancing winter storm. The northeast coast appears uninfluenced by cases of Keaīwa Camp rains; however, a small secondary maximum (>.22) occurs on Pu'u Wa'awa'a (8555). Pu'u Wa'awa'a is directly lee of Mauna Loa for southeasterly flow and may become the center of sea breeze convection.

Kealakekua (3977) (Fig. 15) receives heavy rains due to convection resulting from the Kona sea breeze (Leopold 1949). CI isopleth patterns closely resemble the Kona isohyetal pattern (Taliaferro 1958). A small area of 0.1 values inland from Hilo may testify to the coupling of Kona rains with high elevation windward events.

[1]See Appendix Figure A.1 for location of Hawai'i Island rain gage stations.

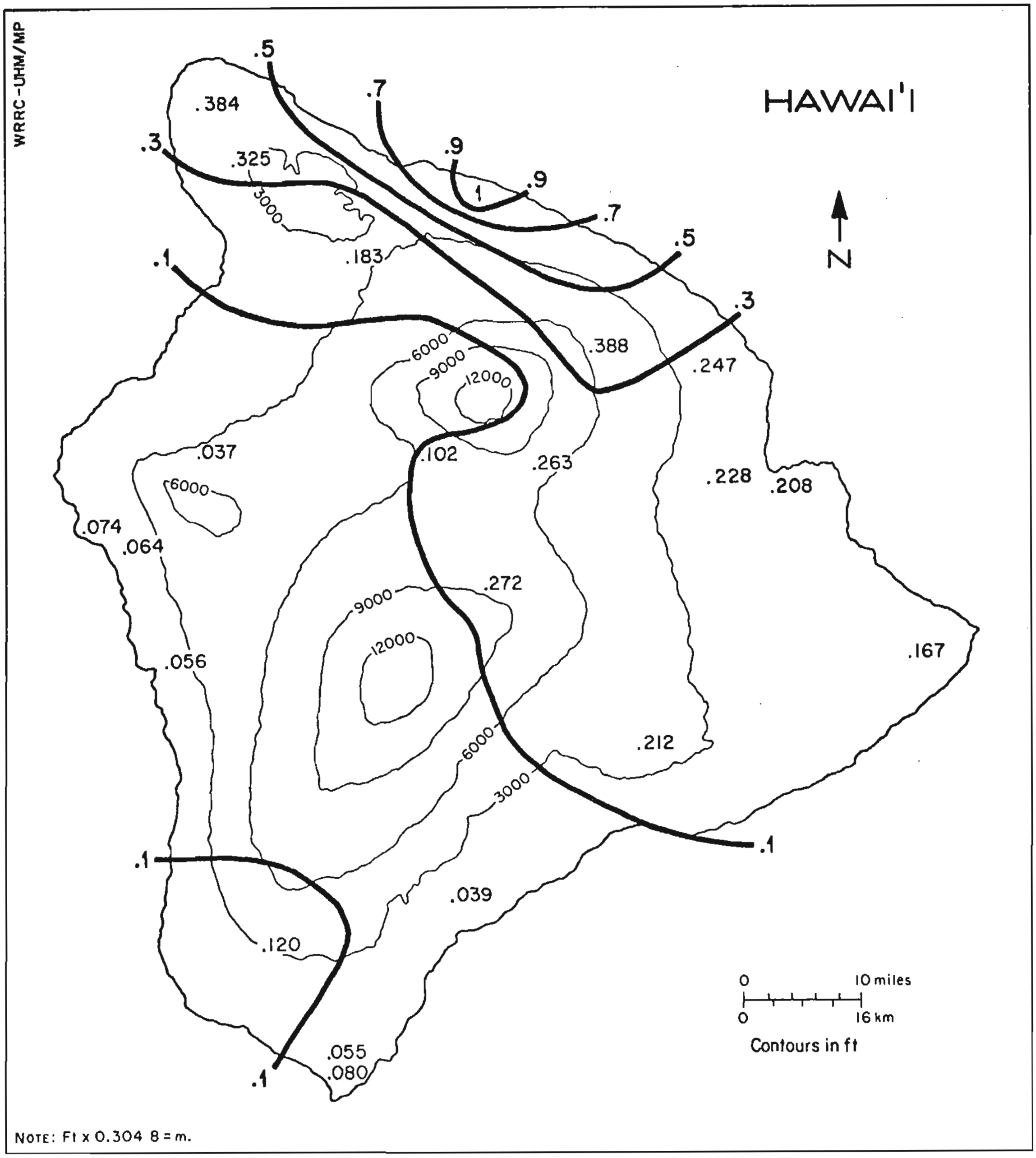

FIGURE 12. MAP OF CI VALUES RELATIVE TO STATION 840 (HAINA, HAWAI'I)

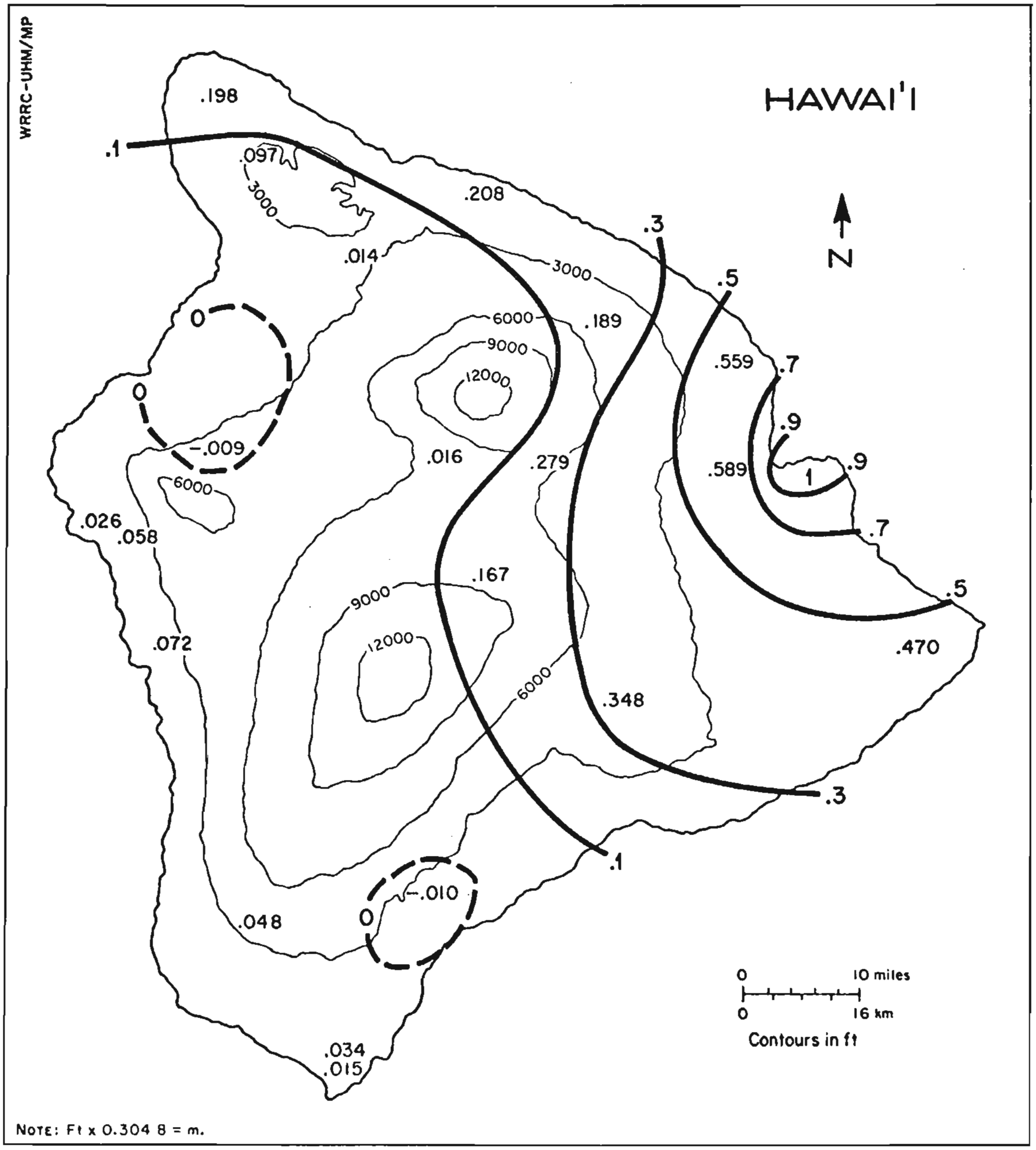

FIGURE 13. MAP OF CI VALUES RELATIVE TO STATION 1492 (HILO AIRPORT, HAWAI'I). DASHED ISOPLETHS ARE EVEN VALUES.

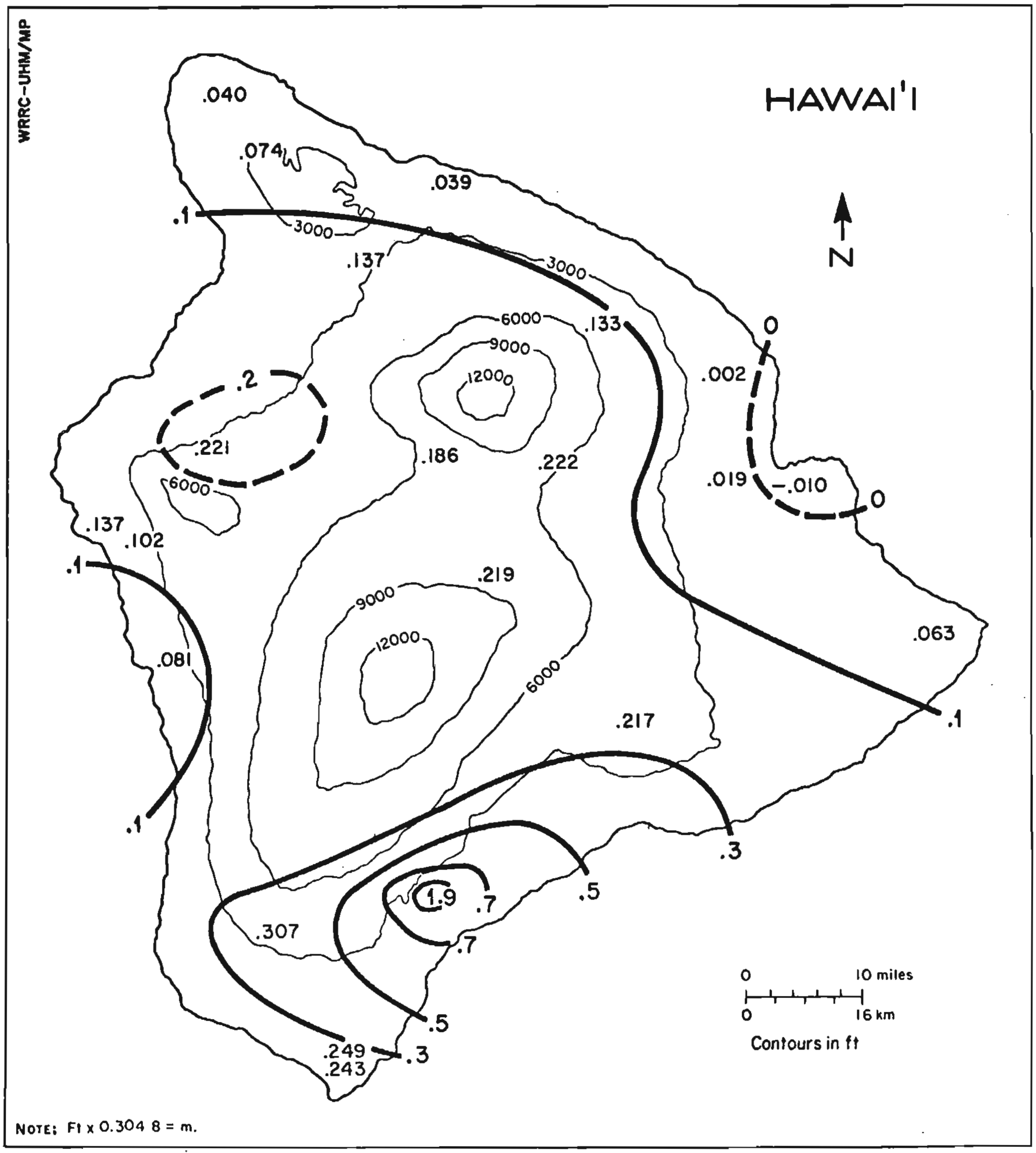

FIGURE 14. MAP OF CI VALUES RELATIVE TO STATION 3925 (KEAĪWA CAMP, HAWAI'I). DASHED ISOPLETHS ARE EVEN VALUES.

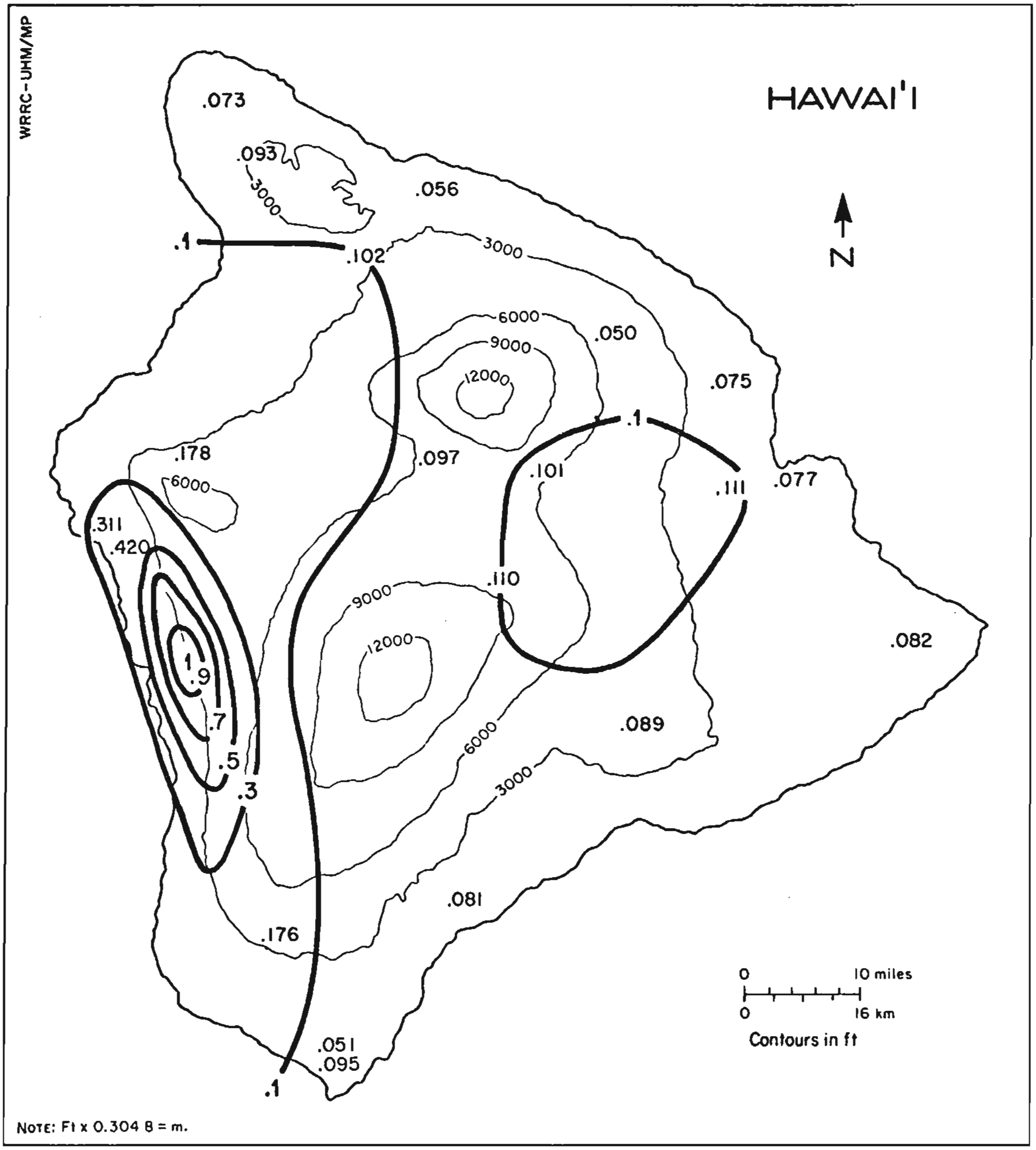

FIGURE 15. MAP OF CI VALUES RELATIVE TO STATION 3977 (KEALAKEKUA, HAWAI'I)

Rainfall rates of 25 mm, which are recorded only twice a year at Lālāmilo Field Office (Table 5), stem from thunderstorms. Lālāmilo seems to be linked to the leeward Kohala Mountains to the northwest, but isolated from other island districts (Fig. 16).

TABLE 5. NUMBER OF DAYS WITH RAINFALL >25 mm FOR HAWAI'I ISLAND BETWEEN 1965 AND 1973

Sta. No.	No. of Events	Record Length (Days)	Percent of Record Length
840	136	3216	4.2
1303	168	3124	5.4
1339	71	3153	2.2
1492	263	3228	8.1
1570	31	1197	2.6
1960	319	3063	10.4
2512	63	3187	2.0
3510	234	1845	12.7
3925	126	3224	3.9
3977	82	3065	2.7
4098	121	3087	3.9
4764	32	3127	1.0
5018	52	2760	1.9
5260	22	3175	0.7
5460	202	3101	6.5
8063	16	3183	0.5
8550	29	792	3.7
8555	49	3212	1.5
8675	18	1226	1.5
8679	22	1694	1.3
9350	51	2862	1.8

Hawaii National Park Headquarters and Kūlani Mauka are high level windward stations. The CI pattern (Figs. 17, 18) reflects extensive regions of heavy rains. In the case of the Hawaii National Park Headquarters, isopleths suggest coupling with northeast and southeast coastal rainfall regimes.

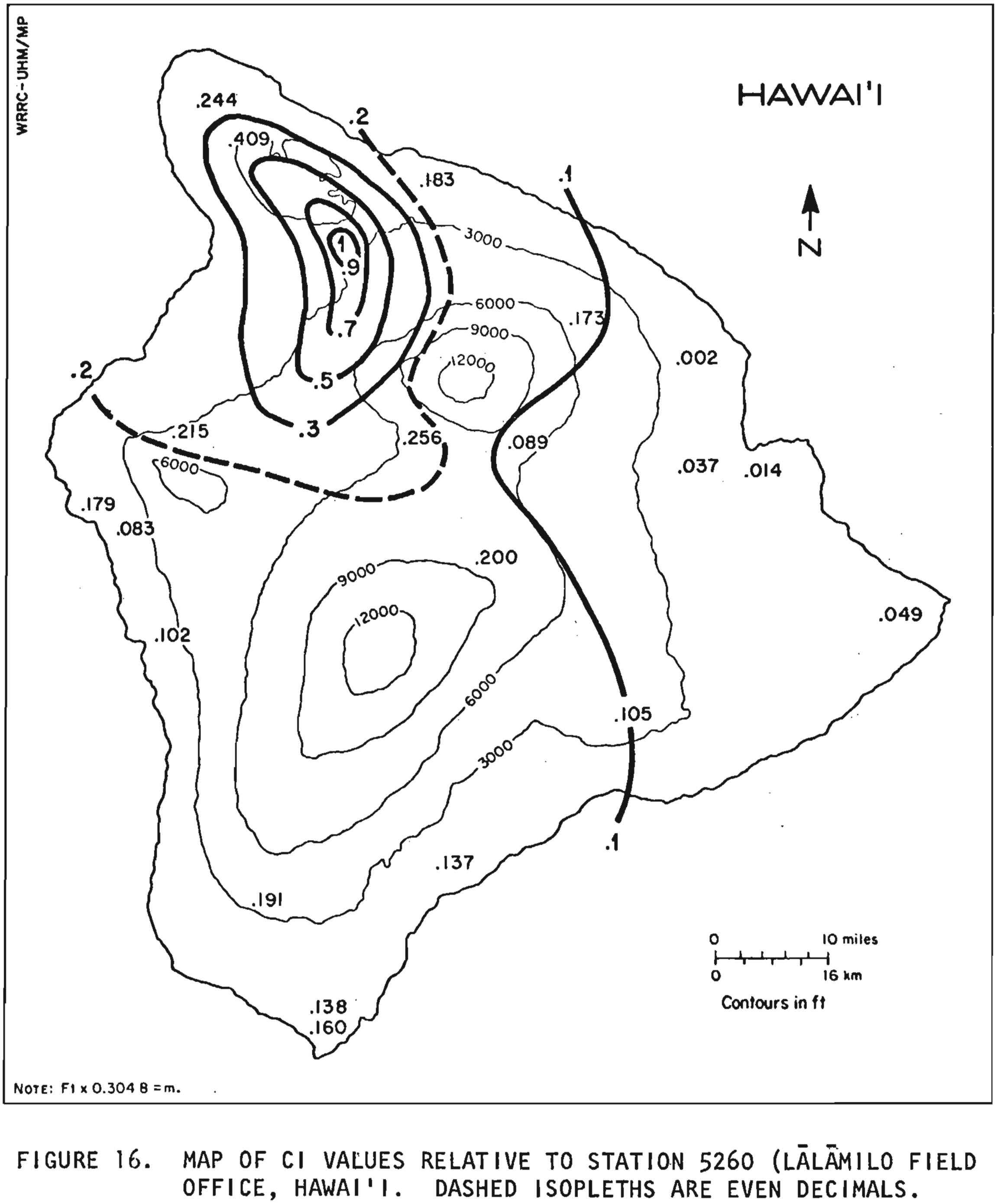

FIGURE 16. MAP OF CI VALUES RELATIVE TO STATION 5260 (LĀLĀMILO FIELD OFFICE, HAWAI'I. DASHED ISOPLETHS ARE EVEN DECIMALS.

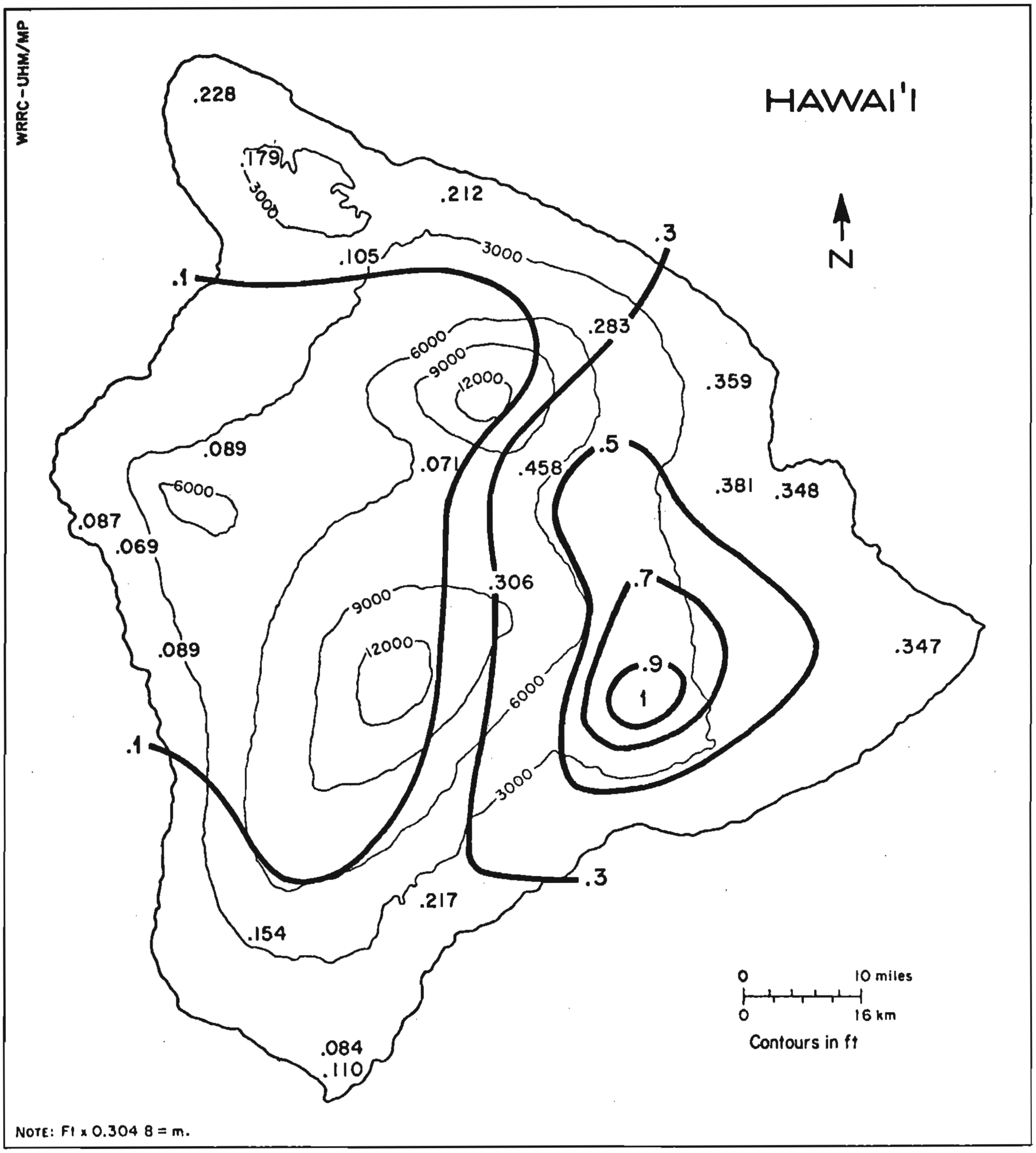

FIGURE 17. MAP OF CI VALUES RELATIVE TO STATION 1303 (HAWAII VOLCANOES NATIONAL PARK HEADQUARTERS, HAWAI'I)

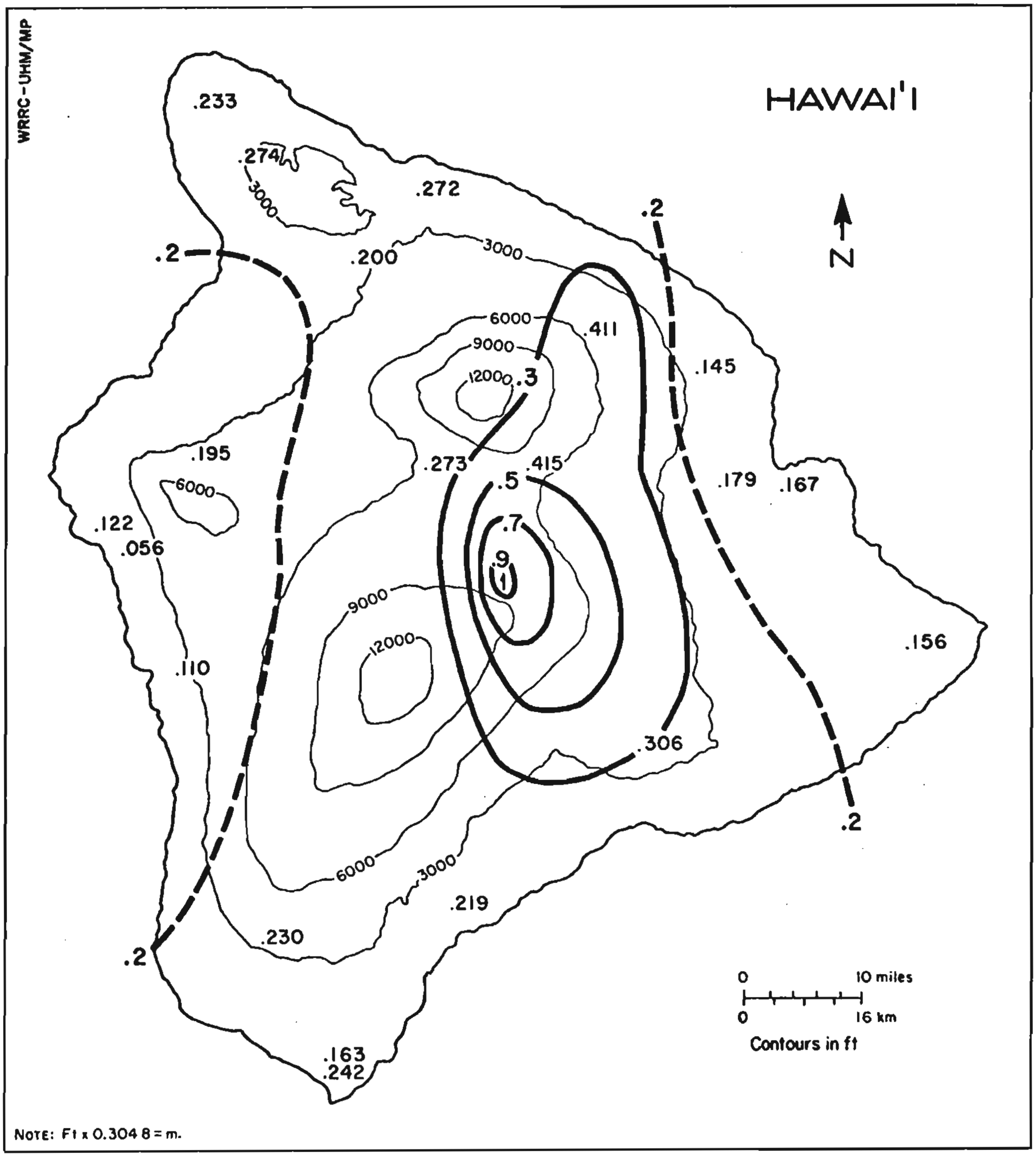

FIGURE 18. MAP OF CI VALUES RELATIVE TO STATION 5018 (KŪLANI MAUKA, HAWAI'I). DASHED ISOPLETHS ARE EVEN VALUES.

Due to its comparative size Hawai'i produces the strongest local influences among the islands. The remaining islands will be examined in order of decreasing size.

Maui[1]

Pa'akea (7194) typifies a wet windward East Maui station. Rainfall rates of 25 mm occur on 12.7% of all days—a frequency equal to Kaūmana (3510) at almost the same elevation on Hawai'i. Leeward Maui stations are completely out of phase with windward sections while West Maui possesses a secondary maximum of CI (Fig. 19). West Maui (Fig. 20) is better correlated with Central Maui, e.g., Kahului (2572), than are the East Maui slopes. The CI pattern for Kīhei (4489), a dry leeward station (Fig. 21), resembles a Kona storm isohyetal pattern. Kīhei is closely linked to the even drier leeward West Maui station at Lāhainā. Haleakalā summit (1108) is the highest station (3 056 m MSL) in the set. High values of CI are limited to the upper slopes (Fig. 22). The West Maui stations have higher CI values than the windward Haleakalā slopes, indicative of winter storm contributions.

O'ahu[2]

O'ahu has the most dense recording rain gage network in the state, but urbanization has caused frequent station moves and resulted in reduced record lengths. Twenty-five of 38 possible records were used in the study. As with the other islands, secondary CI maxima are not evident. Helemano Intake (1384) typifies a wet Ko'olau Range station (Fig. 23). The CI isopleths resemble storm isohyets for recent O'ahu floods (Schroeder 1977) with a maximum over the northern Ko'olaus. Inasmuch as totals less than 25 mm also contribute to the CI, the pervasive influence of the trade winds may also be present. Honolulu Airport (1919) (Fig. 24) receives 25-mm rains from winter storms and southerly winds. That storm rains can encompass all of O'ahu much more readily than its larger neighbors is reflected in O'ahu's CI distribution. The values never fall as low as for the larger islands.

Kailua Fire Station (2683) (Fig. 25) is sufficiently removed from the mountains that only storms produce significant rainfalls. Thunderstorm spacing is evident along the windward coast. A secondary maximum of CI is found 10 000 to 20 000 m northwest of Kailua. Mt. Ka'ala (6553) is apparently linked to systems drifting from the east and south (Fig. 26).

---

[1]See Appendix Figure A.2 for location of Maui rainfall gage stations.
[2]See Appendix Figure A.3 for location of O'ahu rainfall gage stations.

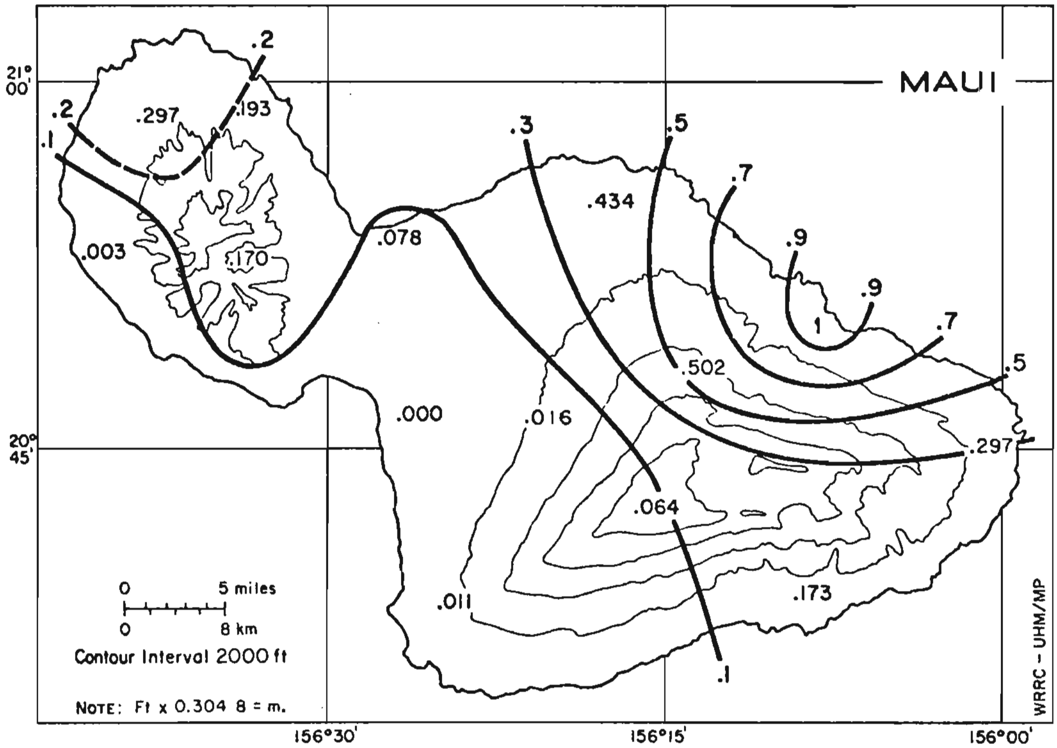

FIGURE 19. MAP OF CI VALUES RELATIVE TO STATION 7194 (PA'AKEA, MAUI). DASHED ISOPLETHS ARE EVEN VALUES.

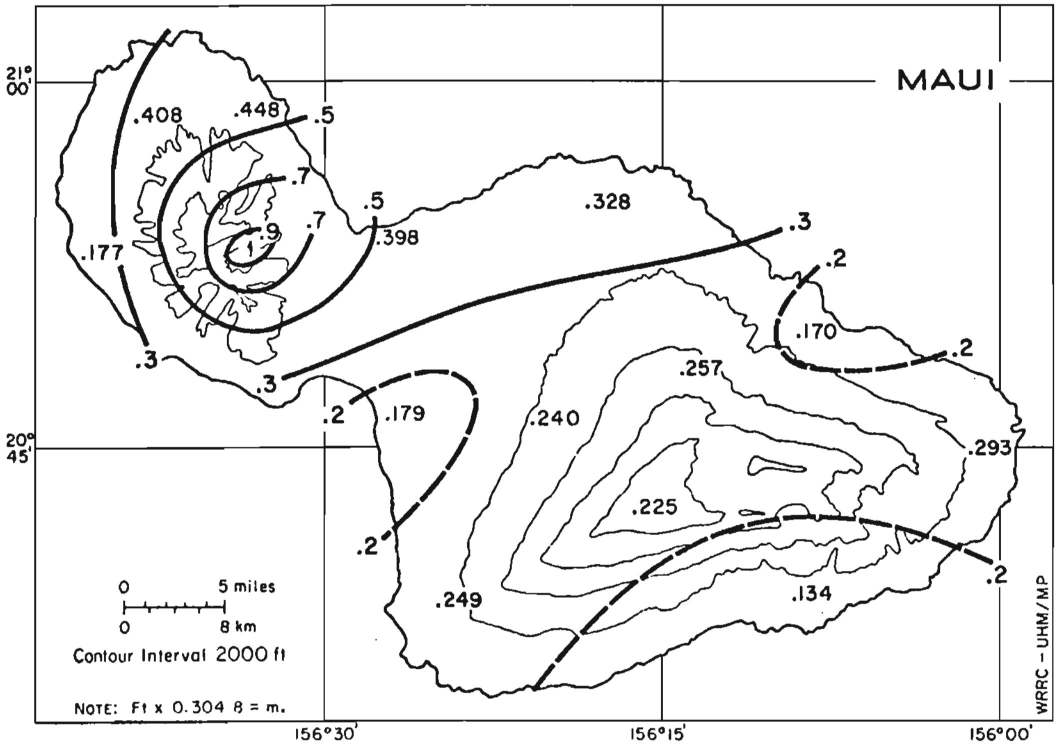

FIGURE 20. MAP OF CI VALUES RELATIVE TO STATION 2008 ('ĪAO NEEDLE, MAUI). DASHED ISOPLETHS ARE EVEN VALUES.

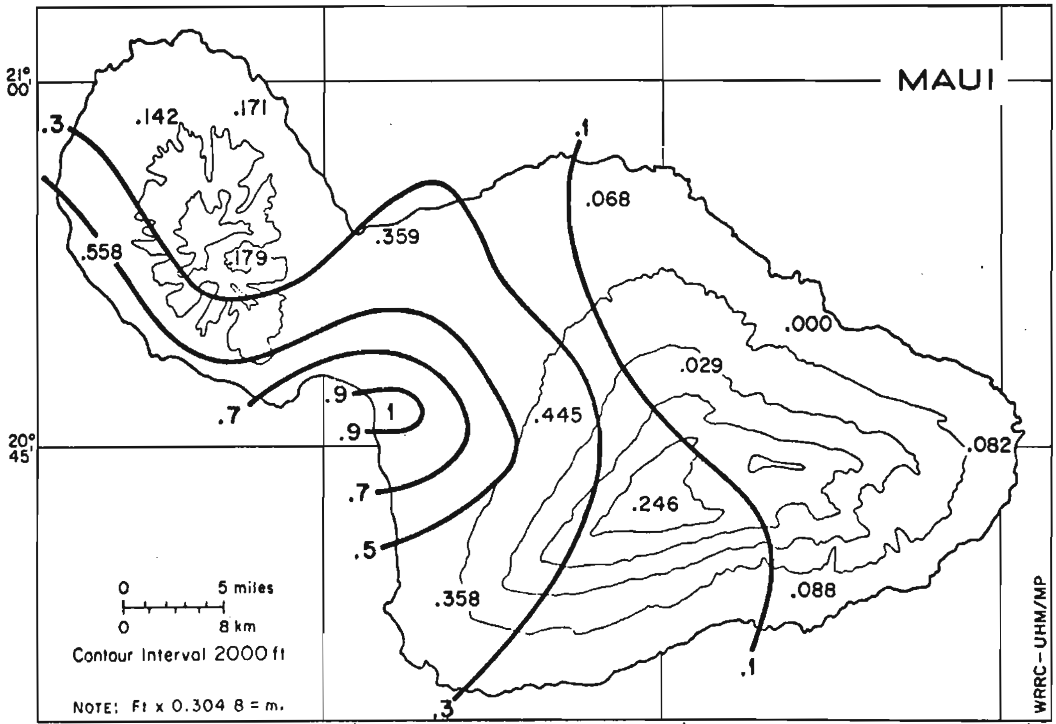

FIGURE 21. MAP OF CI VALUES RELATIVE TO STATION 4489 (KĪHEI, MAUI)

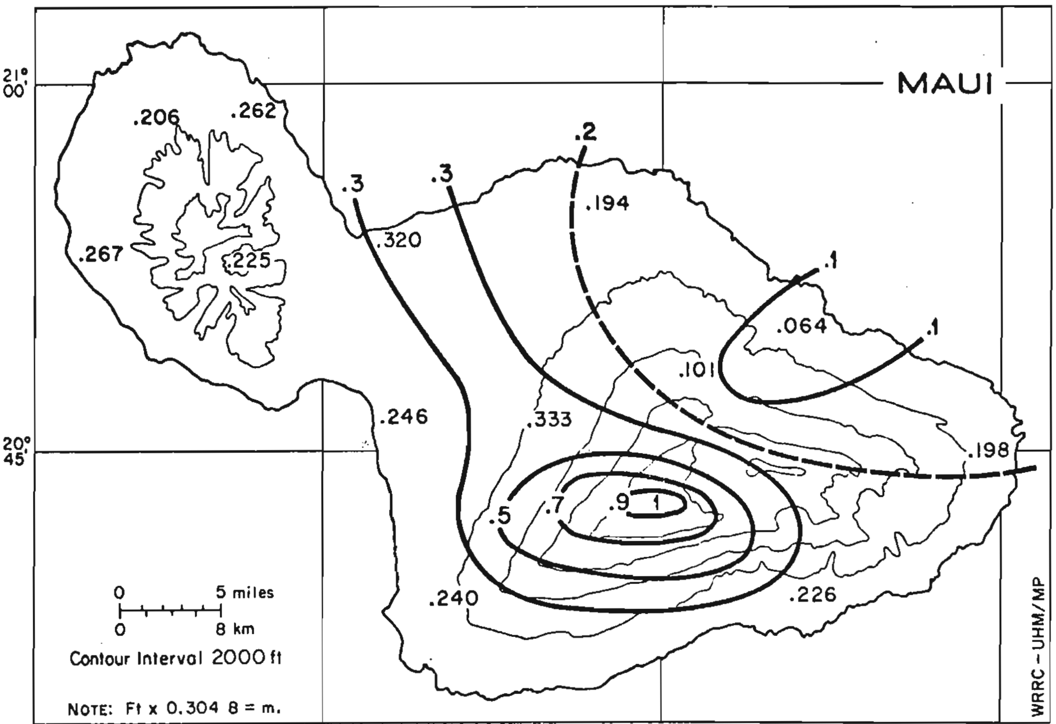

FIGURE 22. MAP OF CI VALUES RELATIVE TO STATION 1008 (HALEAKALĀ SUMMIT, MAUI). DASHED ISOPLETHS ARE EVEN VALUES.

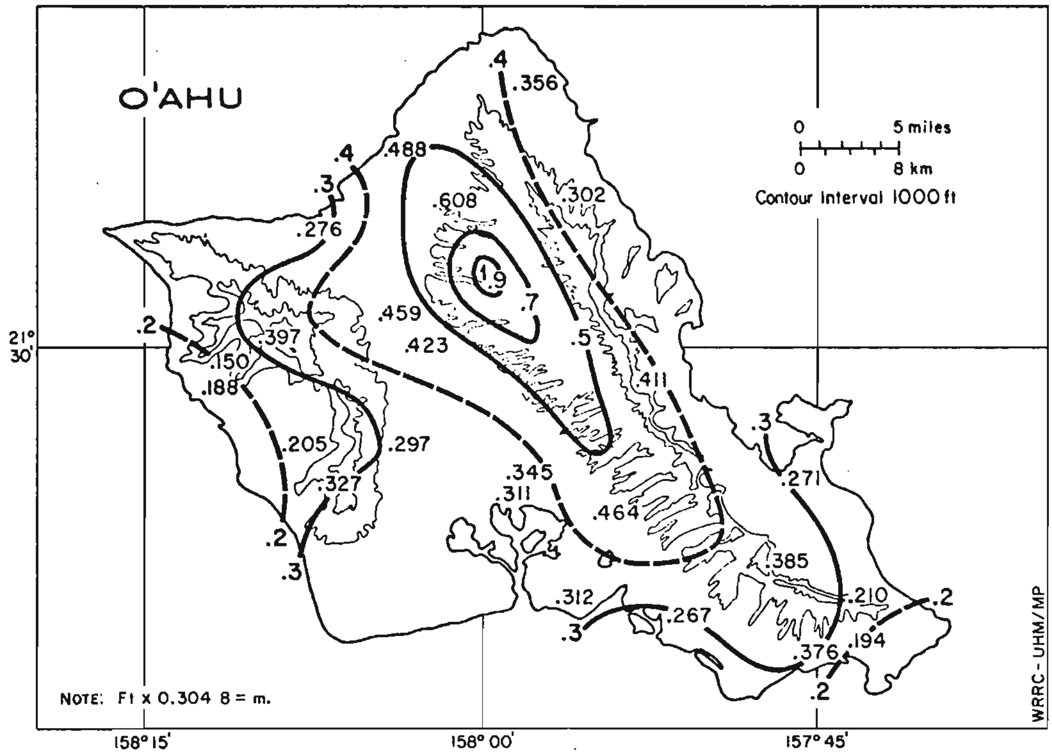

FIGURE 23. MAP OF CI VALUES RELATIVE TO STATION 1384 (HELEMANO INTAKE, O'AHU). DASHED ISOPLETHS ARE EVEN VALUES.

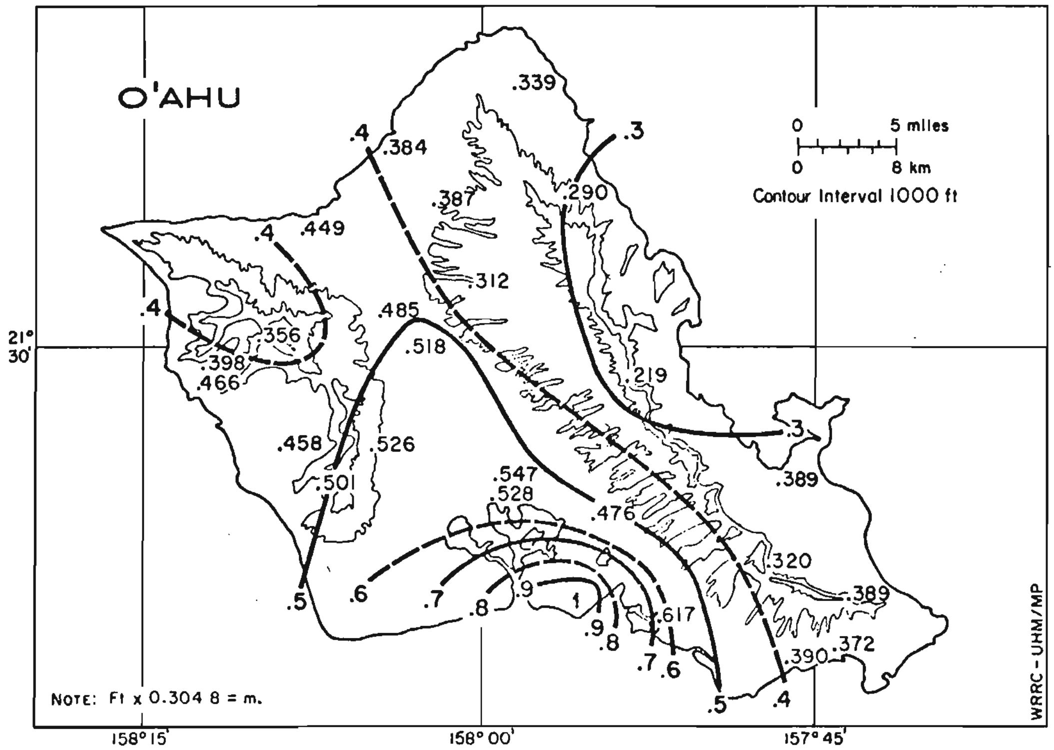

FIGURE 24. MAP OF CI VALUES RELATIVE TO STATION 1919 (HONOLULU AIRPORT, O'AHU). DASHED ISOPLETHS ARE EVEN VALUES.

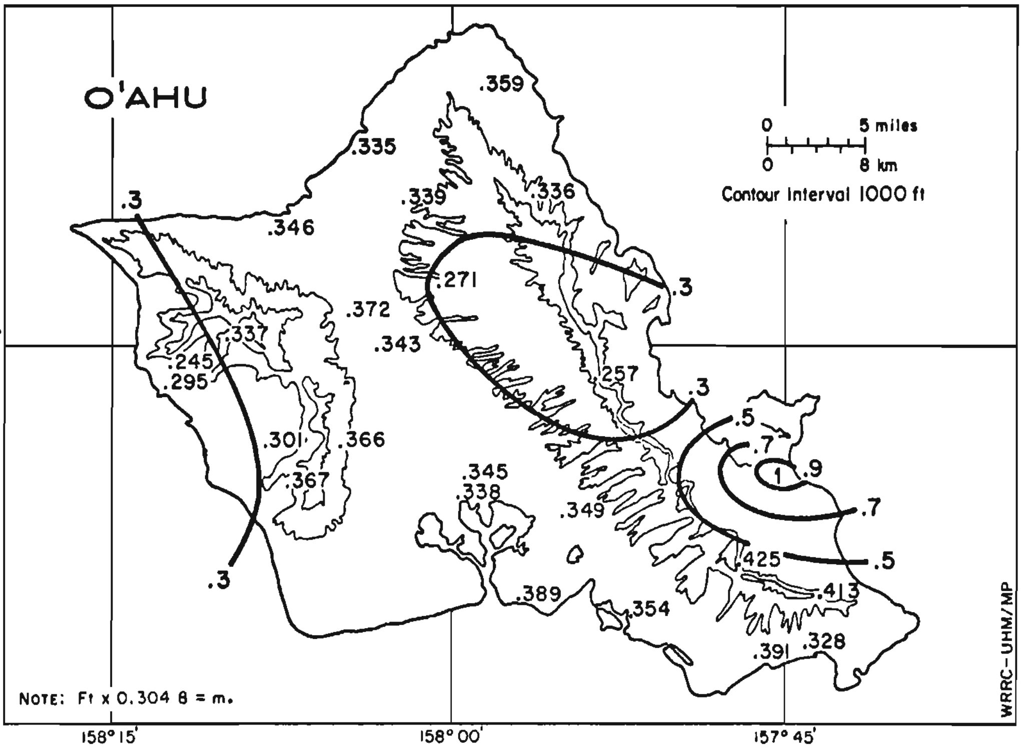

FIGURE 25. MAP OF CI VALUES RELATIVE TO STATION 2683 (KAILUA FIRE STATION, O'AHU)

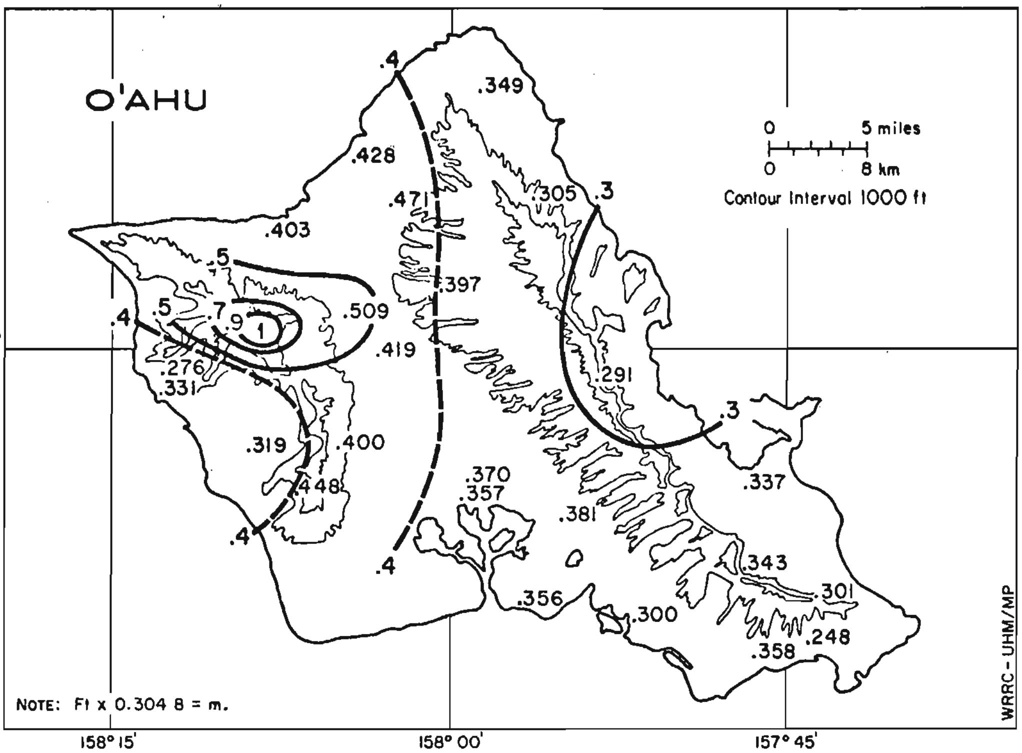

FIGURE 26. MAP OF CI VALUES RELATIVE TO STATION 6553 (MT. KA'ALA, O'AHU). DASHED ISOPLETHS ARE EVEN VALUES.

Kaua'i[1]

Although smaller than O'ahu, Kaua'i rises higher (1 598 m MSL) and desiccates both trade winds and Kona winds more efficiently. This is demonstrated by the low CI Values for Kekaha (4272) when paired with windward (Fig. 27) and mountain (Fig. 28) stations. The low CIs of northeast mountain stations (Fig. 29) are due to their high frequency of 25-mm rains with trade winds.

Moloka'i[2]

Moloka'i receives significant tradewind rains on the eastern mountains (Fig. 30), but west Moloka'i experiences heavy rains with winter storms (Fig. 31). Unusual CIs at Puko'o Kai (8221) are due primarily to a short record length. Stations with similar short records were generally deleted from the study (App. Table B.5).

Lāna'i[3]

Lāna'i is very dry; 60% of all event pairs for the contingency tables were paired zeros (App. Table B.6). Lāna'ihale (5301) is the highest and wettest point; the associated CI pattern appears as that of trade winds (Fig. 32). The Kaumalapau Harbor isopleth pattern (Fig. 33) is the reverse of the Lāna'ihale pattern. Relatively low CI values for closely-spaced leeward gages hint that convective elements over Lāna'i may be of smaller dimension than is the case for larger islands.

Orographic influences dominate convective storm systems in the production of intense Hawaiian rains. The influences of orography are most obvious on the largest islands, Hawai'i and Maui; influences are smaller but clearly detectable over the other islands. In most cases no secondary maximum presents itself. This is due to the orographic nature of many heavy rains and to migrating storm cells in winter storms.

---

[1]See Appendix Figure A.4 for location of Kaua'i rain gage stations.
[2]See Appendix Figure A.5 for location of Moloka'i rain gage stations.
[3]See Appendix Figure A.6 for location of Lāna'i rain gage stations.

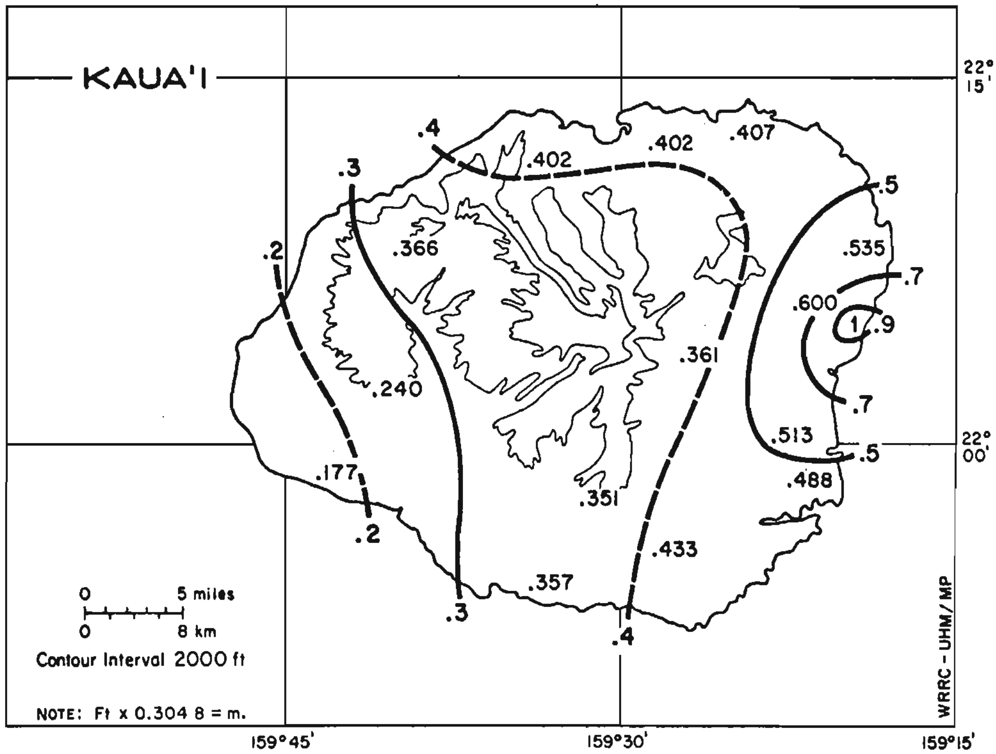

FIGURE 27. MAP OF CI VALUES RELATIVE TO STATION 3159 (KAPA'A STABLES, KAUA'I). DASHED ISOPLETHS ARE EVEN VALUES.

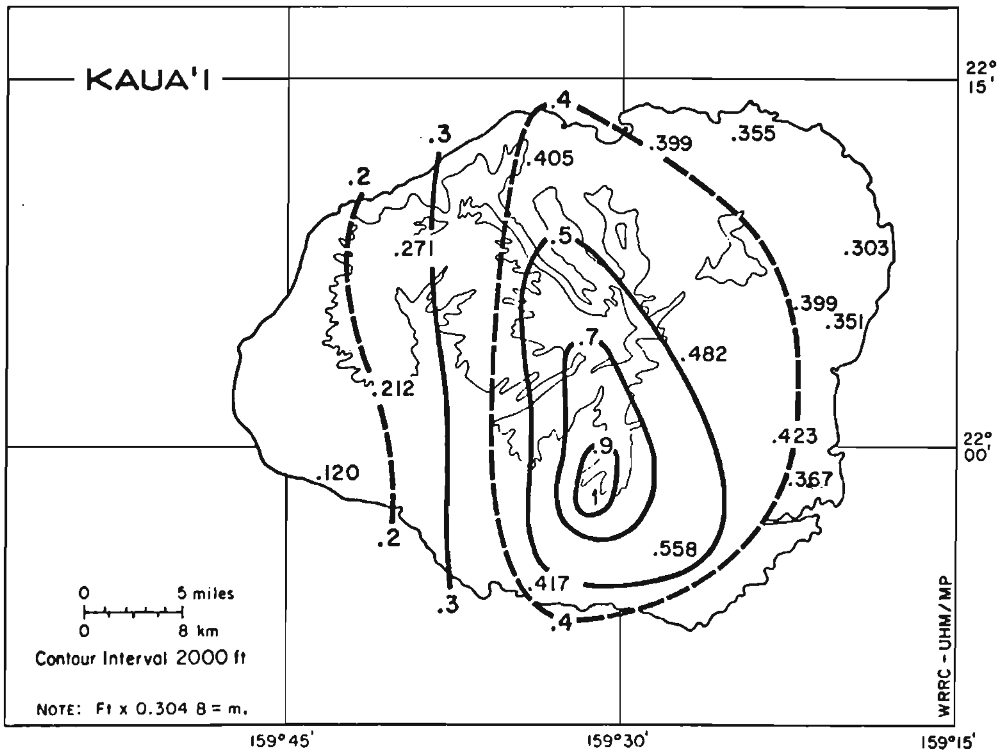

FIGURE 28. MAP OF CI VALUES RELATIVE TO STATION 0140 (ALEXANDER RESERVOIR, KAUA'I). DASHED ISOPLETHS ARE EVEN VALUES.

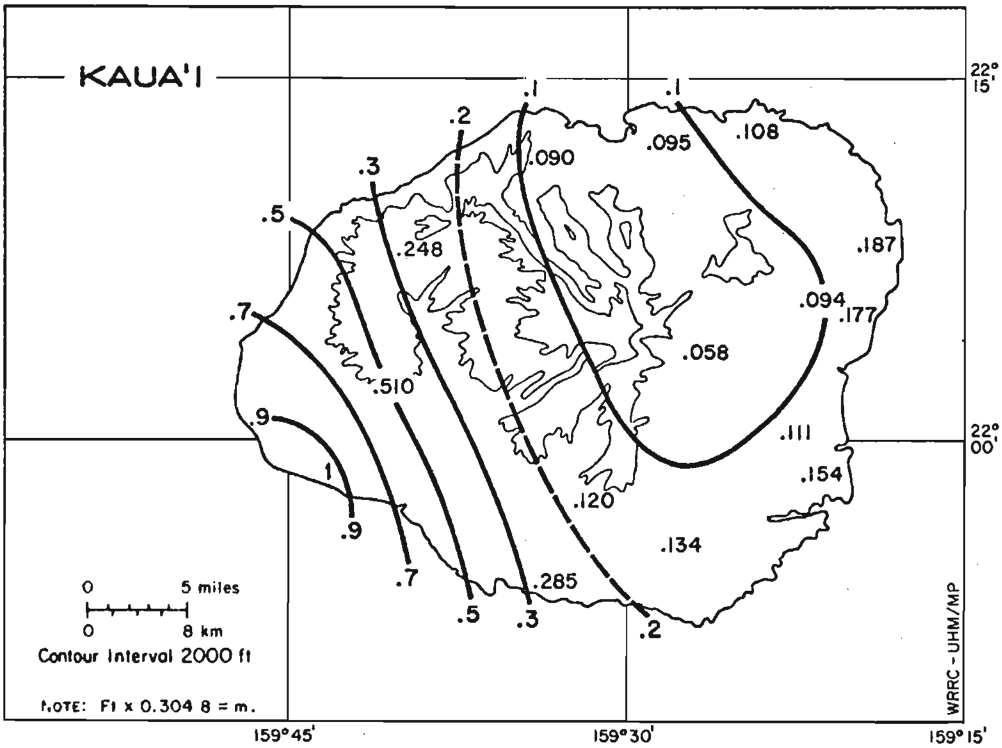

FIGURE 29. MAP OF CI VALUES RELATIVE TO STATION 4272 (KEKAHA, KAUA'I). DASHED ISOPLETHS ARE EVEN VALUES.

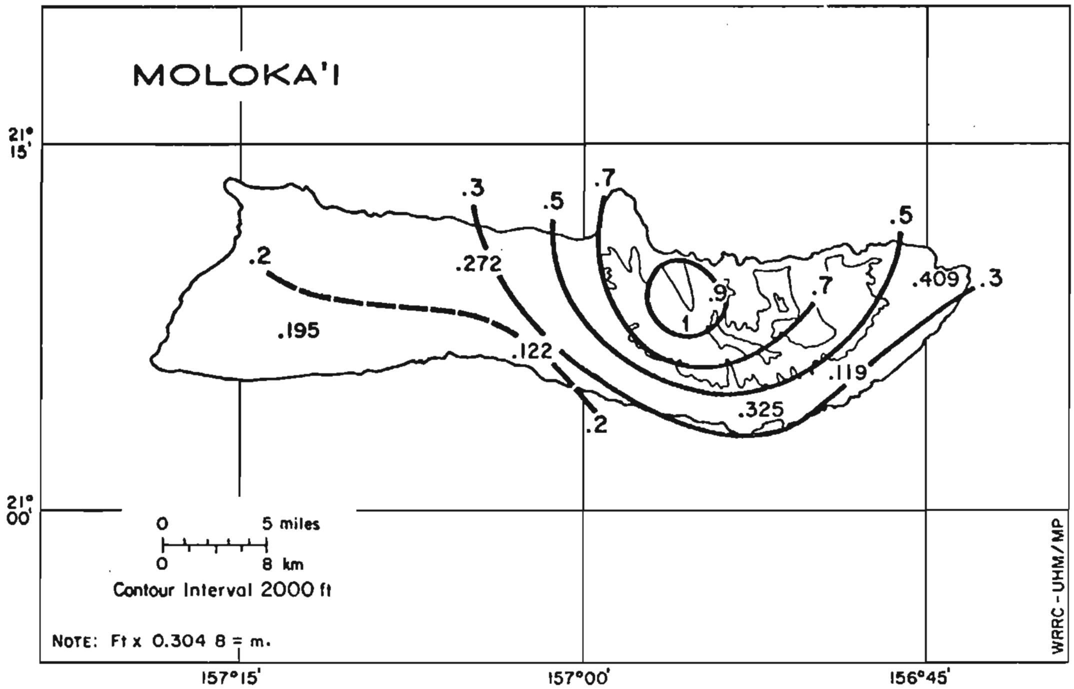

FIGURE 30. MAP OF CI VALUES RELATIVE TO STATION 9404 (WAIKOLU, MOLOKA'I). DASHED ISOPLETHS ARE EVEN VALUES.

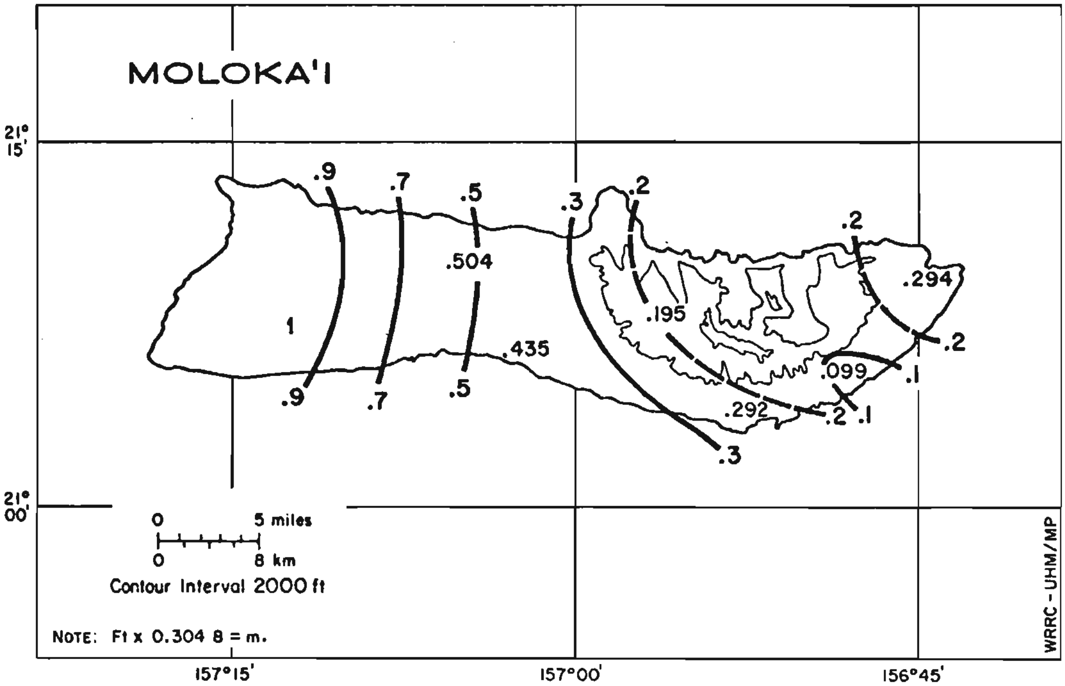

FIGURE 31. MAP OF CI VALUES RELATIVE TO STATION 6190 (MAUNALOA, MOLOKA'I). DASHED ISOPLETHS ARE EVEN VALUES.

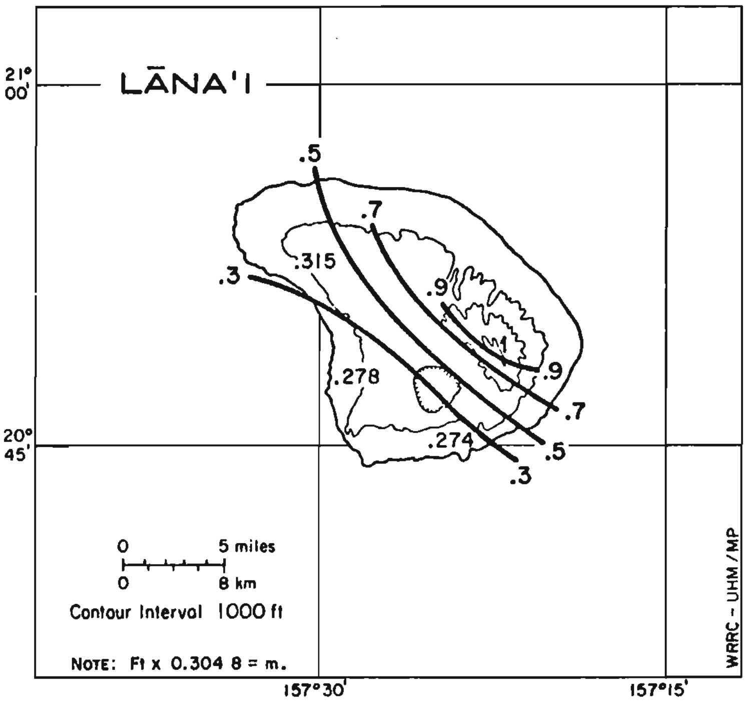

FIGURE 32. MAP OF CI VALUES RELATIVE TO STATION 5301 (LĀNA'IHALE, LĀNA'I). DASHED ISOPLETHS ARE EVEN VALUES.

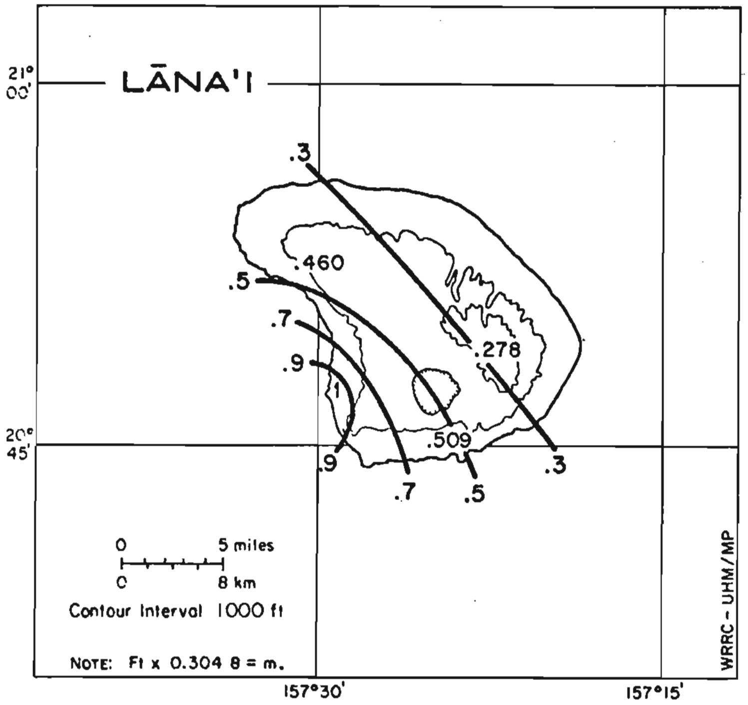

FIGURE 33. MAP OF CI VALUES RELATIVE TO STATION 3461 (KAUMALAPAU HARBOR, LĀNA'I). DASHED ISOPLETHS ARE EVEN VALUES.

INTERISLAND CI

To extend the scale of comparisons, representative windward and leeward stations were selected for each of the six major islands. Mountain locations were not used since elevation differences among islands are too great. Table 6 lists the stations selected and their annual rainfalls (Taliaferro 1959).

CIs computed for each six-station set show a general decrease in values with station separation especially apparent in the case of windward stations (Table 7). Note that Lāna'i's windward station is randomly (near zero CI) related to any other windward station. Lāna'i lies in the lee of Maui, and thus no station is truly "windward." Lāna'i does relate to other islands for winter storm rains in leeward exposures (Table 8).

The results of the interisland comparison reflect observed meteorological features. Migratory features may miss entire sections of the state. Winter rains often occur in fronts and squall lines which are sufficiently narrow to influence only a couple of islands at a time.

TABLE 6. WINDWARD AND LEEWARD STATIONS FOR INTERISLAND STUDIES

Island	Station No.	Name	Annual Rainfall (mm)
		Windward	
Kaua'i	8694	Stable Storm Ditch	3 175
O'ahu	8964	Waiāhole	3 810
Moloka'i	9404	Waikolu	1 905
Lāna'i	5301	Lāna'ihale	890
Maui	7194	Pa'akea	5 080
Hawai'i	1492	Hilo (WSO) Airport	3 810
		Leeward	
Kaua'i	4272	Kekaha	510
O'ahu	5647	Lualualei	635
Moloka'i	6190	Maunaloa	710
Lāna'i	3461	Kaumalapau Harbor	380
Maui	5177	Lāhainā	380
Hawai'i	4764	Kona Airport	635

TABLE 7. MATRIX OF CONTINGENCY INDEX VALUES FOR REPRESENTATIVE WINDWARD STATIONS

Island	Station No.	Weather Bureau Number					
		8694	8964	9404	5301	7194	1492
Kaua'i	8694	1.000	0.288	0.195	0.002	0.232	0.205
O'ahu	8964	0.288	1.000	0.315	0.075	0.254	0.165
Moloka'i	9404	0.195	0.315	1.000	0.113	0.259	0.155
Lāna'i	5301	0.002	0.075	0.113	1.000	0.004	-0.017
Maui	7194	0.232	0.254	0.259	0.004	1.000	0.394
Hawai'i	1492	0.205	0.165	0.155	-0.017	0.394	1.000

NOTE: 0.0 indicates station pair in question had no overlapping time periods.

TABLE 8. MATRIX OF CONTINGENCY INDEX VALUES FOR REPRESENTATIVE LEEWARD STATIONS

Island	Station No.	Weather Bureau Number					
		4272	5647	6190	3461	5177	4767
Kaua'i	4272	1.000	0.310	0.182	0.195	0.233	0.080
O'ahu	5647	0.310	1.000	0.323	0.261	0.298	0.103
Moloka'i	6190	0.182	0.323	1.000	0.323	0.340	0.082
Lāna'i	3461	0.195	0.261	0.323	1.000	0.428	0.150
Maui	5177	0.233	0.298	0.340	0.428	1.000	0.115
Hawai'i	4764	0.080	0.103	0.082	0.150	0.115	1.000

NOTE: 0.0 indicates station pair in question had no overlapping time periods.

SUMMARY

The contingency index is useful in determination of mesoscale organization of rainfalls. The application to Hawai'i is different than previous uses since orographic influences tend to mask cumulus-scale elements. A secondary maximum of CI at increasing station separations was seldom apparent due to orographic constraints and, in some instances, small island sizes.

Maps of CI with respect to stations in representative island locations resemble isohyetal maps. CI minima on small islands exceed CI minima on large islands, such as Hawai'i and Maui. Interisland comparisons show that CI diminishes with distance for both windward and leeward exposures. Interisland results can be explained in terms of the dimensions of tradewind disturbances, alignment of the islands, and preferred orientation and width of winter convective cloud lines.

ACKNOWLEDGMENTS

Dr. L. Stephen Lau, Director of the Water Resources Research Center, University of Hawaii, recognized the importance of flash flooding as a water resources problem for Hawai'i.

Mr. Paul Haraguchi of the National Weather Service Forecast Office, Honolulu International Airport, provided a considerable amount of meteorological data. Mr. Irving C.Y. Lam developed the computational routines used to prepare contingency indices.

REFERENCES

American Meteorological Society. 1978. Flash floods—A national problem. *Bull. Am. Meteorol. Soc.* 59:585-86.

Battan, L.J. 1973. *Radar observation of the atmosphere.* Chicago: University of Chicago Press.

Beran, D.W.; Hooke, W.H.; Little, C.G.; and Coons, F. 1977. Airport weather service: Some future trends. *Bull. Am. Meteorol. Soc.* 58:1182-86.

Blanchard, D.C. 1953. Raindrop size distribution in Hawaiian rains. *J. Meteorol.* 10:457-73.

Blumenstock, D.L., and Price, S. 1967. Climates of the states—Hawaii. No. 60-51, Climatography of the United States, Environmental Science Services Administration, U.S. Dept. of Commerce.

Burnash, R.J.C., and Twedt, T.W. 1978. Event-reporting instrumentation for real-time flash flood warnings. *Preprints*, Conference on Flash Floods-Hydrometeorological Aspects, American Meteorological Society, Los Angeles, California, pp. 96-101.

Eccles, P.J. 1978. Automatic flash flood warnings from dual-wavelength radar—are they worth it? *Preprints*, Conference on Flash Floods-Hydrometeorological Aspects, American Meteorological Society, Los Angeles, California, pp. 52-57.

Fawbush, E.J.; Miller, R.C.; and Starrett, L.G. 1951. An empirical method for forecasting tornado development. *Bull. Am. Meteorol. Soc.* 32:1-9.

George, J.J. 1960. *Weather forecasting for aeronautics.* New York: Academic Press.

Greene, D.R., and Saffle, R.E. 1978. Radar analysis of the 1977 Johnstown flash flood. *Preprints*, Conference on Flash Floods-Hydrometeorological Aspects, American Meteorological Society, Los Angeles, California, pp. 176-80.

Griffith, C.G.; Woodley, W.L.; Browner, S.; Teijerio, J.; Maier, M.; Martin, D.W.; Stout, J.; and Sikdar, D.N. 1976. *Rainfall estimation from geosynchronous satellite imagery during daylight hours.* Tech. Rep. ERL 356-WMP07, National Oceanic and Atmospheric Administration.

Hales, J.E. 1978. The Kansas City flash flood of September 12, 1977. *Preprints*, Conference on Flash Floods-Hydrometeorological Aspects, American Meteorological Society, Los Angeles, California, pp. 158-62.

Haraguchi, P. 1977. Forecasting floods in Hawaii (excluding Hawaii Island). Tech. Memo NWSTM PR-16, National Oceanic and Atmospheric Administration.

Henry, W.K., and Griffiths, J.F. 1963. Research on tropical rainfall patterns and associated meso-scale systems. Rep. No. 4 to U.S. Army Electron. Res. and Develop. Lab., Texas A&M Research Foundation, College Station, Texas.

Hoxit, L.R.; Maddox, R.A.; Mogil, H.M.; and Zuckerberg, F.L. 1978. Meteorological analysis of the Johnstown, Pennsylvania, flash flood, 19-20 July 1977. *Preprints*, Conference on Flash Floods-Hydrometeorological Aspects, American Meteorological Society, Los Angeles, California, pp. 168-75.

Kilonsky, B.J., and Ramage, C.S. 1976. A technique for estimating tropical open-ocean rainfall from satellite observations. *J. Appl. Meteorol.* 15:972-75.

Land, L.F. 1978. Analysis of flood resulting from the Toccoa Falls, Georgia, dam break. *Preprints*, Conference on Flash Floods-Hydrometeorological Aspects, American Meteorological Society, Los Angeles, California, pp. 127-30.

Larson, L.W., and Vochatzer, J.W. 1978. A case study—Kansas City flood September 12-13, 1977. *Preprints*, Conference on Flash Floods-Hydrometeorological Aspects, American Meteorological Society, Los Angeles, California, pp. 163-67.

Leopold, L.B. 1949. The interaction of trade wind and sea breeze, Hawaii. *J. Meteorol.* 6:312-20.

Maddox, R.A.; Caracena, F.; Hoxit, L.R.; and Chappell, C.F. 1977. Meteorological aspects of the Big Thompson flash flood of 31 July 1976. Tech. Rep. ERL 388-APCL 41, National Oceanic and Atmospheric Administration.

______, and Chappell, C.F. 1978. Meteorological aspects of twenty significant flash flood events. *Preprints*, Conference on Flash Floods-Hydrometeorological Aspects, American Meteorological Society, Los Angeles, California, pp. 1-9.

Miller, R.C. 1972. Notes on analysis and severe weather forecasting procedures of the Air Force Global Weather Central. Tech. Rep. 200, Air Weather Service.

National Oceanic and Atmospheric Administration. 1976. Big Thompson flash flood of July 31-August 1, 1976. Rep. 76-1, Natural Disaster Survey, U.S. Dept. of Commerce.

______. 1977*a*. Johnstown, Pennsylvania, flash flood of July 19-20, 1977. Rep. 77-1, Natural Disaster Survey, Dept. of Commerce.

______. 1977*b*. Kansas City flash flood of September 12-13, 1977. Rep. 77-2, Natural Disaster Survey, Dept. of Commerce.

Rainbird, A.F. 1968. Weather disturbances over tropical continents and their effect on ground conditions. Dept. of Atmospheric Sci., Colorado State University, Fort Collins, Colorado.

Ramage, C.S. 1971. *Monsoon meteorology*. New York: Academic Press.

______. 1976. Prognosis for weather forecasting. *Bull. Am. Meteorol. Soc.* 57:4-10.

______. 1978*a*. Further outlook—hazy. *Bull. Am. Meteorol. Soc.* 59:18-21.

______. 1978*b*. Response to "Comments on further outlook—hazy." *Bull. Am. Meteorol. Soc.* 59:644-45.

Rao, M.S.V., and Theon, J.S. 1977. New features of global climatology revealed by satellite-derived oceanic rainfall maps. *Bull. Am. Meteorol. Soc.* 58:1285-89.

Schroeder, T.A. 1976. *Meteorological aspects of the Oahu flood of April 19, 1974.* Tech. Rep. No. 97 (UHMET 76-03), Water Resources Research Center, University of Hawaii.

______. 1977. Meteorological analysis of an Oahu flood. *Mon. Wea. Rev.* 105:458-68.

______. 1978. Meteorology of Hawaiian flash floods. *Preprints*, Conference on Flash Floods-Hydrometeorological Aspects, American Meteorological Society, Los Angeles, California, pp. 17-20.

______; Kilonsky, B.J.; and Meisner, B.N. 1977. *Diurnal variation in rainfall and cloudiness.* Tech. Rep. No. 112, Water Resources Research Center, University of Hawaii.

Scofield, R.A., and Oliver, V.J. 1977. A scheme for estimating convective rainfall from satellite imagery. Tech. Memo. NESS 86, National Oceanic and Atmospheric Administration.

Showalter, A.K., and Fulks, J.R. 1943. A preliminary report on tornadoes. U.S. Weather Bureau, Washington, D.C.

Simpson, R.H. 1952. Evolution of the Kona storm, a subtropical cyclone. *J. Meteorol.* 9:24-35.

Taliaferro, W.J. 1958. *Kona rainfall.* Prov. Report, Hawaii Water Authority, Honolulu, Hawaii.

______. 1959. *Rainfall of the Hawaiian Islands.* Rep. No. R12, Hawaii Water Authority, Honolulu, Hawaii.

Wang, R.; Wu, I.P.; and Lau, L.S. 1970. *Instantaneous unit hydrograph analysis of Hawaiian small watersheds.* Tech. Rep. No. 42, Water Resources Research Center, University of Hawaii.

Woodley, W.L.; Sancho, B.; and Miller, A.H. 1972. Rainfall estimation from satellite cloud photographs. Tech. Memo. ERL OD-11, National Oceanic and Atmospheric Administration.

______; Griffith, C.G.; Griffin, J.; and Augustine, J. 1978. Satellite rain estimation in the Big Thompson and Johnstown flash floods. *Preprints*, Conference on Flash Floods-Hydrometeorological Aspects, American Meteorological Society, Los Angeles, California, pp. 44-51.

APPENDICES

Appendix A Figures

Appendix B Tables

APPENDIX A. ISLAND RAIN GAGE STATION MAPS

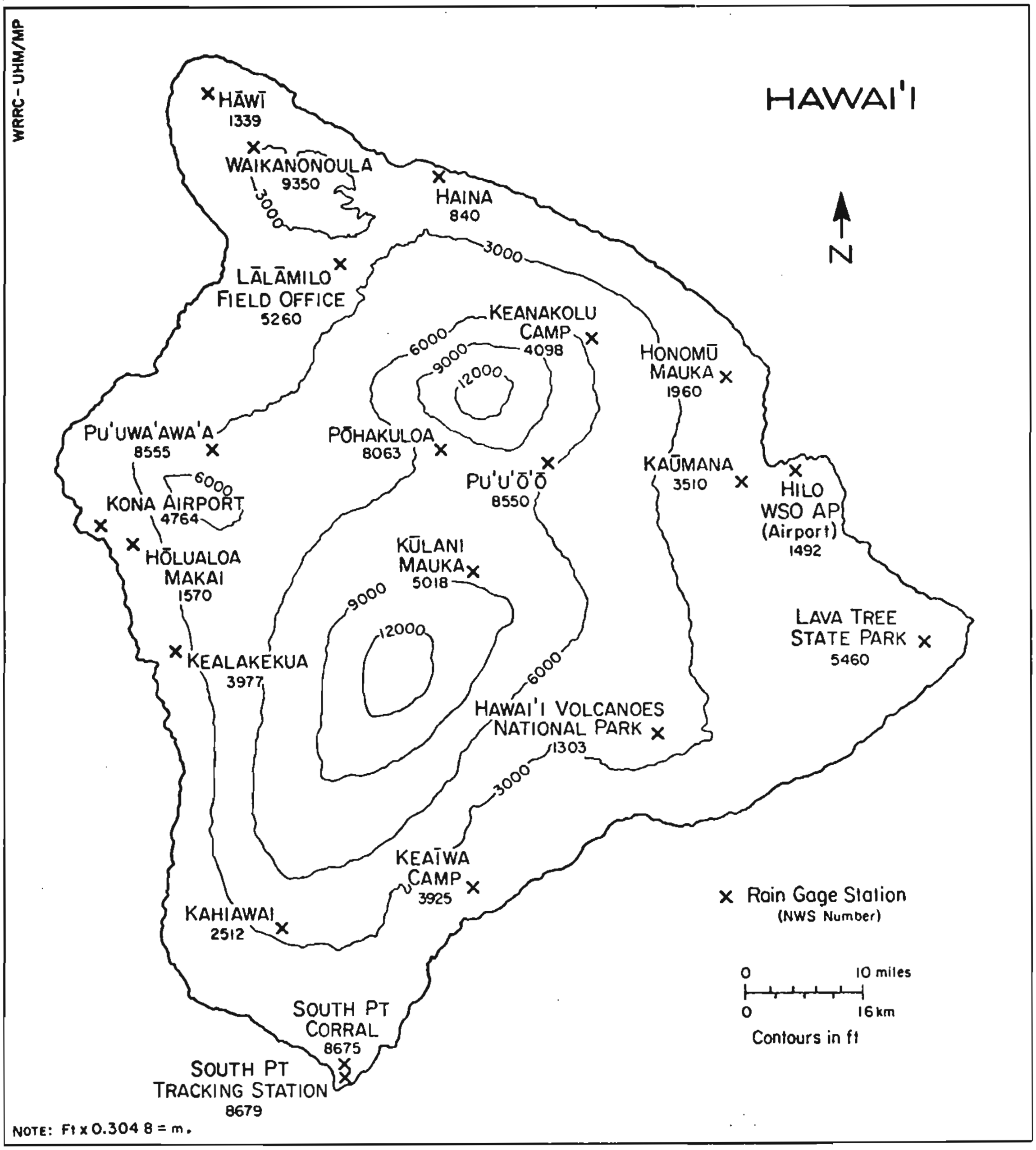

FIGURE A.1. MAP OF RAIN GAGE STATIONS, HAWAI'I ISLAND

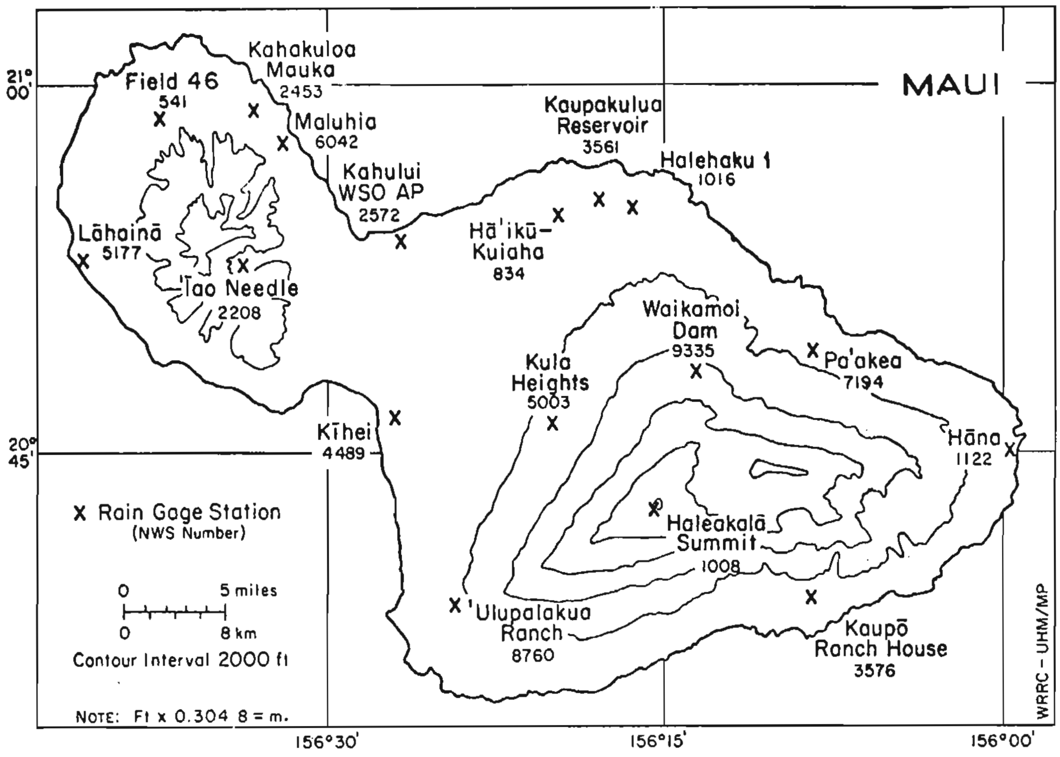

FIGURE A.2. MAP OF RAIN GAGE STATIONS, MAUI

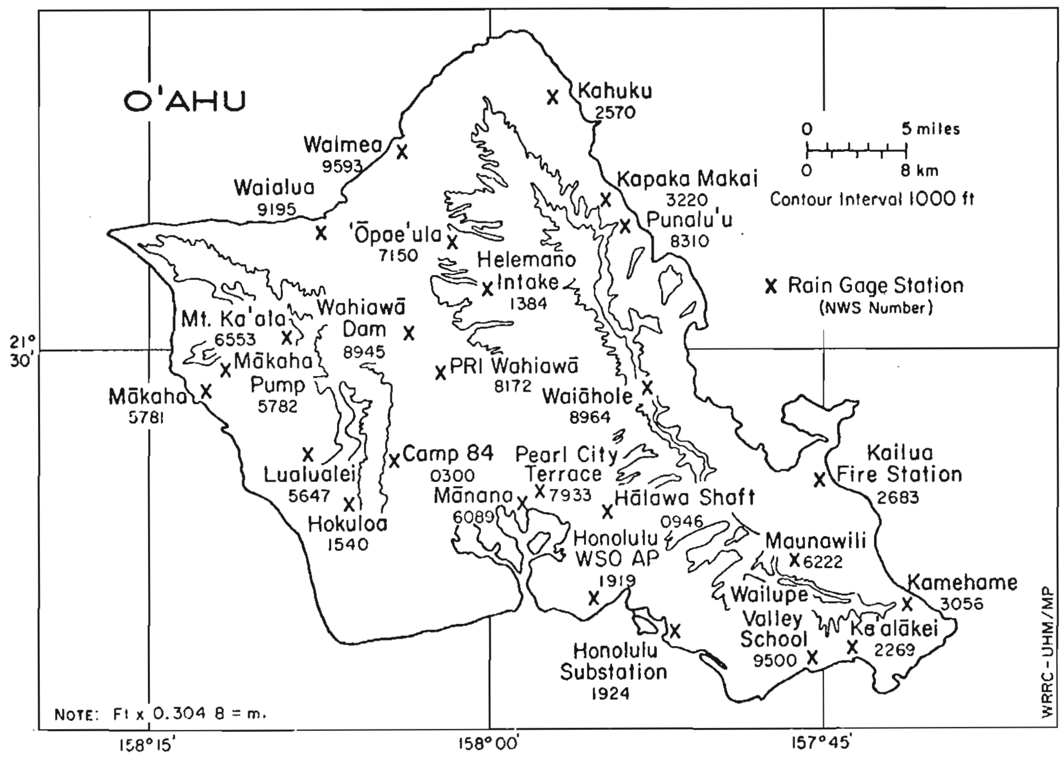

FIGURE A.3. MAP OF RAIN GAGE STATIONS, O'AHU

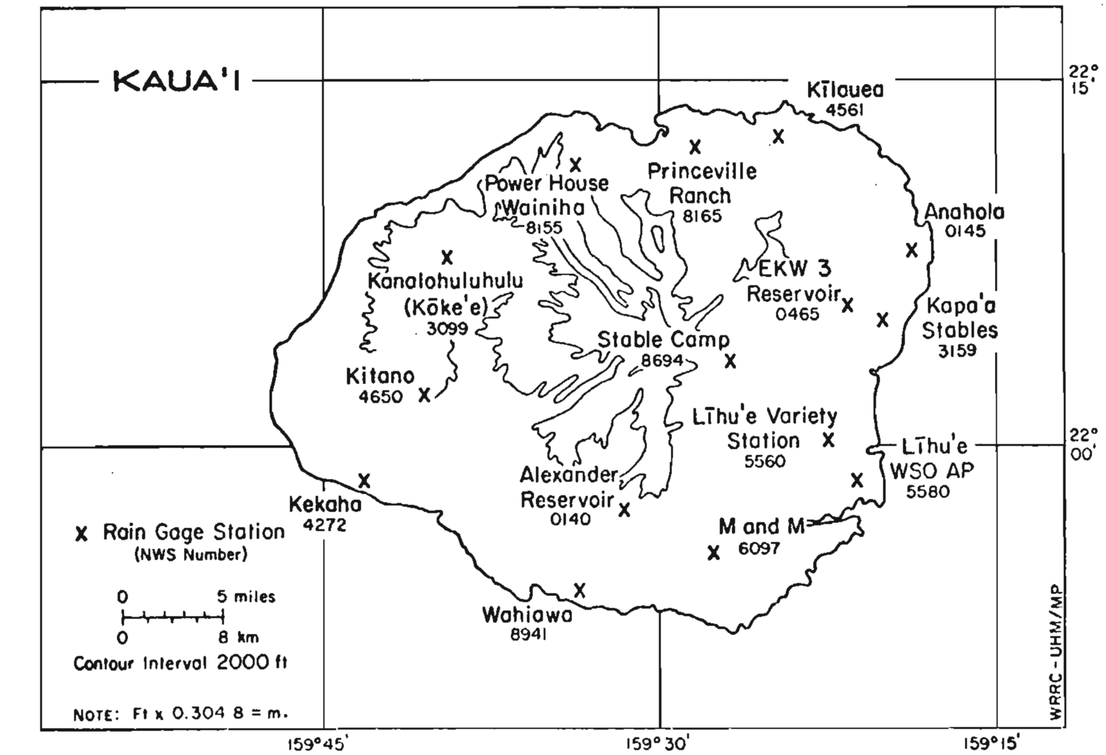

FIGURE A.4. MAP OF RAIN GAGE STATIONS, KAUA'I

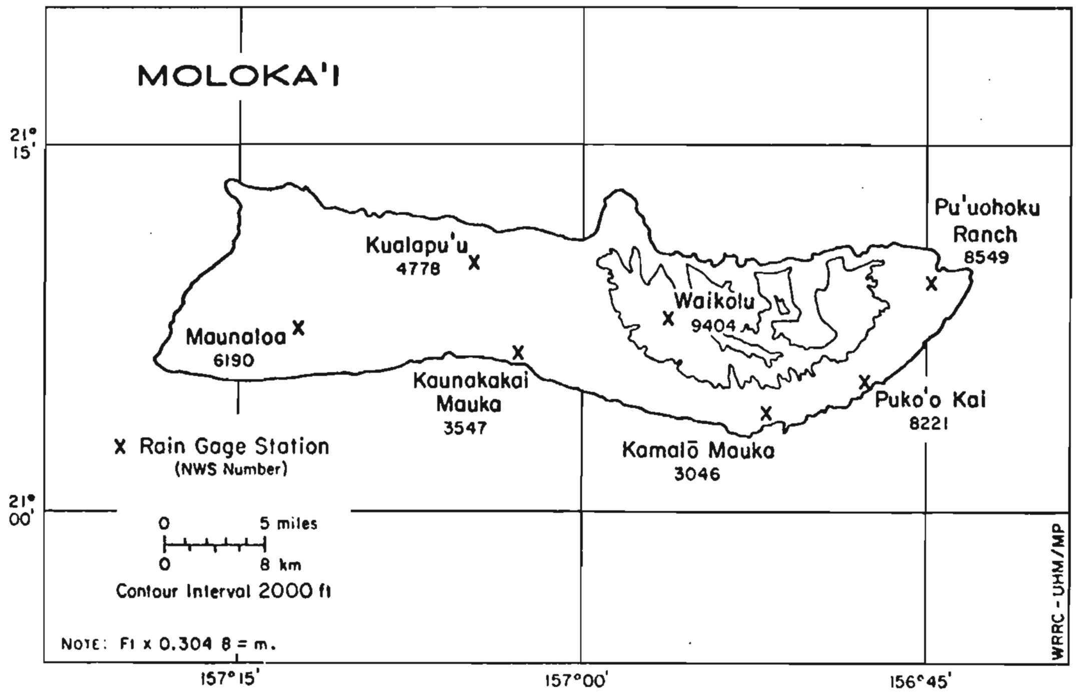

FIGURE A.5. MAP OF RAIN GAGE STATIONS, MOLOKA'I

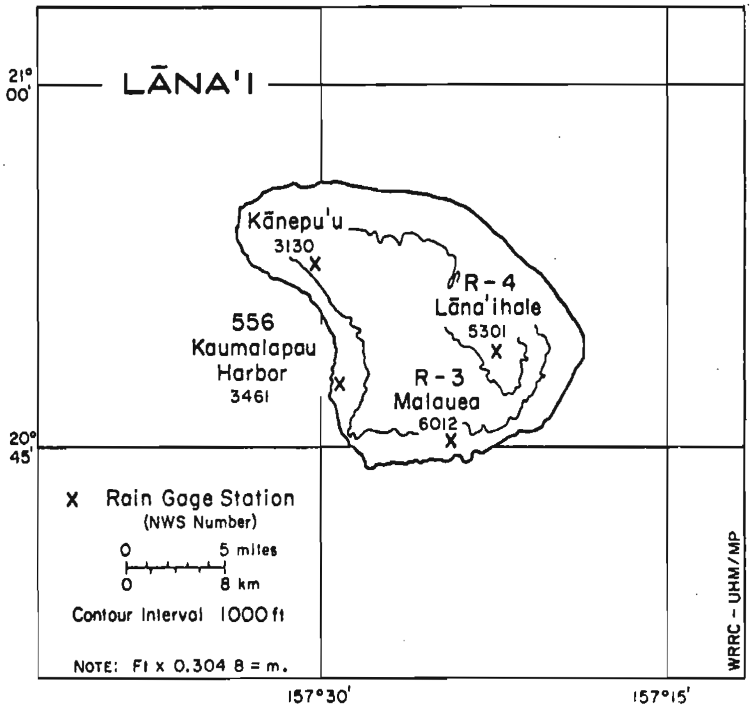

FIGURE A.6. MAP OF RAIN GAGE STATIONS, LANA'I

APPENDIX B. MATRIX OF CONTINGENCY INDEX VALUES

TABLE B.1. MATRIX OF CONTINGENCY INDEX VALUES FOR STATIONS ON HAWAI'I ISLAND

Sta.	Weather Bureau Number																				
No.	840	1303	1339	1492	1570	1960	2512	3510	3925	3977	4098	4764	5018	5260	5460	8063	8550	8555	8675	8679	9350
840	1.000	0.212	0.384	0.208	0.064	0.247	0.120	0.228	0.039	0.056	0.388	0.074	0.272	0.183	0.167	0.102	0.263	0.037	0.055	0.085	0.325
1303	0.212	1.000	0.228	0.348	0.069	0.359	0.154	0.381	0.217	0.089	0.283	0.087	0.306	0.105	0.347	0.071	0.458	0.089	0.084	0.110	0.177
1339	0.384	0.228	1.000	0.198	0.031	0.197	0.095	0.175	0.040	0.073	0.251	0.082	0.233	0.244	0.208	0.110	0.274	0.104	0.074	0.092	0.423
1492	0.208	0.348	0.198	1.000	0.058	0.559	0.048	0.589	-.010	0.077	0.189	0.026	0.167	0.014	0.470	0.016	0.279	-.009	0.015	0.034	0.097
1570	0.064	0.069	0.031	0.058	1.000	0.024	0.162	0.000	0.102	0.420	0.057	0.355	0.056	0.083	0.059	0.120	0.122	0.178	0.039	0.000	0.039
1960	0.247	0.359	0.197	0.559	0.024	1.000	0.038	0.585	0.002	0.075	0.234	0.026	0.145	0.002	0.386	0.019	0.279	0.007	0.016	0.025	0.102
2512	0.120	0.154	0.095	0.048	0.162	0.038	1.000	0.053	0.307	0.176	0.179	0.200	0.230	0.191	0.089	0.260	0.114	0.225	0.215	0.217	0.164
3510	0.228	0.381	0.175	0.589	0.000	0.585	0.053	1.000	0.019	0.111	0.200	0.046	0.179	0.037	0.391	0.031	0.000	0.025	0.075	0.027	0.144
3925	0.039	0.217	0.040	-.010	0.102	0.002	0.307	0.019	1.000	0.081	0.133	0.137	0.219	0.137	0.063	0.186	0.222	0.221	0.249	0.243	0.074
3977	0.056	0.089	0.073	0.077	0.420	0.075	0.176	0.111	0.081	1.000	0.050	0.311	0.110	0.102	0.082	0.097	0.101	0.178	0.051	0.095	0.093
4098	0.388	0.283	0.251	0.189	0.057	0.234	0.179	0.200	0.133	0.050	1.000	0.094	0.411	0.173	0.178	0.151	0.437	0.090	0.081	0.128	0.266
4764	0.074	0.087	0.082	0.026	0.355	0.026	0.200	0.046	0.137	0.311	0.094	1.000	0.122	0.179	0.037	0.223	0.115	0.260	0.111	0.131	0.129
5018	0.272	0.306	0.233	0.167	0.056	0.145	0.230	0.179	0.219	0.110	0.411	0.122	1.000	0.200	0.156	0.273	0.415	0.195	0.163	0.242	0.274
5260	0.183	0.105	0.244	0.014	0.083	0.002	0.191	0.037	0.137	0.102	0.173	0.179	0.200	1.000	0.049	0.256	0.089	0.215	0.138	0.160	0.409
5460	0.167	0.347	0.208	0.470	0.059	0.386	0.089	0.391	0.063	0.082	0.178	0.037	0.156	0.049	1.000	0.035	0.293	0.031	0.052	0.045	0.134
8063	0.102	0.071	0.110	0.016	0.120	0.019	0.260	0.031	0.186	0.097	0.151	0.223	0.273	0.256	0.035	1.000	0.109	0.263	0.204	0.302	0.153
8550	0.263	0.458	0.274	0.279	0.122	0.279	0.114	0.000	0.222	0.101	0.437	0.115	0.415	0.089	0.293	0.109	1.000	0.117	0.085	0.000	0.162
8555	0.037	0.089	0.104	-.009	0.178	0.007	0.225	0.025	0.221	0.178	0.090	0.260	0.195	0.215	0.031	0.263	0.117	1.000	0.230	0.193	0.112
8675	0.055	0.084	0.074	0.015	0.039	0.016	0.215	0.075	0.249	0.051	0.081	0.111	0.163	0.138	0.052	0.204	0.085	0.230	1.000	0.000	0.095
8679	0.085	0.110	0.092	0.034	0.000	0.025	0.217	0.027	0.243	0.095	0.128	0.131	0.242	0.160	0.045	0.302	0.000	0.193	0.000	1.000	0.134
9350	0.325	0.177	0.423	0.097	0.039	0.102	0.164	0.144	0.074	0.093	0.266	0.129	0.274	0.409	0.134	0.153	0.162	0.112	0.095	0.134	1.000

NOTE: 0.0 indicates station pair in question had no overlapping time periods.

TABLE B.2. MATRIX OF CONTINGENCY INDEX VALUES FOR STATIONS ON MAUI

Sta. No.	Weather Bureau Number 541	1008	1016	1122	2208	2453	2572	3576	4489	5003	5177	7194	8760	9335
541	1.000	0.206	0.517	0.379	0.408	0.544	0.319	0.231	0.142	0.163	0.113	0.297	0.170	0.330
1008	0.206	1.000	0.194	0.198	0.225	0.262	0.320	0.226	0.246	0.333	0.267	0.064	0.240	0.101
1016	0.517	0.194	1.000	0.435	0.328	0.382	0.286	0.255	0.068	0.112	0.054	0.434	0.097	0.412
1122	0.379	0.198	0.435	1.000	0.293	0.375	0.255	0.253	0.082	0.124	0.056	0.297	0.151	0.316
2208	0.408	0.225	0.328	0.293	1.000	0.448	0.398	0.134	0.179	0.240	0.177	0.170	0.249	0.257
2453	0.544	0.262	0.382	0.375	0.448	1.000	0.430	0.173	0.171	0.226	0.160	0.193	0.209	0.231
2572	0.319	0.320	0.286	0.255	0.398	0.430	1.000	0.163	0.359	0.346	0.311	0.078	0.267	0.098
3576	0.231	0.226	0.255	0.253	0.134	0.173	0.163	1.000	0.088	0.143	0.111	0.173	0.142	0.151
4489	0.142	0.246	0.068	0.082	0.179	0.171	0.359	0.088	1.000	0.445	0.558	0.000	0.358	0.029
5003	0.163	0.333	0.112	0.124	0.240	0.226	0.346	0.143	0.445	1.000	0.417	0.016	0.369	0.084
5177	0.113	0.267	0.054	0.056	0.177	0.160	0.311	0.111	0.558	0.417	1.000	-.003	0.337	0.015
7194	0.297	0.064	0.434	0.297	0.170	0.193	0.078	0.173	0.000	0.016	-.003	1.000	0.011	0.502
8760	0.170	0.240	0.097	0.151	0.249	0.209	0.267	0.142	0.358	0.369	0.337	0.011	1.000	0.085
9335	0.330	0.101	0.412	0.316	0.257	0.231	0.098	0.151	0.029	0.084	0.015	0.502	0.085	1.000

NOTE: 0.0 indicates station pair in question had no overlapping time periods.

TABLE B.3. MATRIX OF CONTINGENCY INDEX VALUES FOR STATIONS ON O'AHU

Sta. No.	Weather Bureau Number 300	964	1384	1540	1919	1924	2269	2570	2683	3056	3220	5647	5781	5782	6089	6222	6553	7150	7933	8172	8945	8964	9195	9500	9593
300	1.000	0.417	0.297	0.600	0.526	0.462	0.369	0.355	0.366	0.370	0.280	0.534	0.469	0.475	0.484	0.293	0.400	0.378	0.530	0.555	0.521	0.201	0.482	0.318	0.373
964	0.417	1.000	0.464	0.412	0.476	0.420	0.311	0.396	0.349	0.304	0.345	0.292	0.272	0.236	0.523	0.396	0.381	0.526	0.514	0.479	0.502	0.338	0.337	0.416	0.519
1384	0.297	0.464	1.000	0.327	0.312	0.267	0.194	0.356	0.271	0.210	0.362	0.205	0.188	0.150	0.311	0.385	0.397	0.608	0.345	0.423	0.459	0.411	0.276	0.376	0.488
1540	0.600	0.412	0.327	1.000	0.501	0.442	0.317	0.399	0.367	0.352	0.310	0.469	0.452	0.369	0.473	0.330	0.448	0.390	0.504	0.516	0.516	0.250	0.437	0.358	0.397
1919	0.526	0.476	0.312	0.501	1.000	0.617	0.372	0.339	0.389	0.389	0.290	0.458	0.466	0.398	0.528	0.320	0.356	0.387	0.547	0.518	0.485	0.219	0.449	0.390	0.384
1924	0.462	0.420	0.267	0.442	0.617	1.000	0.379	0.307	0.354	0.398	0.248	0.441	0.480	0.379	0.447	0.292	0.300	0.332	0.513	0.460	0.398	0.170	0.412	0.374	0.345
2269	0.369	0.311	0.194	0.317	0.372	0.379	1.000	0.264	0.328	0.521	0.259	0.302	0.356	0.272	0.299	0.280	0.248	0.256	0.360	0.340	0.277	0.165	0.359	0.381	0.272
2570	0.355	0.396	0.356	0.399	0.339	0.307	0.264	1.000	0.359	0.298	0.482	0.285	0.249	0.261	0.371	0.391	0.349	0.439	0.310	0.380	0.399	0.313	0.370	0.329	0.455
2683	0.366	0.349	0.271	0.367	0.389	0.354	0.328	0.359	1.000	0.413	0.336	0.301	0.295	0.245	0.338	0.425	0.337	0.339	0.345	0.343	0.372	0.257	0.346	0.391	0.335
3056	0.370	0.304	0.210	0.352	0.389	0.398	0.521	0.298	0.413	1.000	0.262	0.302	0.349	0.302	0.305	0.338	0.301	0.299	0.335	0.320	0.344	0.187	0.383	0.413	0.292
3220	0.280	0.345	0.362	0.310	0.290	0.248	0.259	0.482	0.336	0.262	1.000	0.216	0.207	0.169	0.278	0.399	0.305	0.408	0.262	0.315	0.353	0.375	0.314	0.333	0.376
5647	0.534	0.292	0.205	0.469	0.458	0.441	0.302	0.285	0.301	0.302	0.216	1.000	0.575	0.511	0.400	0.233	0.319	0.264	0.446	0.434	0.392	0.145	0.410	0.254	0.271
5781	0.469	0.272	0.188	0.452	0.466	0.480	0.356	0.249	0.295	0.349	0.207	0.575	1.000	0.000	0.000	0.189	0.331	0.250	0.405	0.453	0.391	0.112	0.502	0.301	0.268
5782	0.475	0.236	0.150	0.369	0.398	0.379	0.272	0.261	0.245	0.302	0.169	0.511	0.000	1.000	0.330	0.191	0.276	0.239	0.192	0.350	0.308	0.118	0.417	0.204	0.245
6089	0.484	0.523	0.311	0.473	0.528	0.447	0.299	0.371	0.338	0.305	0.278	0.400	0.000	0.330	1.000	0.300	0.357	0.407	0.000	0.560	0.501	0.216	0.394	0.322	0.436
6222	0.293	0.396	0.385	0.330	0.320	0.292	0.280	0.391	0.425	0.338	0.399	0.233	0.189	0.191	0.300	1.000	0.343	0.390	0.309	0.342	0.338	0.458	0.277	0.476	0.353
6553	0.400	0.381	0.397	0.448	0.356	0.300	0.248	0.349	0.337	0.301	0.305	0.319	0.331	0.276	0.357	0.343	1.000	0.471	0.370	0.419	0.509	0.291	0.403	0.358	0.428
7150	0.378	0.526	0.608	0.390	0.387	0.332	0.256	0.439	0.339	0.299	0.408	0.264	0.250	0.239	0.407	0.390	0.471	1.000	0.420	0.507	0.556	0.354	0.423	0.410	0.668
7933	0.530	0.514	0.345	0.504	0.547	0.513	0.360	0.310	0.345	0.335	0.262	0.446	0.405	0.192	0.000	0.309	0.370	0.420	1.000	0.525	0.521	0.238	0.433	0.372	0.412
8172	0.555	0.479	0.423	0.516	0.518	0.460	0.340	0.380	0.343	0.320	0.315	0.434	0.453	0.350	0.560	0.342	0.419	0.507	0.525	1.000	0.611	0.284	0.476	0.353	0.466
8945	0.521	0.502	0.459	0.516	0.485	0.398	0.277	0.399	0.372	0.344	0.353	0.392	0.391	0.308	0.501	0.338	0.509	0.556	0.521	0.611	1.000	0.300	0.475	0.376	0.511
8964	0.201	0.338	0.411	0.250	0.219	0.170	0.165	0.313	0.257	0.187	0.375	0.145	0.112	0.118	0.216	0.458	0.291	0.354	0.238	0.284	0.300	1.000	0.181	0.334	0.303
9195	0.482	0.337	0.276	0.437	0.449	0.412	0.359	0.370	0.346	0.383	0.314	0.410	0.502	0.417	0.394	0.277	0.403	0.423	0.433	0.476	0.475	0.181	1.000	0.301	0.429
9500	0.318	0.416	0.376	0.358	0.390	0.374	0.381	0.329	0.391	0.413	0.333	0.254	0.301	0.204	0.322	0.476	0.358	0.410	0.372	0.353	0.376	0.334	0.301	1.000	0.378
9593	0.373	0.519	0.488	0.397	0.384	0.345	0.272	0.455	0.335	0.292	0.376	0.271	0.268	0.245	0.436	0.353	0.428	0.668	0.412	0.466	0.511	0.303	0.429	0.378	1.000

NOTE: 0.0 indicates station pair in question had no overlapping time period.

TABLE B.4. MATRIX OF CONTINGENCY INDEX VALUES FOR STATIONS ON KAUA'I

Sta. No.	Weather Bureau Number 140	145	465	3099	3159	4272	4561	4650	5560	5580	6097	8155	8165	8694	8941
140	1.000	0.303	0.399	0.271	0.351	0.120	0.355	0.212	0.423	0.367	0.558	0.405	0.399	0.482	0.417
145	0.303	1.000	0.488	0.339	0.535	0.187	0.371	0.246	0.430	0.439	0.366	0.361	0.358	0.304	0.339
465	0.399	0.488	1.000	0.304	0.600	0.094	0.480	0.175	0.574	0.479	0.473	0.426	0.463	0.476	0.349
3099	0.271	0.339	0.304	1.000	0.366	0.248	0.284	0.398	0.290	0.324	0.281	0.356	0.285	0.214	0.374
3159	0.351	0.535	0.600	0.366	1.000	0.177	0.407	0.240	0.513	0.488	0.433	0.402	0.402	0.361	0.357
4272	0.120	0.187	0.094	0.248	0.177	1.000	0.108	0.510	0.111	0.154	0.134	0.090	0.095	0.058	0.285
4561	0.355	0.371	0.480	0.284	0.407	0.108	1.000	0.176	0.422	0.393	0.386	0.444	0.568	0.398	0.278
4650	0.212	0.246	0.175	0.398	0.240	0.510	0.176	1.000	0.189	0.225	0.221	0.149	0.145	0.105	0.320
5560	0.423	0.430	0.574	0.290	0.513	0.111	0.422	0.189	1.000	0.524	0.510	0.387	0.438	0.482	0.379
5580	0.367	0.439	0.479	0.324	0.488	0.154	0.393	0.225	0.524	1.000	0.480	0.364	0.372	0.358	0.400
6097	0.558	0.366	0.473	0.281	0.433	0.134	0.386	0.221	0.510	0.480	1.000	0.389	0.424	0.458	0.451
8155	0.405	0.361	0.426	0.356	0.402	0.090	0.444	0.149	0.387	0.364	0.389	1.000	0.535	0.386	0.308
8165	0.399	0.358	0.463	0.285	0.402	0.095	0.568	0.145	0.438	0.372	0.424	0.535	1.000	0.417	0.300
8694	0.482	0.304	0.476	0.214	0.361	0.058	0.398	0.105	0.482	0.358	0.458	0.386	0.417	1.000	0.259
8941	0.417	0.339	0.349	0.374	0.357	0.285	0.278	0.320	0.379	0.400	0.451	0.308	0.300	0.259	1.000

NOTE: 0.0 indicates that the station pair in question had no overlapping time period.

TABLE B.5. MATRIX OF CONTINGENCY INDEX VALUES FOR STATIONS ON MOLOKA'I

Sta. No.	Weather Bureau Number 3046	3547	4778	6190	8221	8549	9404
3046	1.000	0.250	0.351	0.292	0.000	0.367	0.325
3547	0.250	1.000	0.409	0.435	0.113	0.224	0.122
4778	0.351	0.409	1.000	0.504	0.090	0.353	0.272
6190	0.292	0.435	0.504	1.000	0.099	0.294	0.195
8221	0.000	0.113	0.090	0.099	1.000	0.114	0.119
8549	0.367	0.224	0.353	0.294	0.114	1.000	0.409
9404	0.325	0.122	0.272	0.195	0.119	0.409	1.000

NOTE: 0.0 indicates station pair in question had no overlapping time period.

TABLE B.6. MATRIX OF CONTINGENCY INDEX VALUES FOR STATIONS ON LĀNA'I

Sta. No.	Weather Bureau Number 3130	3461	5301	6012
3130	1.000	0.460	0.315	0.432
3461	0.460	1.000	0.278	0.509
5301	0.315	0.278	1.000	0.274
6012	0.432	0.509	0.274	1.000

NOTE: 0.0 indicates station pair in question had no overlapping time period.